UNIVERSITY OF CALGARY

Estimating Extreme Snow Avalanche Runout for the Columbia Mountains and Fernie Area of British Columbia, Canada

by:

Katherine S. Johnston

A THESIS SUBMITTED TO THE FACULTY OF GRADUATE STUDIES IN PARTIAL FULFILLMENT OF THE REQUIREMENTS FOR THE DEGREE OF MASTER OF SCIENCE

DEPARTMENT

OF CIVIL ENGINEERING

CALGARY, ALBERTA

AUGUST, 2011

©Katherine S. Johnston 2011

ABSTRACT

Extreme snow avalanche runout is typically estimated using a combination of historical and vegetation records as well as statistical and dynamic models. The two classes of statistical models ($\alpha - \beta$ and *runout ratio*) are based on estimating runout distance past the β-point, which is generally defined as the point where the avalanche slope incline first decreases to 10°. The parameters for these models vary from mountain range to mountain range.

In Canada, α – β and runout ratio parameters have been published for the Rocky and Purcell Mountains and for the British Columbia Coastal mountains. Despite active development, no suitable tall avalanche path model parameters have been published for the Columbia Mountains or for the Lizard Range area around Fernie, BC. Using a dataset of 70 avalanche paths, statistical model parameters have been derived for these regions. In addition, the correlation between extreme and average snowfall values and avalanche runout is explored.

ACKNOWLEDGEMENTS

Thank you to Bruce Jamieson for giving me the opportunity to work on this project, and for coordinating the financial support for this project. His thoughtful advice, numerous reviews, and inspirational leadership have helped make this a fantastic experience.

My thanks to Alan Jones for providing numerous hours of guidance, mentoring, and thoughtful discussion throughout this project, and for facilitating data acquisition from outside sources. Thanks also to Chris Stethem (Chris Stethem and Associates), Mark Vesley (Fernie Alpine Resort), Steve Kuijt (Island Lake Catskiing) and Craig Ellis (Imperial Metals) for collecting detailed observations and for sharing field data.

For assistance with summer and winter fieldwork I would like to thank my fellow students Cameron Ross, Mike Smith, Dave Tracz, Cora Shea, Ryan Buhler, and Scott Thumlert, and ASARC technicians Mark Kolasinski, Deanna Andersen and Michael Shynkaryk. For dedicated and detailed proof reading, thanks to Ryan Buhler, Scott Thumlert and Sascha Bellaire.

For field support of the ASARC program and for practical insight I would like to thank Bruce McMahon, Jeff Goodrich, Rob Hemming, and the entire Avalanche Control Section of Glacier National Park.

For financial support of the ASARC program, I would like to acknowledge and thank to Natural Sciences and Research Council and Canada (NSERC), the Helicat Canada Association, the Canadian Avalanche Association, Mike Wiegele Helicopter Skiing, the Canada West Ski Area Association, Parks Canada, the Association of Canadian Mountain Guides, the Backcountry Lodges of British Columbia Association, the Canadian Ski Guide Association and Teck Coal. Thank you to the Alliance Pipeline for supporting me with the Naomi Heffler Memorial Scholarship and to the Alberta Scholarship Programs for supporting me with an Alberta Graduate Student Scholarship.

Table of Contents

LIST OF TABLES

LIST OF FIGURES

LIST OF SYMBOLS AND ABBREVIATIONS

ASARC	Applied Snow and Avalanche Research at the University of Calgary
α	alpha, extreme runout point and angle
α/ β	dimensionless ratio of the field measured α and β angles
β	beta, point and angle where slope first decreases to 10° while descending the slope
CAA	Canadian Avalanche Association
CSA	Chris Stethem and Associates
CDCD	Canadian Daily Climate Data
δ	delta, average slope of the avalanche path runout zone in-between α and β points
D-value	Kolomogrov – Smirinov D statistic
DEM	digital elevation model
E	encounter probability
EC	Environment Canada
F-value	value of F-statistic
FAR	Fernie Alpine Resort
FOS	factor of safety
GPS	Global Positioning System
H_0	vertical drop from top of the start zone to lowest point on the parabola fitted to the avalanche path profile
H_0y''	scale factor, product of H_0 and y"
H_β	vertical drop from the top of the start zone to the β-point
H_α or H	vertical drop from the top of the start zone to the α-point
HN3d	depth of new snow accumulation over 3 days
$HN3d_{crit}$	critical threshold depth of new snow accumulation over 3 days required for long running avalanches
IM	Imperial Metals
k	degrees of freedom
kPa	kilopascals
K – S	Kolmogorov – Smirinov
L	defined return period (years)
MOE	Ministry of Environment
MOT	Ministry of Transportation
n	sample size
NAD83	North American Datum 83

P	non-exceedence probability
p	statistical significance value
PLK	Perla Lied McClung dynamic avalanche runout model
PCM	Perla Cheng McClung dynamic avalanche runout model
PRISM	Parameter elevation Regressions on Independent Slopes Model
Q_0	minimum value from sample set
Q_1	lower quartile from sample set
Q_2	median value from sample set
Q_3	upper quartile from sample set
Q_4	maximum value from sample set
R	Pearson correlation coefficient
r^2 or R^2	Coefficient of determination (adjusted unless otherwise stated)
RZ_Elev	runout zone elevation (m)
SE	Standard error
Ψ	si, slope segment angle of the avalanche path
S_0	slope length of avalanche path from top of start zone to extreme runout positions
SC_{mm}	snow course water equivalent in mm
SR	surface roughness factor
SWE	snow water equivalent
SWE_{ex}	extreme snow water equivalent
SZ_Ang	start zone angle
SZ_Asp	start zone aspect
SZ_Elev	start zone elevation (m)
SZ_Width	width of upper portion of start zone (m)
T	set period of time
t-value	t statistic
θ	theta , average angle of the avalanche path start zone
TP	terrain parameter
UTM	Universal Transverse Mercator
WI	Wind Index
W_Precip	PRISM winter precipitation
X_β	horizontal distance between top of avalanche path start zone and β-point
X_α	horizontal distance between top of avalanche path start zone and α-point
Δx	horizontal distance between β-point and α-point
$\Delta x / X_\beta$	runout ratio fraction
x_p	runout ratio for a specific non-exceedence probability
y''	2^{nd} derivative of the parabolic fit to the avalanche path profile

1.0 INTRODUCTION

This introductory chapter is intended to provide a background on snow avalanches, avalanche terrain and the impacts of avalanches in Canada. Avalanche risk management involves assessing, managing and mitigating avalanche risk. A key component of assessing avalanche risk for land use planning is defining and mapping the extreme avalanche runout. Extreme avalanche runout can be defined as the longest running avalanche that could occur in a specific path. Analogous to predicting and mapping flood zones for land development in valley bottoms, predicting and mapping extreme avalanche runout is an essential step for land development in mountainous terrain. Assessing extreme avalanche runout usually involves collecting oral and written records, aerial photo analysis, field studies of avalanche impacted vegetation, and topographical surveys. The topographical path survey can then be used to estimate extreme avalanche runout using statistical and dynamic avalanche runout models.

This chapter introduces the existing statistical models used in Canada and discusses their use and limitations for avalanche hazard mapping. New parameters for existing statistical models are derived for specific geographic areas, namely the Fernie area of the South Rocky Mountains and the Columbia Mountains in British Columbia, Canada. These parameters can be used in statistical runout models to estimate extreme avalanche runout in the Fernie area and in the Columbia mountains. Section 3.1 includes a detailed description of these two study areas. Additionally, the relationship between extreme runout and snowfall is explored using snowfall and snowpack data from a number of sources.

1.1 Snow Avalanches

Compared to other natural slope hazards such as landslides and debris flows, avalanches are much more common due to the unique properties of snow. Alpine snow is weak compared to other earth materials such as rock, ice or soil and usually consists of about 80% air and 20% ice, with the strength coming from the bonds between ice particles. Additionally, snow exists at or very close to its melting point of 0°C, this allows snow to readily creep and deform under its own weight, which can lead to rapid and dramatic changes in form and strength (McClung and Schaerer, 2006).

Figure 1.1: *Loose snow avalanche (Bruce Jamieson photo)*

A snow avalanche can be defined as a mass of at least several m^3 of snow moving at a visible speed (Jamieson, 2009). The size and destructive potential (CAA, 2007) can range from small (<10 m^3 of snow) and relatively harmless to people, to large (>10^5 m^3 of snow) with the ability to destroy infrastructure and multiple buildings. The two major types of snow avalanches include loose snow avalanches and slab avalanches. Both types of snow avalanches can be either "wet" or "dry" referring to the overall moisture content of the deposit. Loose snow avalanches (Figure 1.1) start at a point and entrain snow as they move down slope; dry, loose snow avalanches are usually small (McClung and Schaerer, 2006).

Slab avalanches (Figure 1.2) start when a slab of cohesive snow releases from the slope and moves as a unit before breaking up; most large and long running avalanches start as slabs (McClung and Schaerer, 2006). In Canada, avalanches are generally classified according to size and destructive potential as shown in Table 1.1.

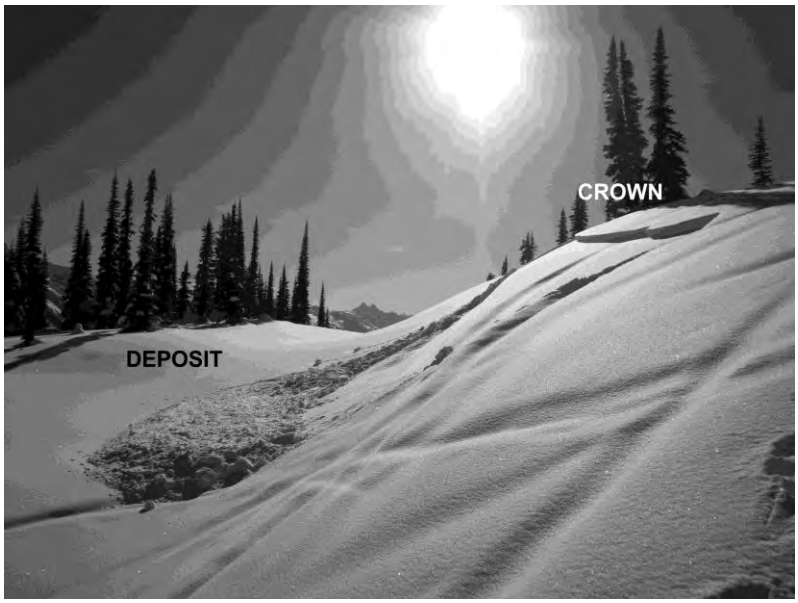

Figure 1.2: *Small slab avalanche (Mike Smith photo)*

Table 1.1: *Canadian snow avalanche size classification (after McClung and Schaerer, 2006).*

Size	Destructive Potential	Typical Mass (t)	Typical Path Length (m)	Typical Impact Pressure (kPa)
1	Relatively harmless to people	<10	10	1
2	Could bury, injure, or kill a person	10^2	100	10
3	Could bury a car, destroy a small building, or break a few trees	10^3	1000	100
4	Could destroy a railway car, large truck, several buildings, or a forest with an area up to 4 hectares	10^4	2000	500
5	Largest snow avalanches known, could destroy a village or forest of 40 hectares	10^5	3000	1000

In practice, avalanche size is generally estimated by the observer based primarily on the destructive potential and secondarily on the mass, length, and impact pressure. The destructive potential is usually the easiest parameter to estimate in the field, which makes avalanche size ratings based on this scale subjective.

1.2 Avalanche Terrain

An avalanche path is a fixed location where avalanches occur. An avalanche area is defined as a location with one or more avalanche paths (McClung and Schaerer, 2006). Avalanche paths range in size from very big with vertical drops over 2000 m and path lengths over 4000 m, or very small with vertical drops less than 50 m and path lengths less than 100 m. Avalanche paths can be very obvious and easy to identify like the one shown in Figure 1.3, which consists of large and overlapping paths that run from mountain top to valley bottom.

Figure 1.3: *A large avalanche path in Juneau, Alaska (Tom Mattice photo)*

Figure 1.4: *Less obvious avalanche terrain obscured by vegetation (Bruce Jamieson photo)*

Avalanche paths may also be subtle consisting of smaller avalanche paths as shown in Figure 1.4 which are not well defined or which are obscured by vegetation. For land use planning, avalanche hazard mapping professionals are generally concerned with the large, easy to identify avalanche paths.

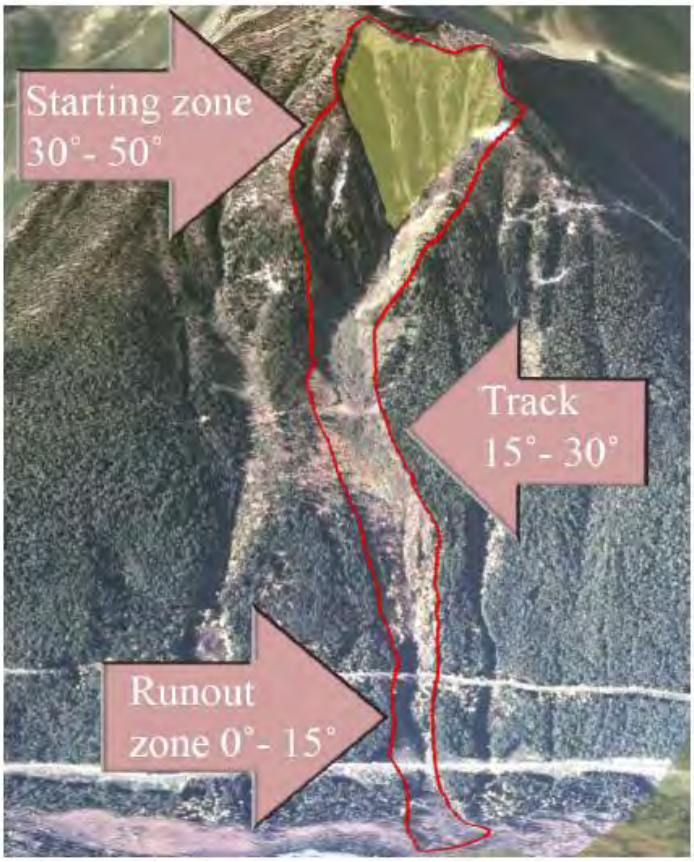

Figure 1.5: *Avalanche path showing typical slope angles and location of the start zone, track and runout zone (Delparte, 2008)*

An avalanche path consists of three main terrain features: a starting zone, a track, and a runout zone (Figure 1.5).

The start zone typically has slope angles over 25° and includes the area where unstable snow releases from the slope and begins to move downhill (McClung and Schaerer, 2006). The track typically has slope angles of 15 – 25° (McClung and Schaerer, 2006) and includes the middle part of the path; snow may be both entrained and deposited in the track. For large avalanches, the speed may increase in the track or remain constant. The runout zone typically has slope angles of less than 15° and includes the area where large avalanches decelerate and stop, the runout zone may cross the valley bottom and extend uphill on the other side of the valley.

1.3 Avalanche Motion

As previously mentioned, avalanches can be divided into two broad categories, namely loose snow and slab avalanches. Either type of avalanche can travel as a dry mass or as a wet mass of snow; some avalanches may start as dry and become wet as they descend to lower elevations and entrain moist snow. According to McClung and Schaerer (2006), wet snow avalanches experience much higher friction at the sliding surface, and typically travel slower and cause less destruction than dry slab avalanches. While dry snow avalanches will tend to travel faster and overrun terrain features, wet avalanches are more likely to follow gullies.

Since dry slab avalanches generally travel farther in the runout zone, reach the highest speeds (compared to wet avalanches) and are capable of producing the largest impact pressures (Mears, 1992), the large dry slab event is typically considered as the design case for land use planning.

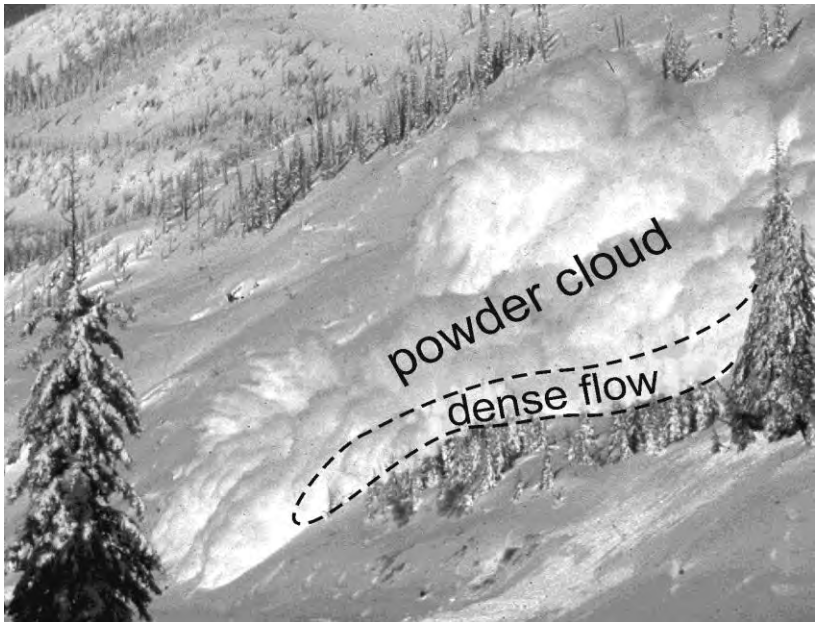

Figure 1.6: *Dense and power flow components of a dry avalanche (Will Geary image)*

As a dry slab avalanche releases, the slab is broken up into smaller and smaller pieces; eventually these pieces break up into a mixture of snow particles and air. The component of the avalanche which breaks up and interacts with the ground or snow cover during motion is referred to as the dense flow component. (Figure 1.6). The component which breaks up and becomes a low density airborne mixture of snow and air is referred to as the powder component. In addition, a large, dry avalanche may also be accompanied by an air blast which typically travels in front of the dense flow and powder component.

According to McClung and Schaerer (2006), the dense flow component is usually less than 5 m high while the powder component can be 10's of meters high, and the density of the powder component is about one tenth that of the dense core. According to Perla and Martinelli (1976) and Gubler (1987), the dense flow can reach velocities up to about 60 m/s (200 km/h), while the powder flow can travel much faster; up to 70 m/s (250 km/h).

A large dry slab avalanche will gain speed rapidly in the starting zone as the slab releases and travels downhill reaching maximum velocity in the avalanche track. Large avalanches will start to decelerate rapidly in the runout zone below slope incline angles of about 15°.

Even though the powder component can travel faster than the dense flow and can be larger in volume, since the density is usually about 10 times lower, the dense flow is generally found to have the most destructive potential. For context, Table 1.2 after McClung and Schaerer (2006) summarizes typical damage from a range of impact pressures.

Table 1.2: *Approximate average impact pressure and potential damage to structures (McClung and Schaerer, 2006)*

Impact Pressure (kPa)	Potential Damage
1	Break windows
5	Push in doors
30	Destroy wood-framed structures
100	Uproot mature spruce
1000	Move reinforced-concrete structures

In general, impact pressure from the powder component is often less than a few kPa, however, in some cases, the powder component can be powerful enough to destroy hectares of mature timber as shown in Figure 1.7.

Figure 1.7: *Powder blast damage to mature timber in Rogers Pass, BC (Sylvia Forrest photo)*

In these situations, differentiating between powder and dense flow damage can be difficult.

1.4 Avalanche Frequency and Return Interval

In a given avalanche path, there may be several small avalanches throughout the season which stop in the starting zone and upper track. Large avalanches extending to the full runout zone usually occur much less frequently. At a given location in the avalanche path, the *return period (T),* is the average time between avalanche events with similar characteristics; usually described by size or runout extent. Avalanche *frequency (1/T)* is the inverse of return period, for example an avalanche with a return period of 10 years has an annual frequency of 0.1. The encounter probability (*E*) is the likelihood that an avalanche with a defined return period (*T*) will occur in a set period of time (*L*). Assuming that avalanche occurrences are statistically independent from year to year, the encounter probability can be described by (McClung, 1999):

$$E = 1 - (1-1/T)^{L} \qquad \text{Equation 1.1}$$

For example, the encounter probability for an avalanche with a 100 year return period is 0.01 in a 1 year observation period, and 0.63 in a 100 year observation period.

1.5 Avalanche Accidents and Costs in Canada

Jamieson (2009) estimates that avalanche impacts in Canada total about $10 M annually not including the loss associated with approximately 15 human lives per year (Campbell et al., 2008). The estimated losses come from a variety of sources including the indirect cost of highway closures, damage to property and infrastructure and the damage or loss of harvestable timber.

From 1782 to 2007, avalanches have been responsible for at least 702 fatalities in Canada (Campbell et al., 2007). Forty-two percent of these accidents involved people who were either in buildings, on transportation corridors, or working in resource industries. Fifty-three percent involved recreationalists and the remaining five percent are either unknown or were engaged in other activities (Campbell et al., 2007). Since about the 1970's, a combination of improved avalanche mitigation and an increase in winter backcountry recreation has led to an increase in recreational fatalities and a decrease in other types of avalanche fatalities.

Figure 1.8: *Damaged school and gymnasium in Kangiqsualujjuaq, Quebec (Bruce Jamieson photo)*

The most recent avalanche accident in Canada involving people in buildings took place in 1999 in the community of Kangiqsualujjuaq, Quebec on January 1, 1999 (Jamieson et al., 2010). An avalanche with a crown height of 1 – 1.8 m released from a slope above the school gymnasium and impacted the wood frame building shown in Figure 1.8. Nine people including five children were killed in the accident; at least seven of the victims were outside the building when the avalanche struck. Following this accident, experts were hired to prepare an avalanche hazard map for the site which identified the school and gymnasium as being within the high risk zone. Subsequently, the school was rebuilt and other buildings were relocated to outside the high-risk avalanche zone.

The most recent avalanche fatality in Canada at an outdoor worksite was caused by an extreme avalanche event in the Lizard Range near Fernie, BC in January 2006 (Jamieson et al., 2010). On

the morning of January 14, 2006, a guide for a local catskiing operation was working in a high elevation snow study plot when a large natural avalanche ran though mature timber and through the study plot burying the guide and the weather observation station. In the previous 15 years of operation, avalanches had never before reached the study plot, the guide was not wearing an avalanche transceiver at the time of the accident.

1.6 Avalanche Hazard Mitigation

In an ideal situation, avalanche terrain would be completely avoided for major development in mountainous terrain. Where avoidance of avalanche terrain is either impossible or impractical, mitigation measures are undertaken. Avalanche hazard mitigation can be separated into two broad categories: active and passive mitigation measures. Active measures require continuous evaluation of the avalanche hazard and application of short term measures such as explosive control or evacuations/closures to mitigate the risk. An example of an active control program is the Trans-Canada Highway avalanche control section at Rogers Pass in British Columbia. Over 130 avalanche paths threaten a 40 km section of the highway through Rogers Pass, and during the winter months a team of forecasters and technicians are constantly monitoring avalanche activity and risk. The avalanche risk at the Pass is mitigated by a combination of highway closures and artillery triggered avalanches.

Passive mitigation measures are permanent defence measures which may not require constant evaluation, but usually consist of engineering works with high capital costs such as catchment dams or reinforced structures. Passive mitigation structures will also likely require some amount of maintenance throughout their lifetime in the form of regular snow removal and/or inspections and repairs. An example of a passive mitigation measure includes the avalanche deflection dyke shown in Figure 1.9 which is located at Mt. Steven in Field, BC.

Figure 1.9: *Deflection dyke at Mt. Steven, near Field, BC (Katherine Johnston photo: September 2009)*

The purpose of this dyke is to deflect avalanches and rock fall from Mt. Steven away from the Trans-Canada Highway. Since construction, the height of the deflection dike has been increased several times; maintenance of the dyke includes removal of rock build-up.

Other types of passive mitigation include snowsheds which are designed to let avalanches pass over roadways without impacting the roads, and reinforced buildings and structures which are designed to withstand the impact force of an avalanche.

1.7 Avalanche Hazard Zoning in Canada

The purpose of performing an avalanche hazard assessment is to identify terrain which could potentially be impacted by avalanches. Depending on the location and type of development, conducting an avalanche hazard assessment may be mandatory or voluntary. After examining similar zoning systems in Europe, the Canadian Avalanche Association (CAA) developed a Canadian Zoning guideline 2002 (CAA, 2002). This guideline advises that development areas in mountainous terrain can be divided into Red, White and Blue Zones which are defined based on impact pressures and expected avalanche return periods shown in Figure 1.10.

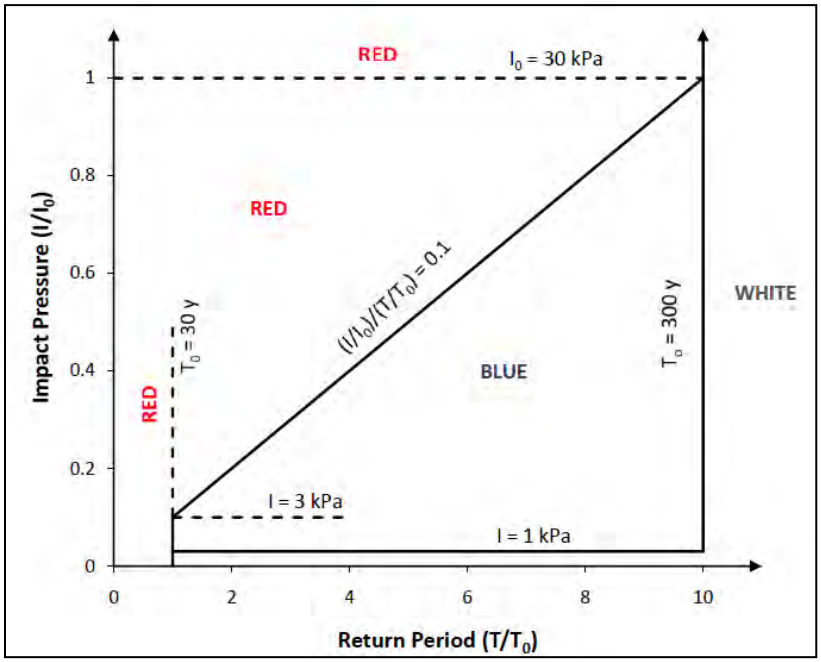

Figure 1.10: *Canadian impact pressure and return period zoning chart (after CAA 2002, with permission)*

The Red Zone (high risk) encompasses the area with an avalanche return period of less than 30 years or with a return period in between 30 and 300 years and impact pressures greater than about 1 kPa. The White Zone (low risk) includes the area with either a return period greater than 300 years, or return periods in between 30 and 300 years and expected impact pressures less than 1 kPa. Impact pressures of about 1 kPa are generally assumed sufficient to break windows (McClung and Schaerer, 2006). The Blue Zone encompasses the area between the red and white zones. An example of an avalanche hazard map for a hypothetical avalanche path is included as Figure 1.11.

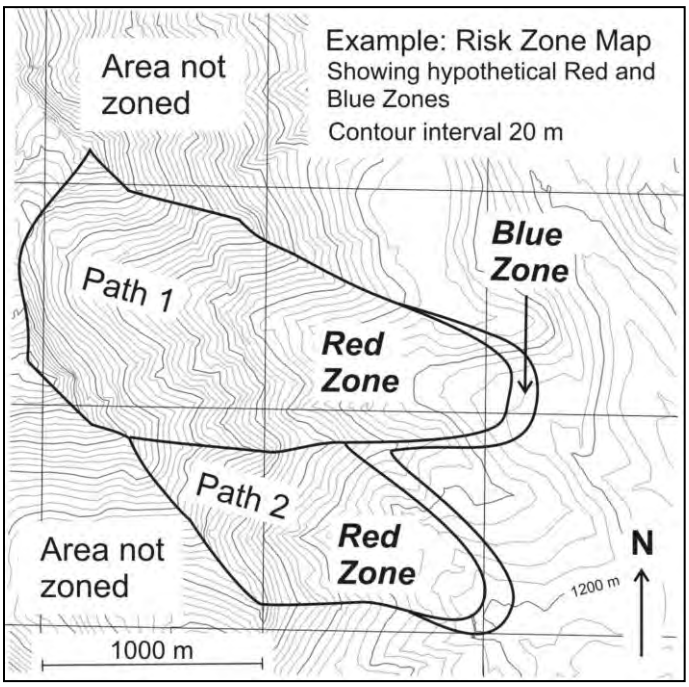

Figure 1.11: *Risk map for a hypothetical avalanche path showing the red and blue risk zones (CAA, 2002, with permission)*

Although the CAA Zoning system is a non-legislated guideline, some jurisdictions have chosen to adopt it and require avalanche hazard assessments prior to development. In addition, the BC Ministry of Transportation (BC MOT) Subdivision Development policy states that residential development should be located where avalanches with a return period of 300 years or less are not expected, and that BC MOT will not build or maintain roads to subdivisions which do not meet the CAA Guidelines.

1.8 Avalanche Runout Models

The two broad classes of avalanche runout models are statistical and dynamic models. Statistical models predict extreme avalanche runout by comparing terrain variables for the path in question to a statistically representative set of avalanche paths from the same mountain range. The two types of statistical models are the $\alpha - \beta$ and the *runout* ratio models, which are described in Chapter 2. In Canada, statistical model parameters have been developed for tall avalanche paths (vertical drops > 350 m) for the combined Rocky and Purcell Mountains (McClung et al., 1989) and for the British Columbia Coastal Mountains (Nixon and McClung, 1993).

Dynamic avalanche runout models such as the Perla, Lied, Kristensen (PLK) (Perla et al., 1984) or Perla, Cheng, McClung (PCM) (Perla et al., 1980) represent avalanche motion as either a fluid or granular flow and calculate avalanche speed along the slope profile. The extreme runout position can be estimated calculating the point along the slope profile where the avalanche

stops. Dynamic models rely on the modeller selecting avalanche parameters such as slab thickness, and representative friction coefficients which account for resistive forces such as basal sliding friction, air drag, and internal resistance. Although seemingly straightforward, these parameters depend on the model and mountain range and require expert judgement and experience by the modeller to obtain useful runout estimates.

1.9 Assessing Avalanche Hazard for Land Use Planning

For land use planning in mountainous areas, avalanche hazards are usually assessed using a combination of historical data, field observations and analytical methods. Specifically, these tasks will include collecting and reviewing historical avalanche occurrence data (both oral and written records), observing vegetation damage in the runout zone, and collecting and analyzing the slope profile of the avalanche path. The avalanche runout return period of interest will depend on what the area is going to be used for and what the proposed development consists of. For example, a temporary structure such as a mining exploration site may only be interested in the 10 or 30 year avalanche while a major highway or large building development may require mapping of the 50 – 100 year event.

A key goal of the avalanche hazard consultant is to provide an accurate avalanche hazard map based on multiple sources of data and estimation methods. As with other engineering works and designs, a *factor of safety (FOS)* may be applied to account for unknowns and to build some level of conservatism into the assessment. A misrepresented avalanche hazard map could result in physical damage to people and property, conversely, an overly conservative avalanche hazard map could result in a loss of valuable development land.

Figure 1.12: *Example of logging in small avalanche path runout zones, Blue River, BC (Katherine Johnston photo)*

Historical observations and ground truth observations of avalanche runout are generally preferred over avalanche runout models since the models contain a number of limiting assumptions. In some parts of the world, such as Norway, oral and written records of avalanche occurrences may be available for periods over 100 years (Lied and Bakkehöi, 1980). In Canada, the record of oral and written avalanche occurrence data is usually much shorter and in many cases there is no historical record for new development. Observations of avalanche damage to vegetation may be non-existent where the vegetative record has been eliminated by logging as shown in Figure 1.12, or in alpine environments lacking mature vegetation or areas north of the tree line. In these cases, the hazard mapper may put more emphasis on estimations derived from avalanche runout models, or a larger factor of safety may be built into the assessment.

For each of these sources of data, there is both temporal and spatial uncertainty. For oral and written records, there is uncertainty in both the timing and runout locations of documented avalanches. The magnitude of this uncertainty will depends on the data quality and recording method.

For historical map and aerial photo analysis, uncertainty is introduced by both the scale and time period of available information. For example, if aerial photographs for a given avalanche path indicate avalanche damage to vegetation between 1955 and 1970, it is unknown if this

damage was caused by an individual event or by several events. In addition, the exact timing of the event between 1955 and 1970 is unknown. Spatial uncertainty with map and air photo analysis depends on the scale of the available images which will vary between locations.

Statistical and dynamic avalanche models are based on the topographic profile which is collected in the field and subject to instrumentation errors and also the selected avalanche path trajectory. For simple and unconfined paths it is usually straightforward to select the trajectory of the large, dry avalanche while for complicated and variable terrain it may be more difficult.

As previously mentioned, dynamic models rely on selection of friction and turbulence parameters, and the accuracy of these models depends on having available calibration information and on the modellers experience with the models in specific regions.

The models primarily used in Canada are 1-D flow models which are depend on the topographic profile of the avalanche path centerline. The hazard mapper will use expert judgment to extend these results laterally while accounting for variability in runout zone terrain.

Although it may be possible to conduct a sensitivity analysis and quantitatively assess the uncertainty in avalanche runout model estimates, the hazard zoning boundaries will be based on a number of different estimates. In an ideal situation, these independent methods and data sources will give the same temporal and spatial information for extreme avalanche runout. However, the uncertainties associated with these different data sources will vary from site to site, and the hazard mapper must use expert judegment to determine the amount of confidence to place on each of the methods. A lower level of confidence will likely result in increased conservatism and larger avalanche hazard zones.

1.10 Influence of Climate on Runout

Although avalanche runout is intrinsically related to the snowpack, all statistical models and most dynamic models do not explicitly include climate or snowpack characteristics in the analysis. The exception is some of the dynamic models developed in Switzerland which include

slab release thickness based on elevation as an input parameter. Since snowfall and snowpack height increase with elevation, this indirectly incorporates a climate variable into the analysis.

The primary reason for excluding climate from extreme runout analysis is the underlying assumption that over a very long period of time, the optimal climate conditions favouring extreme avalanche runout will occur in all mountain ranges and all avalanche paths (Mears, 1984).

A secondary reason is that the variation in snowfall amounts between starting zones located in different mountain ranges and valleys is complex, and is difficult to measure and/or accurately predict. Long and accurate records of local climate and snowpack within avalanche starting zones are rarely available. In Canada, weather stations are generally located at valley bottom elevations, or at locations which would not be impacted by avalanches. Current practice in Canada is to estimate snowfall within avalanche starting zones using a combination of data from nearby weather stations (often in the valley bottoms), and knowledge of wind transport and other local conditions.

Lied and Bakkehöi (1980) attempted to relate extreme avalanche runout to climate by analyzing the relationship between starting zone wind loading and extreme runout. Mears (1984) qualitatively compared the climate and terrain parameters from long running avalanches in Colorado and in Coastal Alaska. Mears (1984) hypothesized that the drier snow climate and higher elevation runout zones of the continental Colorado paths led to longer running avalanches compared to the lower elevation and wetter runout zones in coastal Alaska.

Smith and McClung (1997) analyzed 24 years of avalanche occurrence, terrain, and weather data from 25 avalanche paths in Rogers Pass. They found that avalanche frequency was significantly correlated with the 30 year maximum water equivalent along with wind exposure, runout zone elevation and inclination. However, since 30 year maximum water equivalent is not easily measured or estimated, the snowfall variable was dropped from the correlation.

Schweizer et al. (2009) used 58 years of detailed climate and avalanche occurrence data from the Salezertobel path near Davos, Switzerland to relate the return period of critical new snow

depths to the return period of large avalanches. They found that the return period for the critical snow depths was about half that of the return period of large avalanches for the Salezertobel path.

1.11 Objectives and Overview of Thesis

The major mountain ranges of Western Canada include the Coastal, Columbia and Rocky Mountain ranges. Previous studies by McClung et al. (1989) and Nixon and McClung (1993) have presented $\alpha - \beta$ and runout ratio statistical model parameters for the combined Rocky and Purcell mountains, and for the British Columbia coastal mountains. In addition, Canada wide runout ratio parameters have been derived for short avalanche slopes with vertical drops less than 350 m (Jones and Jamieson, 2004). Several previously mentioned studies have focused on quantitatively relating climate variables to avalanche runout and return period with limited success.

The Columbia mountains are located in central British Columbia, due to the combination of mountainous terrain and favourable snowfall, the Columbia's are home to numerous ski hills and backcountry ski operations. In addition to recreational development, there is also substantial residential and industrial development within avalanche terrain that may require identification of avalanche hazards.

Unlike the central and northern Rocky Mountains which are characterized by a continental snow climate (cold, thin snowpack), the Lizard Range located in the South Rocky Mountains is known for having more of a transitional snow climate with milder temperatures, and a deeper snowpack (McClung and Schaerer 2006). Claus et al. (1984) refer to this climate as "Rocky Mountain Wet". Haegeli and McClung (2007) suggest that there may be a north-south division in snowpack characteristics within the Rocky Mountains. Avalanche hazard mapping professionals conducting work in this region have anecdotally indicated that the existing Rocky/Purcell Mountain statistical models tend to underestimate extreme avalanche runout when compared to field observations.

The primary objectives of this study are to develop α – β and runout ratio model parameters which can be used to assist with estimating extreme avalanche runout for tall avalanche paths (H > 350 m) in the Columbia Mountains and in the Fernie area. A secondary objective of this project is to explore the relationship between snowfall and extreme avalanche runout using snowfall data from a variety of sources and avalanche runout data collected for this study.

2.0 LITERATURE REVIEW

2.1 Introduction

This review focuses on the development and application of statistical runout models for extreme avalanche runout estimation. Section 2.2 provides a summary of key contributions in the development of statistical models. Section 2.3 discusses the theory of the α – β and runout ratio models independently and provides an introduction to the effects of scale, climate and geomorphology. Section 2.4 provides a brief background on dynamic models.

A cross section view through a typical avalanche path centerline along with the geometric terrain variables used by the statistical models is shown in Figure 2.1 below.

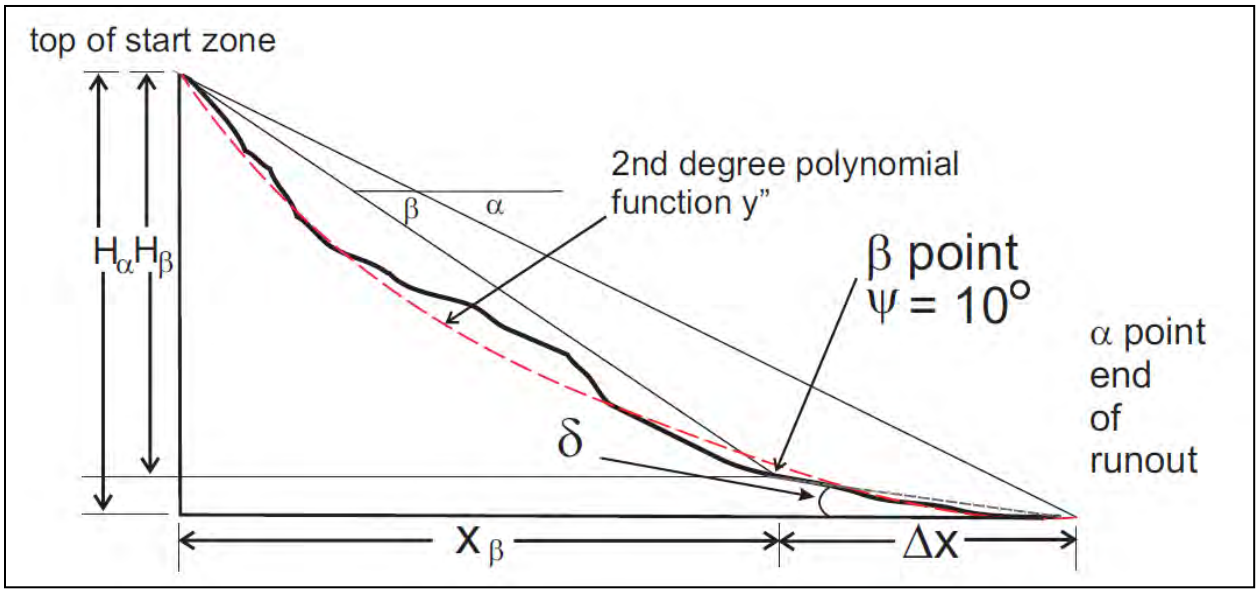

Figure 2.1: *Cross section through a typical avalanche path showing geometric terrain variables used for statistical model extreme runout estimation*

Geometric terrain variables used for statistical runout estimation include the topographic and terrain parameters shown in Figure 2.1. These parameters are further described in Section 4.2. Existing classes of statistical models primarily depend on the location of the β-point which is typically defined as the point where the slope incline first descends to 10° as defined by field-observed breaks in the slope. The corresponding β-angle is the angle between the top of the

start zone and the β-point as measured from the horizontal. The α-angle is defined as the angle between the top of the starting zone and the extreme runout position observed in the field. δ is defined as the average slope of the runout zone which is calculated by measuring the elevation difference and distance between the β and α-points. The runout ratio ($x = \Delta x/X_\beta$) is defined as the ratio of the distance between α and β (Δx) divided by X_β, which is the horizontal distance from the starting position to the β-point. y" refers to the second derivative of the polynomial function fitted to the avalanche path profile of the form:

$$y = ax^2 + bx + c \qquad \text{Equation 2.1}$$

The parabolic fit is used to extract terrain variables used for the multiple regression analysis presented in Section 4.3.

2.2 Key Developments in the Theory of Statistical Models

From 1976 to 1983, the work of Bovis and Mears (1976), Lied and Bakkehöi (1980) and Bakkehöi et al. (1983) introduced the prediction of extreme avalanche runout based solely on avalanche path terrain parameters. In 1976, Bovis and Mears examined a dataset of 67 avalanche paths from Colorado and speculated that extreme runout length may be predicted by the shape of the avalanche path. In 1980 and 1983, Lied and Bakkehöi and Bakkehöi et al. used a dataset of 111 Norwegian avalanche paths with long historical records of avalanche occurrences to develop a predictive model of avalanche runout based on terrain. They found that extreme runout distance could be related to four easily measured predictor variables: 1) starting zone angle; 2) β angle; 3) total vertical displacement (H_0); and 4) the second derivative of the polynomial function best fitted to the path profile (y"). Lied and Bakkehöi (1980) defined the β-point as the point where the slope angle first reaches 10° while descending the slope. This reference β-point has been used in similar form in all subsequent statistical modelling. Although not always defined at the 10° slope angle, later work by Bakkehöi et al. (1983) found that β was the only significant predictor variable, and that extreme avalanche runout was best represented by a model of the form:

$$\propto = C_0 + C_1\beta \qquad \text{Equation 2.2}$$

with α and β in degrees, and the constants C_0 and C_1 obtained by regressing α on β.

Subsequent work by Martinelli (1986), McClung et al. (1989) and Nixon and McClung (1993) confirmed the applicability of the α – β method to other mountain ranges. McClung et al. (1989) used data from four different mountain ranges to show that the terrain parameters differed between mountain ranges and that the constants C_0 and C_1 had to be derived independently from range to range. Using this dataset, they developed α – β parameters unique to the Colorado Rockies, the Canadian Rocky and Purcell Mountains the Sierra Nevada and western Norway.

In 1987, McClung and Lied presented an alternative method for predicting extreme avalanche runout using the same topographical parameters as the α – β model and applying the theory of extreme value statistics. McClung and Lied (1987) introduced the dimensionless runout ratio $x = \Delta x/X_\beta$ and found that it follows an extreme value distribution with respect to a reduced variate or non-exceedence probability:

$$\Delta x/X_\beta = u + b(-\ln(-\ln P)) \qquad \text{Equation 2.3}$$

In this equation, *u* and *b* are the location and scale parameters in a Gumbel (extreme value type 1 or log-Weibull) distribution which are determined by a regression analysis for a set of avalanche paths from the same mountain range. Δx and X_β are determined from individual avalanche path observations. The non-exceedence probability, *P*, is defined as the fraction of avalanche paths (between 0 and 1) in a particular mountain range that do not exceed a specific runout ratio. In 1991, McClung and Mears presented runout ratio parameters for tall paths (H > 350 m) in the Colorado Rockies, the Canadian Rockies and Purcells, the Sierra Nevadas and western Norway. Work by McKittrick and Brown (1993) defined runout ratio parameters for avalanche paths in southwest Montana, they found that moving the β-point upslope from 10° to 18° provided a better fit to the shorter running avalanche paths found in Montana. In 2004, Jones and Jamieson compiled a dataset of 48 Canada wide short slopes (H < 350 m) and found that moving the β-point upslope from 10° to 24° provided a much better fit.

The general method for developing a statistical runout model involves collecting detailed topographical data from a set of "typical" avalanche paths in a given mountain range each of which has a comprehensive record of extreme runout. The avalanche occurrence data may consist of historical written or verbal records, or observations of damage to vegetation. McClung and Mears (1991) found that random error introduced into avalanche occurrences estimated based on vegetative damage diminishes as the number of surveyed paths increases, and proposed that 30 avalanche paths were the minimum required to develop a statistical model.

A suitable avalanche path usually consists of a path with little to no cross valley or uphill runout, and without significant channelization in the avalanche runout zone. Paths with significant components of uphill runout may not be well suited to statistical models because the uphill component will tend to slow down large avalanches faster than paths without uphill runout resulting in shorter runout distances. Paths which are channelized in the track or runout zone will typically run further than paths without confinement. Avalanche paths with multiple β-points or benches can also be troublesome for developing statistical models, as are paths which do not reach a slope angle of 10° prior to the extreme runout position.

Since statistical models are based on estimating avalanche runout based on historical observations and on vegetative damage, they typically estimate runout position for the dense flow component of the avalanche which generally causes the majority of the damage. In cases where the powder component has been destructive enough to cause significant damage such as flagging or destroying timber, a component of the powder effects will be included.

2.3 Statistical Runout Models

2.3.1 Alpha-Beta Statistical Models

The α – β model was originally developed in Norway (Lied and Bakkehöi, 1980) using data from 192 avalanche paths with well defined extreme runout positions and long historical records of avalanche occurrences. Lied and Bakkehöi (1980) initially developed a linear regression of α on

β, H_0, θ (starting zone inclination), y" (curvature of path), and a confinement parameter. They later found that beta was the only significant predictor and since then, α – β models have been developed by others for other mountain ranges. Later work by McClung and Mears (1991), and Johannesson (1998) developed α – β models for the Canadian Rocky and Purcell Mountains, the Sierra Nevadas, Coastal Alaska, Colorado Rockies and for Iceland.

In Canada, α – β models have been developed for the combined Rocky and Purcell Mountains (McClung et al., 1989) and for the Coast Mountains (Nixon and McClung, 1993). A Columbia Mountains model has also been developed by Delparte et al. (2008); however the runouts predicted in this model are based on a 40 year observation period and may not represent extreme runout. As part of their work in 2008, Delparte et al. (2008) also explored the use of high and low resolution digital elevation models (DEMs) to provide the topographical parameters for predicting extreme avalanche runout. Delparte et al. (2008) did not find a significant difference between the results from high and low resolution DEMs. A summary of published α – β model parameters is included as Table 2.1 below.

Table 2.1: *Summary of previously developed α – β statistical model parameters for extreme avalanche runout estimation*

Area	C_0	C_1	R^2	SE	n	Reference
Rocky and Purcell Mountains	0.93	-	0.75	1.75	126	McClung and Mears, 1991
Sierra Nevada	0.67	2.50	0.60	-	90	McClung and Mears, 1991
Coastal Alaska	0.74	3.67	0.58	-	52	McClung and Mears, 1991
Colorado Rockies	0.63	4.68	0.50	-	130	McClung and Mears, 1991
Western Norway	0.93	-	0.93	2.1	192	McClung and Mears, 1991
Coast Mountains	0.90	-	0.74	1.70	31	Nixon and McClung, 1993
Iceland	0.85	-	0.72	2.2	44	Johannesson, 1998
Columbia Mountains (40 year observation period)	0.93	-	0.89	1.10	35	Delparte et al., 2008

A main limitation of the α – β statistical model is the sensitivity of the extreme runout position to the overall slope in the runout zone since the extreme runout position is calculated using the relationship:

$$\frac{\Delta x}{X_\beta} = \frac{tan\beta - tan\alpha}{tan\alpha - tan\delta}$$ Equation 2.4

Where Δx is the distance between the α and β-points and δ is the overall slope in the runout zone. Usually, the person conducting the analysis will extend the topographical path survey well past the β-point to get an overall approximation of the runout zone slope δ, and then use the above relationship to iterate between the calculated value of Δx and the model predicted α angle. This can be troublesome for paths where the overall avalanche trajectory below the β-point is not obvious.

2.3.2 Runout Ratio Statistical Model

The runout ratio model was first developed by McClung et al. (1989) by applying extreme value statistics to avalanche runout data. McClung et al. (1989) found that the runout ratio ($\Delta x/X_\beta$) for extreme events obeyed an extreme value type 1 (EV1 or Gumbel) distribution, and that the Gumbel parameters *u* and *b* could be used to estimate extreme runout for specific non-exceedence probabilities in a given path by the relationship:

$$x_p = u + b(-\ln(-\ln(P))$$ Equation 2.5

The non-exceedence probability, *P*, is defined as the fraction of avalanche paths (between 0 and 1) in a particular mountain range that do not exceed a specific runout ratio.

McClung and Mears (1991) found that the terrain dependent parameters u and b differ from one mountain range to another and later work by Nixon and McClung (1993) and Jones and Jamieson (2004) led to the development of runout ratio parameters for the Coast Mountains and for Canada-wide short slopes (H < 350 m). Table 2.2 summarizes existing runout ratio parameters for north American and Norwegian mountain ranges.

Table 2.2: *Summary of previously developed runout ratio statistical model parameters for extreme avalanche runout estimation*

Area	β (°)	u	b	SE	R^2	n	Reference
Rocky and Purcell Mountains	10	0.079	0.070	0.012	0.98	79	McClung and Mears, 1991
Sierra Nevada	10	0.374	0.206	0.041	0.98	90	McClung and Mears, 1991
Colorado Rockies	10	0.288	0.202	0.040	0.98	130	McClung and Mears, 1991
Western Norway	10	0.143	0.077	0.011	0.98	80	McClung and Mears, 1991
Coastal Alaska	10	0.185	0.108	0.023	0.97	52	McClung and Mears, 1991
Southwest Montana	18	0.0343	0.173	-	0.93	24	McKittrick and Brown, 1993
Canadian Coast Mountains	10	0.096	0.092	0.021	0.96	20	Nixon and McClung, 1993
Canadian Short Slopes	24	0.494	0.441	0.08	0.98	46	Jones and Jamieson, 2004

R^2 refers to the goodness of the fit for each mountain range, and SE is the standard error. For ranked data, only high R^2 values (R^2>0.95) are considered an acceptable fit to a Gumbel distribution, this criteria is met for all regions other than southwest Montana.

As part of the runout ratio analysis, McClung and Mears (1991) also suggested that "censoring" the data to exclude values below $P = e^{-1}$ effectively removes the shorter running avalanches from the dataset. This provides a better fit to the higher values of runout ratio and the longer running avalanches which builds additional conservatism into the models.

According to McClung and Mears (1991), a key advantage of the runout ratio method is that the estimation of Δx is not dependent on δ which is the slope in the runout zone, because the runout position past the β-point is determined independently. This means that the runout ratio method may be more useful for avalanche paths with some component of uphill runout or for paths where it may be difficult to measure or estimate the overall slope in the runout zone.

2.3.3 Scale Effects in Extreme Avalanche Runout Models

Early work on the runout ratio statistical model by McClung and Lied (1987) and McClung and Mears (1991) recognized that short avalanche slopes tended to run significantly further than tall avalanche paths. McClung and Lied (1987) used an example avalanche path from Colorado

with a vertical drop less than 400 m and an abrupt transition from the slope to the valley floor to show the proportionally longer runout distances from shorter slopes. They suggested that the difference in length between the center of mass of the deposit and the tip of the debris becomes more important for short slopes.

McClung and Mears (1991) suggested that some short avalanche slopes (ridge crests and cirque headwalls) favoured proportionally deeper snow accumulations in the starting zones which led to larger release volumes and longer running avalanches. To examine this further, McClung and Mears (1991) arbitrarily separated their dataset between paths over and under 1000 m vertical fall (H). They found a significant difference in runout between the two datasets with the shorter avalanche paths running proportionally further than the tall avalanche paths.

Similar work by Nixon and McClung (1993) partitioned datasets from the Rocky/Purcell Mountains at X_β = 1500 m and for the BC Coast Mountains at X_β = 1000 m and again found that the shorter avalanche paths ran proportionally further. McKittrick and Brown (1993) analyzed data from 24 avalanche paths in southwest Montana with a maximum vertical fall height of 553 m (mean = 248 m) and found that moving the β-point upslope from 10° to 18° provided a better fit to a Gumbel distribution. One reason for moving the β-point is that shorter avalanche slopes do not always runout to a 10° position on the slope. This study was the first analysis of primarily “short” avalanche slopes, and no length-scale effects were apparent in McKittrick and Brown’s (1993) dataset.

Jones and Jamieson (2004) analyzed and developed statistical model parameters for a set of 48 short avalanche slopes in Canada. The avalanche paths analyzed in this dataset were from various mountain ranges across Canada and had vertical fall heights (H) less than 350 m. Jones and Jamieson (2004) redefined the β-point as the position in the path where the slope angle first reached 24° rather than 10°. In his MSc thesis, Jones (2001) suggested that particles of snow in a flowing avalanche start to lock at slope angles of about 25° and that large avalanches will begin to decelerate at this slope angle which may be a physical justification for moving the β-point location. Using the same dataset of 48 short slopes, Jones (2001) also found that scale

effects were more pronounced for the runout ratio model than for the α – β model. This same finding was also previously recognized by McClung and Lied (1987).

Jones and Jamieson (2004) also included a "terrain parameter" to describe the overall shape of the avalanche slope as linear, concave or hockey stick shaped as shown in Figure 2.2.

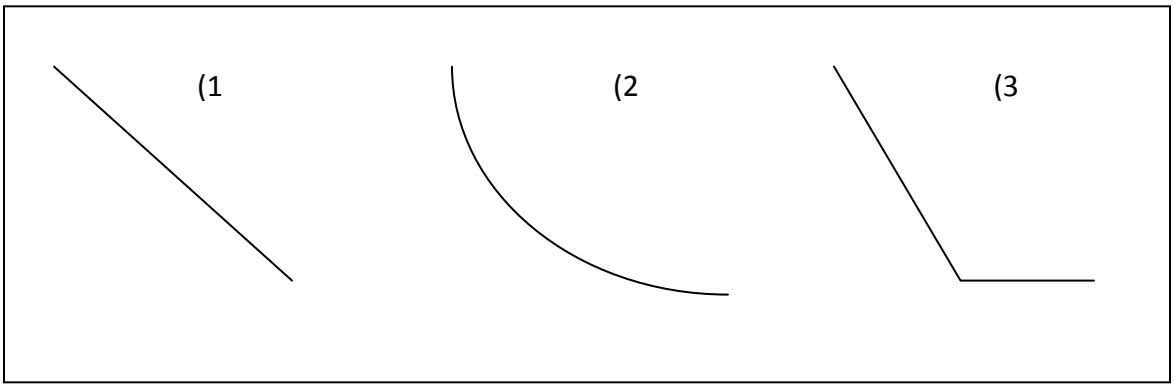

Figure 2.2: *Examples of terrain parameter types 1) Linear, 2) Concave, and 3) Hockey Stick for typical avalanche path profiles (after Jones and Jamieson 2004)*

Jones and Jamieson (2004) found that the hockey stick shaped paths tended to run further than the linear or concave paths. The physical explanation provided for this is the abrupt transition from granular to fluid flow characteristics which may occur when the avalanche hits the abrupt slope transition.

2.3.4 Climate and Geomorphology Effects on Extreme Avalanche Runout Estimation

The α – β and runout ratio models are defined on a mountain range basis depending primarily on topographic terrain parameters, and excluding climate variables such as snowpack height or snowfall. The boundaries of these mountain ranges are usually based on physical geographic boundaries such as rivers, and to a lesser extent on geology and climate.

McClung et al. (1989) examined extreme avalanche runout data from four mountain ranges: the Canadian Rockies and Purcells, western Norway, the Colorado Rockies, and the Sierra Nevadas. This work defined extreme avalanche runout as the avalanche with a return period of approximately 100 years. Their experience suggested that in the majority of cases, the 100 year avalanche was caused by a large dry avalanche, and that the climatic conditions required for

this event would occur in each of the four mountain ranges over a 100 year period. They also found that the longest running avalanches occurred in the Colorado Rockies and the Sierra Nevadas which are characterized by a continental (Colorado) and a maritime (Sierra) snow climate. Conversely, the shorter running avalanches occurred in western Norway and the Canadian Rockies and Purcells which are characterized by a maritime (Norway) and continental (Canada) snow climate. This suggests that the differences in avalanche runout distances cannot be explained by regional snow-climate classifications.

Smith and McClung (1997) used 24 years of avalanche occurrence and climate data from Rogers Pass to develop a regression model relating avalanche frequency to terrain and climate variables. They found that the start-zone elevation, terrain roughness, and 30 year maximum water equivalent were the significant predictor variables, and that 30 year maximum water equivalent and terrain roughness were the strongest predictors. Since terrain roughness and 30 year maximum water equivalent are both linked to snow supply, Smith and McClung (1997) suggested that avalanche frequency is strongly related to climate. The key challenge with this model is that it is often difficult to measure or estimate the 30 year maximum water equivalent for a given avalanche path.

In 2008 Schweizer at al. examined the relationship between snowfall and runout using 58 years of avalanche occurrence and snowfall data from the Salezertobel avalanche path near Davos, Switzerland. Schweizer at al. (2008), defined $HN3d_{crit}$, which is the critical new snow accumulation over a period of 3 days, required for long running avalanches. Using 58 years of avalanche occurrence and snowfall observations from high and low elevation study plots near the Salezertobel path, they found that the $HN3d_{crit}$ had a return period of about 2 years, while the long running avalanche return period was on the order of 5 years. They also found that the snowfall data from the high elevation weather plot correlated better with the long running avalanches, but also caused more false alarms (days when the $HN3d_{crit}$ was reached, but long running avalanches did not occur) than the snowfall data from the valley bottom station. Examination of the weather and snowpack data leading up to the long running avalanches showed that in addition to $HN3d_{crit}$, other important variables included the snow depth above

the terrain roughness, the presence of a weak basal layer in the snowpack at the track and runout zone elevation, and increasing air temperatures.

2.4 Dynamic Runout Models

Prior to the development of the first statistical models in 1980, quantitative avalanche runout was typically estimated using dynamic avalanche models. Traditional dynamic models use the avalanche path topographic profile in addition to a friction parameter to estimate avalanche velocity and stopping point along the path. Along with knowledge of typical avalanche flow densities and heights, the modeller can use these results to estimate potential impact pressures at different points along the path.

Current avalanche dynamic models are based on the principles of granular, fluid or visco-elastic flow. All of these models require the user to input a value for the sliding friction at the base of the snow, most include at least one other coefficient such as a turbulence factor. This friction coefficient or overall resistance likely also includes components of other resistive forces such as ploughing, air drag, viscous shear and entrainment/ deposition of snow. Friction coefficients must also be determined on a model-by-model basis and cannot be used interchangeably. Useful application of these models requires user familiarity with applying friction coefficients in a given area.

More recent avalanche dynamic models such as AVAL-1D (Margreth and Gruber, 1998) also incorporate snow release volumes which are entered by the modeller as a starting zone snow depth. AVAL-1D models the dense and powder components of the flow separately and can estimate flow height, velocity and impact pressure at any point along the avalanche path. This model is widely used in Europe and is gaining popularity in North America.

Depending on the region where the work is being conducted and on the scale and scope of the project, hazard mappers will typically use a combination of statistical and dynamic avalanche models for estimating extreme runout. The level of confidence placed on the various model

estimates will depend on the analyst's experience with specific models in the region and on expert judgement.

2.5 Summary

When estimating extreme avalanche runout for a specific avalanche path, hazard mappers will typically apply both the α – β and runout ratio statistical models as well as dynamic runout models suited to the project and location. The estimates from these models will be compared to historical and field observations of avalanche runout, with greater confidence usually being placed on field observations.

Previous work by McClung at al. (1989) has shown that the runout ratio model is less sensitive than the α – β model to the slope of the runout zone and that the runout ratio model can be applied to paths with some component of uphill runout. Work by McClung and Lied (1987) used examples of avalanche runout from Switzerland and Colorado to show that the runout ratio method may be more suited to paths with particularly long runout which may be of interest for land use planning applications.

In western Canada, statistical model parameters (α – β and runout ratio) have been developed for the Rocky and Purcell Mountains and for the Coastal Mountains. Despite active residential, industrial and commercial development, extreme runout parameters have not yet been published for the Columbia Mountains. Unlike the central and northern Rocky Mountains which are characterized by a continental snow climate (cold, thin snowpack), the Lizard Range area around Fernie, BC is known for having more of a transitional snow climate with milder temperatures, and a deeper snowpack (McClung and Schaerer 2006). Avalanche hazard mapping professionals conducting work in this region have anecdotally indicated that the existing Rocky/Purcell Mountain statistical models tend to underestimate extreme avalanche runout when compared to field observations (Johnston and Jamieson, 2010).

The primary objectives of this study are to develop α – β and runout ratio model parameters which can be used to assist with estimating extreme avalanche runout for tall avalanche paths (H > 350 m) in the Columbia Mountains and in the Lizard Range. Chapter 3 describes the study

areas and data collection methods used for this study. Chapter 4 presents a statistical analysis and the derivation of $\alpha - \beta$ and runout ratio parameters for these regions.

3.0 STUDY AREA AND METHODS

3.1 Study Areas

The study areas for this project include the Lizard Range area around Fernie and the Columbia Mountains of British Columbia.

3.1.1 Fernie Area

Fernie is located in the south eastern corner of British Columbia, adjacent to the Lizard Range of the Canadian Rocky Mountains (Figure 3.1).

Figure 3.1: *Location of Fernie, British Columbia and the Canadian Rocky Mountains (Base map layers from NR Canada – GeoGratis, 2010)*

Unlike the central and northern Rocky Mountains which are characterized by a continental snow climate (cold, thin, snowpack), the Fernie area has more of a transitional snow climate (McClung and Schaerer, 2006) with milder temperatures and a deeper snowpack. Claus et al. (1984) refer to this climate as "Rocky Mountain wet". Haegeli and McClung (2007) suggest that there may be a north-south division in snowpack characteristics within the Rocky Mountains. Unlike the majority of the Rocky Mountains which have the biogeoclimatic classification of *Montane Spruce*, the valley bottoms in the Fernie are classified as *Interior Cedar* and *Hemlock* (BC MOF, 2008). Local knowledge suggests that this heavy snowfall area is limited to the Lizard Range and the area immediately surrounding the City of Fernie. For example, the community of Sparwood is located about 30 km north of Fernie and has a more typical Rocky Mountain winter climate characterized by a thinner snowpack and colder temperatures.

Development in the mountainous terrain of the Fernie area includes residential lots and subdivisions, mechanized backcountry ski operations, a ski hill (Fernie Alpine Resort), and coalbed methane resource exploration. Many of these developments have had some degree of avalanche hazard mapping conducted. Avalanche hazard mapping professionals working in this region have anecdotally indicated that the existing Rocky and Purcell Mountain statistical models tend to underestimate extreme avalanche runout when compared to field observations in this area (Jones, A. pers. comm., 2008). Work by Johnston and Jamieson (2010) used a dataset of 28 avalanche paths from this area to show that the Rocky/ Purcell and Coast Mountain models consistently underestimate extreme avalanche runout for Fernie avalanche paths.

3.1.2 Columbia Mountains

The Columbia Mountains are located in south central British Columbia and encompass an area of approximately 135,000 km^2 which includes the Monashee, Cariboo, Selkirk and Purcell sub-ranges (Figure 3.2). Work by Schaerer (1977), showed that in the Rogers Pass area of the Selkirk Mountains, precipitation decreases by 20% from west to east across the mountain range. The biogeoclimatic mapping for the Columbia Mountains shows that at the valley bottom the climate is mostly within the *Interior Cedar Hemlock* zone, except for the drier east slopes of the Purcells which are characterized as *Montane Spruce* or *Interior Douglas Fir*.

Elevation in the Columbia Mountains ranges from about 500 m-asl in the valley bottoms up to 3519 m-asl at the highest peak (Mt. Sir Sandford). Within the Columbia Mountains there are also several icefields and many glaciers. There is a wide variety of land use and land development in the Columbia Mountains impacted by snow avalanches including (but not limited too):

Figure 3.2: *Location of Columbia Mountains (Base map layers from NR Canada – GeoGratis, 2010)*

- Mineral exploration and development;
- Mechanized (helicopter and cat-skiing) backcountry ski operations;
- Ski hill operations and associated residential land development;
- Micro and small-hydro power; and
- Infrastructure (roads etc.) associated with the above.

Other than the existing Canadian short slope model of Jones and Jamieson (2004), there are no published statistical model parameters for estimating extreme (30 – 100 year return period) avalanche runout in the Selkirk, Cariboo and Monashee mountains. Likely because of climatic effects, McClung et al. (1989) combined the Purcell Mountain sub range with the Rocky Mountains when developing statistical model parameters for Canada. Avalanche hazard mapping professionals working in this region have been using both the Coastal and Rocky/ Purcell mountain models when a statistical estimate of avalanche runout is desired.

3.2 Avalanche Path and Precipitation Data

Avalanche path survey data for this project was obtained from fieldwork conducted in the summer of 2010 and from the outside sources listed below:

- Chris Stethem and Associates (CSA) provided 26 avalanche path surveys from a variety hazard mapping projects undertaken in British Columbia;

- Fernie Alpine Resort (FAR) provided avalanche path survey data collected by hazard mapping professionals for six tall avalanche paths in the Lizard Range;
- Imperial Metals (IM) provided avalanche path surveys for six tall avalanche paths in the Ruddock Creek area of the Monashee Mountains; and,
- The Canadian Avalanche Association (CAA) provided six path surveys collected as part of professional avalanche hazard mapping courses taught in BC.

The criteria for avalanche paths used in this study included tall paths *(H* > 350 m) with little to no uphill (i.e. cross valley) runout (maximum 5% of path height) and paths which were not confined or channelized in the track or runout zone. These types of paths are typically better represented by statistical runout models. The surveyed paths were also chosen based on ease of access (road or trail access) and because they had a mature vegetation record of avalanche impacts in the runout zone (minimal logging, fire, or human impact in the runout zone). To the extent possible, an attempt was made to choose paths from a variety of aspects and elevations, although reasonable access by foot and vehicle was often the limiting factor.

3.2.1 Avalanche Path Data for the South Rocky Mountains

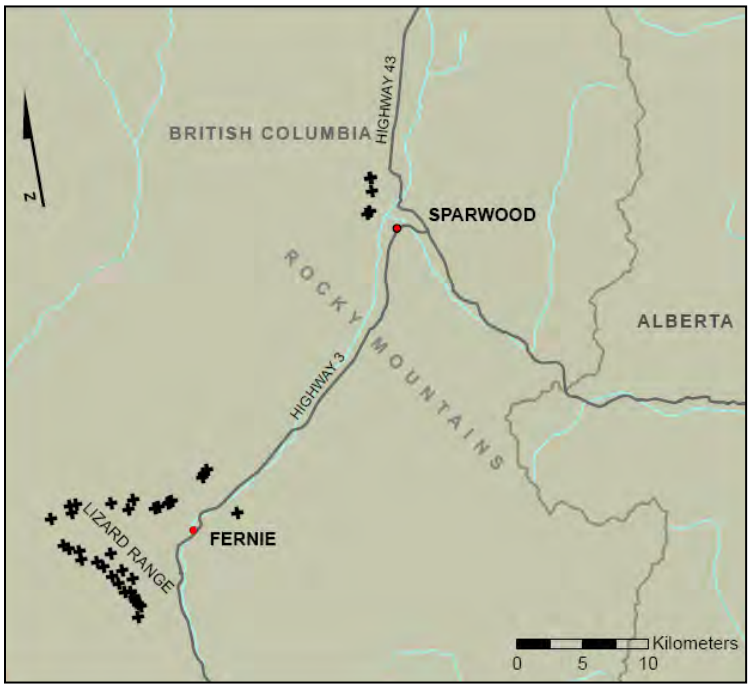

Figure 3.3: *Surveyed avalanche path locations within the Fernie and Sparwood area (Base map layers from NR Canada – GeoGratis, 2010)*

Figure 3.3 shows Fernie, Sparwood and the surrounding South Rocky Mountains including the locations of avalanche path survey sites used for this study. Specific site details are summarized in Table 3.1. ASARC refers to data collected specifically for this study by Katherine Johnston and field assistants from the University of Calgary.

Table 3.1: *Avalanche path survey data sources and locations for the Fernie area*

Sub-Range/ Area	Location	Data Collected By	Study Site
Lizard Range	Mt. Fernie	ASARC	Mt. Fernie 1
		ASARC	Mt. Fernie 2
		ASARC	Mt. Fernie 3
		ASARC	Mt. Fernie 4
		ASARC	Mt. Fernie 5
		CSA	Alpine Trails Path 3
		CSA	Alpine Trails Path 2
	Mt. Proctor	CSA	Central Path
		CSA	North Gully
		CSA	Northeast Bowl
		CSA	Split Path
	Island Lake	CSA	Cedar Bowl – West
		CSA	Cedar Bowl – East
		CSA	Hilda/Pearl
		CSA	Orca
		CSA	Hunters
		CSA	Geisha
		CSA	Baldy FS West
		CSA	Baldy FS West Low SZ
		CSA	Central Baldy FS East
		CSA	Hot Tub Chute
		CSA	Big Steep Mother
		CSA	Fish Bowl
		CSA	Liverwurst Main
		CSA	Liverwurst East
		ASARC	Thirstquencher
		ASARC	Cabin Bowl
		ASARC	Wolverine Bowl
	Fernie Alpine Resort	FAR	Arrow
		FAR	Bow
		FAR	Cascade
		FAR	Dancer
		FAR	Big Hummer
		FAR	Cedar Bowl
Sparwood	Whiskey Jack Development	CSA	Central Path
		CSA	South Path
		CSA	North Path
	DL8523	CSA	South Path
		CSA	North Path, Finger A

UTM NAD83 Zone 11 coordinates for avalanche paths in the Fernie area vary from 629087 to 643100 Easting and 5479628 to 5490620 Northing. Starting zone elevations range from 1500 m

to 2300 m-asl, and the starting zone aspects are mostly northeast and southeast due to the overall orientation of the mountains in this area.

This summary also includes five paths from the Sparwood area, although these paths were not used for statistical model development, they are used for the snowfall and runout analysis and comparison presented in Section 4.4, and are included here for completeness. The UTM NAD83 Zone 11 coordinates for the Sparwood area paths range from 649691 to 650034 Easting and from 5511677 to 5514389 Northing. Starting zone elevations range from 1725 to 1825 m-asl, and the aspects are primarily east.

3.2.2 Avalanche Path Data for the Columbia Mountains

Figure 3.4 shows the location of avalanche path surveys in the Columbia Mountains which were used for this project.

Figure 3.4: *Extent of Columbia Mountains with surveyed avalanche path locations (Base map layers from NR Canada – GeoGratis, 2010)*

A summary of specific site details is included as Table 3.2:

Table 3.2: *Avalanche path survey data sources and locations for the Columbia Mountains*

Sub-Range	Location	Data Collected By	Study Site
Monashee Mountains	MacPherson	ASARC	The Womb
		ASARC	Fingers
		ASARC	MacPherson 3
	Ruddock Creek	IM	Oliver E 6.3 – 6.5
		IM	Oliver Ck 11.1 – 11.4
		IM	Oliver CW 12.7 – 14.0
		IM	Zone 2: 13
		IM	Oliver W 16.2 – 16.8
		IM	Oliver W 20
	Eagle Pass	CAA	Eagle Pass
	Gorge Forest Service Road	ASARC	Gorge km 20 Path 5
		ASARC	Gorge km 20 Path 4
		ASARC	Gorge km 20 Path 3
Selkirk Mountains	Whitewater Road	CAA	9.5 Whitewater Road
		CAA	9.0 Whitewater Road
	Nelson	CAA	Grohman Creek
	Kootenay Pass	CAA	Wolf Peak
	Retallack	CAA	Reco Peak
	Bulmer Creek	CSA	Bulmer Creek
	Mt. Cartier	ASARC	Greenslide Creek
	Enterprise Creek	ASARC	Enterprise 2
		ASARC	Enterprise 3
	Kokanee Glacier Park	ASARC	Kokanee Trail
		ASARC	Kokanee Road Path 4
		ASARC	Kokanee Road Path 3
		ASARC	Kokanee Road Path 2
		ASARC	Kokanee Road Path 1
Cariboo Mountains	Mica Mountain	ASARC	Mica Mountain 1
		ASARC	Mica Mountain 2
	Westridge Forest Service Road	ASARC	Westridge FSR Path 1
		ASARC	Westridge FSR Path 2
		ASARC	Westridge FSR Path 3
		ASARC	Westridge RSR km 20

UTM NAD83 Zone 11 coordinates for avalanche paths in the Columbia Mountains vary from 330197 to 510360 Easting and 5438240 to 5864910 Northing. Starting zone elevations range from 1420 m to 2640 m-asl, and cover a wide range of aspects.

3.2.3 Precipitation Data

Precipitation data for the avalanche paths were acquired from several sources including the Precipitation – Elevation Regressions on Independent Slopes Model (PRISM), BC Ministry of Environment Snow Course stations and Environment Canada valley bottom weather stations. The PRISM model was developed by researchers at Oregon State University (Daly et al., 1993). The PRISM model includes estimations of average monthly and annual precipitation at the scale of a 2 km pixel Digital Elevation Model (DEM) accounting for orographic effects and distance from the ocean. For western Canada, PRISM uses known data points from Environment Canada weather stations, snow course survey sites, and highways weather stations to estimate precipitation by the following:

- Estimating the orographic elevation of each precipitation station using the DEM;
- Assigning each DEM grid cell a topographic "facet" based on the grid cell aspect;
- Using a windowing technique to develop a precipitation – DEM elevation regression function from nearby rainfall stations on the cell's facet; and
- Predicting the precipitation at the cell's elevation with this regression function.

The dataset used for this project includes average monthly and annual precipitation for British Columbia from 1971 – 2000. To turn monthly precipitation data into average annual snowfall, the raster datasets for the months of November to April were added together using the "raster calculator" tool in ArcGIS to obtain the average winter snowfall in mm equivalent of water. Figure 3.5 shows the analyzed PRISM data along with avalanche path locations.

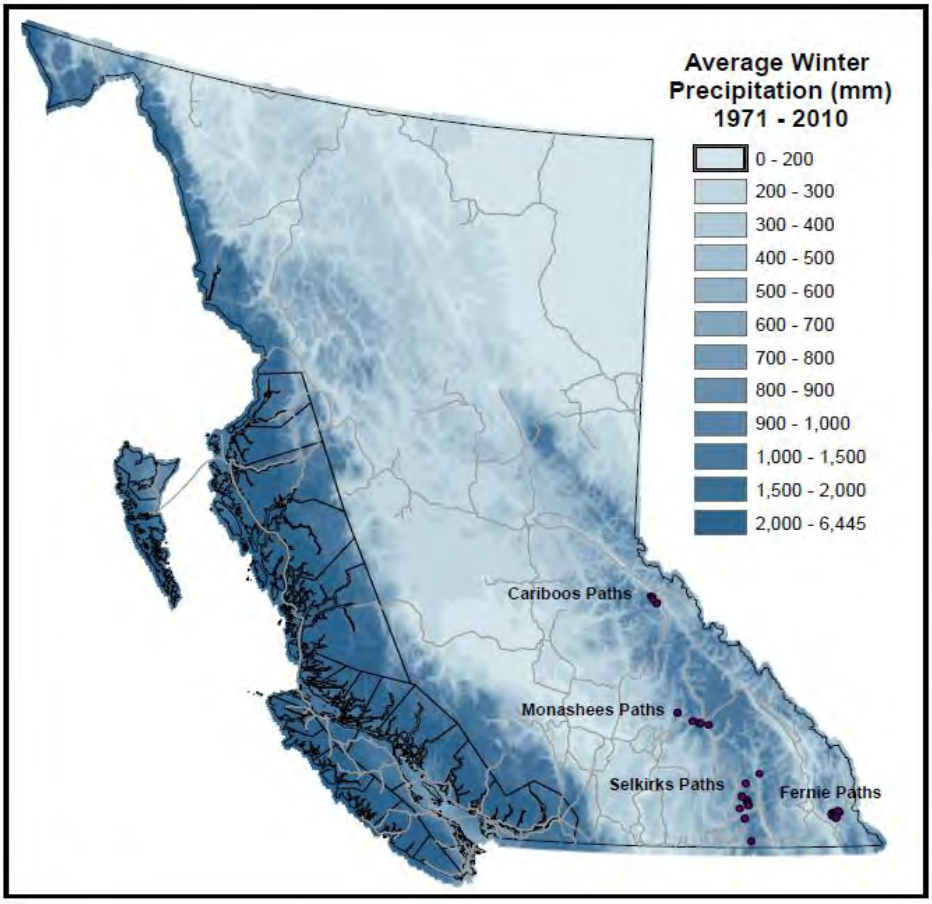

Figure 3.5: Map of British Columbia showing PRISM winter precipitation and surveyed avalanche path locations in the Columbia Mountains and Fernie area *(Base map layers from NR Canada – GeoGratis, 2010)*

Snow course stations in British Columbia are installed and maintained by the BC Ministry of Environment (MOE) River Forecast Centre for the purpose of forecasting stream and lake runoff conditions around the province. The snow course stations are located at a variety of elevations and have variable record lengths up to about 80 years. Snowpack water equivalent (SWE) data for the closest site to each avalanche path starting zone was acquired from the BC MOE website.

Environment Canada weather stations are usually located in and around cities and airports and have variable record lengths up to around 100 years. Snow depth data for the closest station with the most complete record for each avalanche path was obtained from the Canadian Daily Climate Data (CDCD) database (Environment Canada, 2007) which includes records up to 2007.

3.3 Field Methods and Equipment

Based on the criteria described in Section 3.2, avalanche paths were initially identified using digital imagery from Google Earth (Version 5.1, 2010). Topographic maps (1:20,000) obtained from the Terrain Resource Inventory (BC Government, 2010) with 20 m contour intervals were used to estimate the initial boundaries of the avalanche paths. Using the topographic maps; slope angles and slope segment lengths were measured from the top of the starting zone to a position located downslope of the expected extreme runout position. To assist with the extreme runout estimate, historical aerial photographs were obtained and examined for the avalanche paths of interest. Specific observations obtained through the aerial photographs included the following:

- Historical evidence of long running avalanches such as damage to vegetation;
- Type and distribution of vegetation in the runout zones; and
- Evidence of fire, logging, or other human impact in the avalanche path runout zones.

Prior to the field survey, the approximate location of the β-point was identified from the topographic maps to help facilitate the starting point of the detailed field survey.

The field surveys were conducted during July and August, 2010. During the surveys, slope angles and slope segment lengths were measured starting from a point located above the β-point to a location approximately 50+ m beyond the extreme runout position (α-point). Extending the topographic survey past the α-point allows for a better parabolic fit to the avalanche path profile.

A SUUNTO clinometer was used to measure the slope segment angles to an accuracy of ± 0.5° and a Bushnell Yardage Pro laser rangefinder (accuracy ± 1 m) or hip chain (accuracy ± 0.2%) were used to measure the slope distances. A Garmin 60CSX GPS was used to collect waypoints with a horizontal accuracy ranging from ± 3 to ± 15 m (average ± 7 m) and a SUUNTO Vector wristwatch altimeter was used to collect elevation at the waypoints with an accuracy of ± 5 m. Laser rangefinder and hip chain data were used as the primary measurement of slope segment length – when these were not available, GPS waypoints were substituted.

The β-point was identified in the field as the point where the slope incline first decreased to 10° as measured with the clinometer. For paths with multiple β-points or bench-like features in the lower track and runout zone, the lower elevation β-point was used.

The α-point was identified in the field by observing patterns of vegetative growth and damage in the runout zone. To the extent possible, this vegetative damage is assumed to represent damage from the dense flow component of the avalanche, but where it was difficult to differentiate between the damage from the dense flow and from the powder component, the later likely influenced identification of the α-point by favouring a longer runout or smaller α angle.

The intent of the runout survey was to identify the runout position of the 100 year avalanche event; however, the average return period associated with a runout position identified from observations of vegetative damage is likely on the order of 50 – 300 years (McClung and Mears, 1991), introducing unavoidable random error into the analysis.

3.3.1 Survey Procedures

The avalanche sites were all accessed by foot and vehicle. The surveys were all completed by a team of two people. The avalanche path survey involved collecting slope incline angles and vegetation observations from a position in the mid-track of the avalanche path all the way to the bottom of the runout zone. Starting at a mid-track location above the β – point, the first person would walk downhill to either a break in slope or a good sighting position and would measure the slope segment angle using a clinometer aimed at the approximate eye level of the uphill surveyor. The uphill or second person would record the elevation of the survey point, and would measure the slope segment distance between the two people using either a hip chain, a laser rangefinder, or GPS. Typical slope segments ranged from about 20 m to 100 m; however, slope segments as short as 7 m were used where obstacles such as thick vegetation prevented a clear line of sight between the two surveyors. Laser rangefinder and altimeter readings were used as the primary source of information, and where thick vegetation or other obstacles obscured the laser rangefinder, hip chain or GPS data were used to calculate slope segment lengths.

The α and β angles were measured in the field using the clinometer where possible, and calculated from the topographic slope profile where vegetation, terrain and/or weather prevented taking a field measurement. An example of the field notes collected during the avalanche path surveys in included as Appendix A.

3.3.2 Field Indicators of Avalanche Size and Frequency

Snow avalanches have the ability to damage or impact forests and vegetation within the runout zones. These impacts are usually best observed during the summertime when the ground is free of snow and when vegetation is not obscured by the seasonal snowpack or by avalanche debris. Large avalanche paths are generally identified as vertical swaths in the mountainside marked by uniform vegetative changes referred to as trimlines. The types and appearance of vegetation and trimlines in avalanche paths can be used to estimate the frequency, intensity and history of avalanches within the path. The dense and powder components of avalanche flow have different impacts on vegetation which can be used to construct the avalanche history of a given path.

Figure 3.6: *Photograph of an avalanche path in Fernie, BC showing "flagging" and downhill bending of 15 year old timber*

In areas where avalanches will runout on a yearly basis, large trees will not have time to establish themselves, and the vegetation will be characterized by "disaster" species which include grasses, shrubs, and flexible trees up to about 2 m high (Mears, 1992). Lower in the runout zone, where avalanches only reach every 5 – 10 years there may be small trees which are bent over entirely in the downhill direction or which have deformed trunks within a few meters of the ground. Damage to small trees in this zone can indicate repeated

impact from the dense flowing portion of the avalanche, an example of this is shown in Figure 3.6.

These deformed trees may also have new growth or leaders re-establishing themselves in a vertical position. Other examples of avalanche damage to vegetation include the absence of tree branches or "flagging" up to several meters off the ground on the uphill side (Figure 3.6).

Figure 3.7: *Photograph of an avalanche path near Nelson, BC showing avalanche damage to a stand of mature timber*

Large and extreme avalanche events can be powerful enough to completely destroy or remove large trees over 100 years old, and either push them completely over, or in some cases carry them with the avalanche debris to the end of the runout zone (Figure 3.7).

According to McClung and Schaerer (2006), avalanche frequency and return period can be related to vegetative damage using the clues summarized in Table 3.3.

Table 3.3: *Examples of vegetation as an indicator of avalanche frequency (after McClung and Schaerer, 2006)*

Frequency – At Least One Large Avalanche in an Interval of:	Vegetation Clues
1 – 2 Years	Alder and willow, bare patches, and shrubs; no trees higher than about 1 to 2 m
3 – 10 Years	No large trees and no dead wood from large trees; presence of trees higher than 1 to 2 m
10 – 30 Years	Dense growth of small trees; young trees of climax species (e.g. conifers); increment core data useful
25 – 100 Years	Mature trees of pioneer species (e.g. non-coniferous); young trees of climax species; increment core data useful
More than 100 Years	Mature trees of climax species. Increment core data useful

Figure 3.8: *Photograph showing an example of tree ring growth with evidence of avalanche impacts*

In addition to vegetative clues, hazard mapping professionals can date trees and inspect the growth rings to understand the history of avalanches in a particular path. Small trees can be cut through the trunk to allow for observation of growth rings. Changes in the appearance and shape of the tree growth rings on the uphill side can indicate avalanche damage as shown in Figure 3.8.

For larger trees, an increment borer can be used to obtain a core sample of tree growth rings. The core sample can be inspected to evaluate the age of the tree and also potential avalanche damage by changes in tree growth rings (Figure 3.9).

Figure 3.9: *Photograph showing a tree core obtained using an increment borer*

As with any natural science, there is a wide range of variability in field observations, and field indicators are often observed in combination with each other. The most reliable field information is obtained when similar patterns of vegetative damage are observed. An example of this would be observing multiple trees of the same age with the same type of damage in the runout zone.

3.4 Avalanche Path Characteristics

In addition to the topographical survey, other avalanche characteristics including starting zone aspect and angle, surface roughness and wind index were also observed and recorded during the field survey. Specific starting zone characteristics included the average angle in the middle of the starting zone, the average starting zone aspect, and the width of the upper portion of the starting zone. After Schaerer (1977), a qualitative *wind index (WI)* from 1 – 5 was assigned to each avalanche path starting zone in accordance with the criteria shown in Table 3.4.

Table 3.4: *Qualitative wind index for snow supply in an avalanche path starting zone (after Schaerer, 1977)*

W = 1	starting zone completely sheltered from wind by surrounding dense forest
W = 2	starting zone sheltered by an open forest or facing the direction of the prevailing wind
W = 3	starting zone an open slope with rolls or other irregularities where local drifts can form
W = 4	starting zone on the lee side of a sharp ridge
W = 5	starting zone on the less side of a wide, rounded ridge or open area where large amounts of snow can be moved by wind

A *surface roughness* factor "*SR*" was assigned to each avalanche path in accordance with the classification scheme developed by Schaerer (1971) to describe the surface roughness in the avalanche path starting zones. The classification scheme is shown in Table 3.5, which describes the height of snow required in the start zones to overcome ground roughness.

Table 3.5: *Snow retained on ground SR (m) due to terrain features such as the roughness of the ground (after Schaerer, 1971)*

Character of Terrain	Depth, SR (m)
Open slope with smooth bare rock, screen or grass	0.15
Gullies with small boulders	0.20
Gullies with large boulders, rough sides	0.25
Open slope with boulders	0.25
Open slopes covered with scrub and small trees	0.30

After Jones and Jamieson (2004), a qualitative *terrain parameter (TP)* from 1 – 3, was assigned to each topographical path profile to describe the path profile as "linear", "concave" or "hockey-stick" shaped as described in Section 2.3.3.

The average winter precipitation for the centre of the starting zone was extracted from the PRISM dataset by first summing the average monthly precipitation for November, December, January, February, March and April and then extracting the pixel value for the centre of the start zone coordinates for each path.

3.5 Sources of Uncertainty

The intent of the runout survey was to identify the runout location of the 100 year event; however, the true runout event identified is likely on the order of 50 – 300 years (McClung et al., 1991), introducing random error into the analysis.

The method used to estimate start zone winter precipitation is based on a modelled dataset which extrapolates between measured weather stations that are usually located in valley bottoms near populated centers. Most of the avalanche paths surveyed for this study were located a considerable distance away from populated centers introducing uncertainty into the PRISM snowfall estimates. Although the PRISM model accounts for orographic effects and distance from the ocean, there will inherently be less certainty in data from areas with fewer weather stations. In addition to the uncertainty with the monthly PRISM precipitation estimates, we assumed that at the elevation of the avalanche path start zones, precipitation during the months of November, December, January, February, March and April is snow. This assumption may not be valid for every avalanche path or for every season. For example, in the

area around Fernie, BC, it is not unusual to have rainstorms at mountain top during any month of the winter. Similarly, for most BC mountain ranges, it would be normal to have rain fall at mountain top elevations during the months of November and April.

Additional errors and uncertainty are associated with the measurement devices and also with human error during field data collection.

4.0 ANALYSIS AND RESULTS

4.1 Introduction

α – β and runout ratio statistical models predict extreme avalanche runout based on terrain parameters which are usually defined on a regional (mountain range) basis. Previous studies of tall avalanche paths have shown that extreme runout within a mountain range can be related to topographical terrain parameters, particularly the β-point which is usually defined as the point where the slope incline first reaches 10°. In this chapter, multiple regression methods are used to explore the relationship between α and other avalanche path terrain variables. In addition, α – β and runout ratio parameters are derived for tall avalanche paths in the Columbia Mountains and in the Lizard range area near Fernie BC. The relationship between extreme runout and snowfall is explored using the PRISM dataset for average annual and monthly precipitation (Daly et al., 1993), and also using snow course and Environment Canada weather stations from these areas.

4.2 Data

The data used for the statistical analysis include avalanche path characteristics obtained from the various sources described in Chapter 3. The dataset used for the snowfall analysis includes the precipitation data obtained from the PRISM dataset, snowpack water equivalent data obtained from the BC Ministry of the Environment (MOE) snow courses, and snow height data obtained from Environment Canada (EC) weather stations. For the PRISM precipitation data, it is assumed that at the starting zone elevation, precipitation falling during the months of November, December, January, February, March and April falls as snow.

4.2.1 Description of Variables

Table 4.1 summarizes the data collected or evaluated for each avalanche path. Out of the 23 variables, 21 are classified as interval or ratio, and 2 are classified as ordinal. The variables are named in convention with previous studies on extreme avalanche runout (Lied and Bakkehöi, 1980; McClung et al., 1989; Jones and Jamieson, 2004). The key terrain variables were described previously in Section 1.9 and 2.1; additional variables are shown in Figure 4.1 and described in Table 4.1.

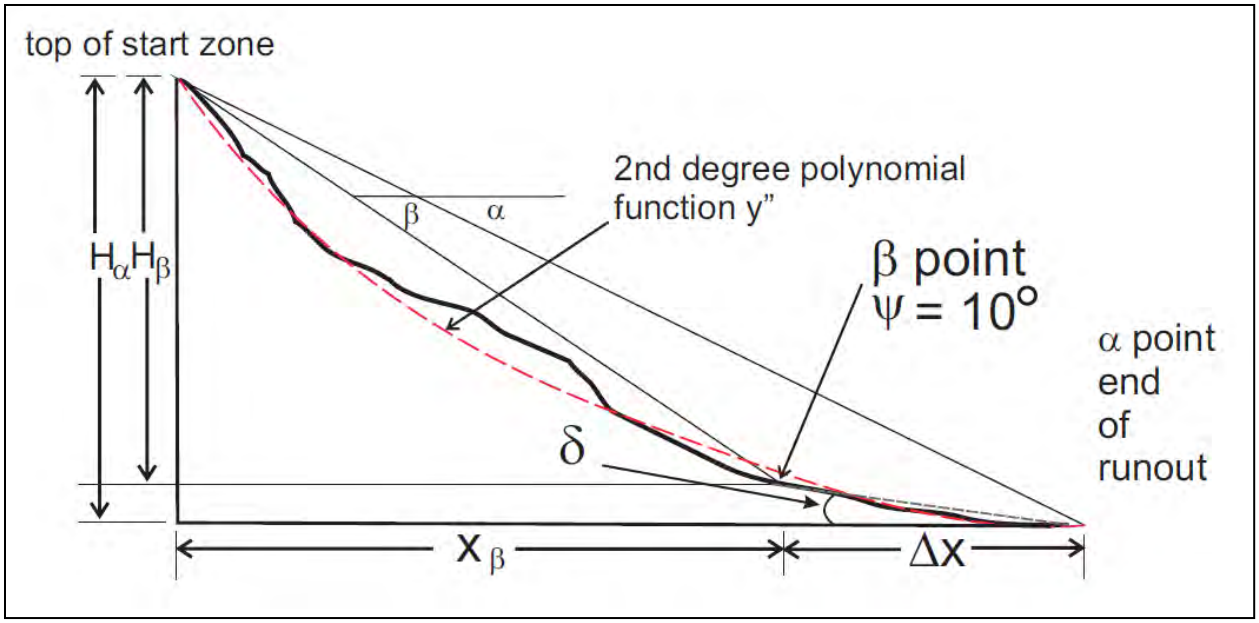

Figure 4.1: *Avalanche path schematic showing terrain parameters used for statistical analysis of extreme runout*

Table 4.1: *Description of avalanche path terrain parameters and variables used for statistical analysis of extreme avalanche runout*

Variable	Abbreviation	Type	Description
Beta angle, β (°)	β	interval	angle from β-point to top of starting zone
Alpha angle, α (°)	α	interval	angle from extreme runout position to top of starting zone
Delta angle, δ (°)	δ	interval	average angle of runout zone, between α and β
Reference angle ratio α/β	α/β	interval	dimensionless ratio of the α and β angles
Slope angle, ψ (°)	ψ	interval	ground slope between two points along the avalanche path centreline
Vertical fall to β, H_β (m)	H_β	interval	vertical distance between top of starting zone and β-point
Horizontal reach to β, X_β (m)	X_β	interval	horizontal distance from top of starting zone to β-point
Vertical fall to α, H_α (m)	H_α	interval	vertical distance between top of starting zone and extreme runout position
Horizontal reach to α, X_α (m)	X_α	interval	horizontal distance from top of starting zone to extreme runout position
Runout distance, Δx (m)	Δx	interval	horizontal distance between α and β-points
Runout ratio, $\Delta x/X_\beta$ (unitless)	$\Delta x/X_\beta$	interval	runout ratio fraction
Slope length of path, S_0 (m)	S_0	interval	distance measured in the field along the path from the top of the starting zone to the

			extreme runout position
Second derivative of slope function, y " (m^{-1})	y"	interval	2nd derivative of the fitted parabola (Equation 1)
Vertical height to low point on parabola, H_0 (m)	H_0	interval	difference between top of starting zone and lowest position on fitted parabola
Scale parameter for path profile, H_0y" (unitless)	H_0y"	interval	product of y" and H_0
Starting Zone Inclination, θ (°)	SZ_Ang	interval	average slope angle in the middle of the start zone
Starting Zone Aspect, (SZ_Asp) (deg)	SZ_Asp	interval	average aspect in the middle of the start zone
Starting Zone Elevation, SZ Elev (m)	SZ_Elev	interval	elevation at the top of the start zone
Runout Zone Elevation, RZ Elev (m)	RZ_Elev	interval	elevation of lower runout zone
Surface Roughness, SR (m)	SR	interval	0.15 – 0.30 (after Schaerer, 1971)
Wind Index, WI (unitless)	WI	ordinal	1 – 5 (after Schaerer, 1977)
Width of Start Zone, W (m)	SZ_Width	interval	width of the upper portion of the start zone
Terrain Profile, TP (unitless)	TP	ordinal	1 – 3 (after Jones and Jamieson, 2004)
Winter Precipitation, WP, (mm)	W_Precip	interval	mm water equivalent at the center of the starting zone

The delta angle, δ, is the average slope of the runout zone in between the α and β position, calculated using the field observed runout distance (Δx) and the elevation difference between α and β. The runout ratio and α/β ratios are dimensionless ratios used to compare the β-point locations to the extreme runout positions.

The slope length of the path, S_0, is the sum of the slope segment lengths from the top of the avalanche path starting zone to the extreme runout position.

For each avalanche path, 2nd order parabolas of the form:

$$y = ax^2 + bx + c \qquad \text{Equation 4.1}$$

were fitted to the topographic terrain profile from the top of the starting zone to past the extreme runout position (Figure 4.1), an example is also included in Appendix B. For all paths except one, the coefficient of determination for each parabolic fit was R^2 of 0.98 or greater. The path named "Zone 2, km 13" from the Columbia Mountains had an R^2 value of 0.975 which appears to be related to some bench-like features in the topography; this path is discussed further in Section 4.5.

The parameter y" is the 2nd order derivative of Equation 4.1 and describes the curvature of the path after Lied and Bakkehöi, 1980. H_0 is the vertical distance from the top of the starting zone to the low point on the fitted parabola, and H_0y" is termed the "scale parameter" also after Lied and Bakkehöi (1980). The starting zone elevation was taken from the top of the starting zone, and the starting zone aspect, inclination and width are taken for the middle or most representative portion of the starting zone. For example, if the starting zone included several large fingers which coalesced into one main path, the aspect, width and inclination of the middle section were used.

The runout zone elevation is measured at the β-point, and the surface roughness was evaluated for the starting zone area after Schaerer (1977). The wind index and terrain profile were qualitatively evaluated on scales of 1-5 and 1-3, respectively, in accordance with the criteria described in Sections 3.5 and 2.3.3. The winter precipitation was extracted from the PRISM raster dataset for the UTM coordinates in the middle of the avalanche path starting zone.

4.2.2 Descriptive Statistics and Distribution of Variables

Descriptive statistics including the mean, standard deviation, minimum (Q_0), lower quartile (Q_1), median (Q_2), upper quartile (Q_3) and maximum (Q_4) for the Fernie, Sparwood and Columbias datasets are summarized in Tables 4.2 (Fernie), 4.3 (Columbias), and 4.4 (Sparwood) on the following pages.

A total of 70 avalanche paths are included in this summary; 32 in the Fernie area, 33 in the Columbia Mountains, and 5 in the Sparwood area.

Table 4.2: *Descriptive statistics of terrain parameters and avalanche path variables for the Fernie area (n = 32)*

Variable	Mean	Standard Deviation	Q_0 Minimum	Q_1, Lower Quartile	Q_2 Median	Q_3, Upper Quartile	Q_4 Maximum
Beta angle, β (°)	26.2	2.8	21.7	24.3	25.6	27.6	33.7
Alpha angle, α (°)	23.4	2.1	20.2	22.2	22.9	24.4	27.9
Delta angle, δ (°)	9.3	3.9	-2.8	7.7	9.1	10.7	21.6
Reference angle ratio α/β	0.90	0.07	0.64	0.85	0.92	0.94	1.02
Vertical fall to β, H_β (m)	745.1	126.59	385	695	762.5	830.2	965
Horizontal reach to β, X_β (m)	1529	315	860	1342	1518	1744	2210
Vertical fall to α, H_α (m)	798	128	398	758	818	883	983
Horizontal reach to α, X_α (m)	1865	364	965	1655	1922	2097	2650
Runout distance, Δx (m)	336	236	-50	198	269	434	1184
Runout ratio, $\Delta x/X_\beta$	0.233	0.196	-0.045	0.118	0.165	0.944	1.076
Slope length of path, S_0 (m)	2138	397	1065	1917	2136	2322	2925
Second derivative of slope function, y" (m^{-1})	3.0E-04	1.3E-04	2.0E-04	2.0E-04	3.0E-04	3.0E-04	8.0E-04
Vertical height to low point on parabola, H_0 (m)	830	137	435	776	850	905	1111
Scale parameter for path profile, H_0y"	0.245	0.093	0.139	0.181	0.212	0.280	0.574
Starting Zone Inclination, θ (°)	36.3	6.6	23	32.25	36	41	49
Starting Zone Aspect, (SZ_Asp) (deg)	90.0	52.4	45	45	45	135	180
Starting Zone Elevation, SZ Elev (m)	1995.0	132.6	1640	1922	2000	2072	2300
Runout Zone Elevation, RZ Elev (m)	1262.0	111.6	1060	1194	1260	1288	1620
Surface Roughness, SR (m)	0.22	0.058	0.15	0.15	0.25	0.25	0.30
Wind Index, WI (unitless)	3.3	0.8	1	3	4	4	4
Width of Start Zone, W (m)	474.4	309.8	100	250	375	740	1430
Terrain Profile, TP (unitless)	1.8	0.5	1	1.75	2	2	3
Winter Precipitation (mm)	732.9	42.8	656	698	743	770	800

Table 4.3: *Descriptive statistics of terrain parameters and avalanche path variables for the Columbia Mountains (n = 33)*

Variable	Mean	Standard Deviation	Q_0 Minimum	Q_1, Lower Quartile	Q_2 Median	Q_3, Upper Quartile	Q_4 Maximum
Beta angle, β (°)	29.3	4.6	21.4	26.0	29.3	33.0	41.0
Alpha angle, α (°)	27.0	4.3	19.4	24.0	27.3	29.6	37.2
Delta angle, δ (°)	7.7	9.3	-12.9	2.7	7.5	13.1	27.3
Reference angle ratio α/β	0.92	0.05	0.79	0.91	0.93	0.95	0.99
Vertical fall to β, H_β (m)	898.6	389.37	395	645	745	1065	1980
Horizontal reach to β, X_β (m)	1618	881	760	1133	1292	1919	5055
Vertical fall to α, H_α (m)	960	425	447	670	765	1214	2045
Horizontal reach to α, X_α (m)	1876	921	1002	1321	1494	2106	5175
Runout distance, Δx (m)	259	214	56	121	171	327	995
Runout ratio, $\Delta x/X_\beta$	0.184	0.170	0.024	0.070	0.143	0.236	0.884
Slope length of path, S_0 (m)	2183	9	1140	1538	1687	2552	5661
Second derivative of slope function, y'' (m^{-1})	3.5E-04	2.1E-04	1.0E-04	2.0E-04	3.0E-04	5.0E-04	8.0E-04
Vertical height to low point on parabola, H_0 (m)	1197	611	419	743	987	1559	2837
Scale parameter for path profile, H_0y''	0.327	0.113	0.142	0.244	0.324	0.382	0.652
Starting Zone Inclination, θ (°)	35.9	5.6	27	30	35	40	50
Starting Zone Aspect, (SZ_Asp) (deg)	152.7	89.3	45	90	135	225	315
Starting Zone Elevation, SZ Elev (m)	2151.0	253.7	1420	2075	2140	2220	2724
Runout Zone Elevation, RZ Elev (m)	1253.0	332.2	534	1040	1365	1440	1865
Surface Roughness, SR (m)	0.258	0.0547	0.15	0.20	0.20	0.25	0.30
Wind Index, WI (unitless)	3.3	1.0	1	3	3	4	5
Width of Start Zone, W (m)	426.4	334.0	100	160	320	550	1500
Terrain Profile, TP (unitless)	1.8	0.7	1	1	2	2	3
Winter Precipitation (mm)	861.3	191.09	486	838	886	965	1208

Table 4.4: *Descriptive statistics of terrain parameters and avalanche path variables for the Sparwood Area (n = 5)*

Variable	Mean	Standard Deviation	Q_0 Minimum	Q_1, Lower Quartile	Q_2 Median	Q_3, Upper Quartile	Q_4 Maximum
Beta angle, β (°)	31.5	3.2	28.6	29.2	31.3	31.4	36.8
Alpha angle, α (°)	28.9	3.0	25.0	27.2	28.9	30.7	32.8
Delta angle, δ (°)	15.3	11.0	5.7	11.2	11.5	14.0	34.3
Reference angle ratio α/β	0.93	0.12	0.74	0.87	0.98	0.99	1.05
Vertical fall to β, H_β (m)	628.2	185.80	530	540	554	557	960
Horizontal reach to β, X_β (m)	1010	160	886	910	973	996	1285
Vertical fall to α, H_α (m)	632	188	516	540	550	590	966
Horizontal reach to α, X_α (m)	1063	227	839	926	936	1268	1345
Runout distance, Δx (m)	53	147	-71	-60	40	60	295
Runout ratio, $\Delta x/X_\beta$	0.051	0.152	-0.078	-0.060	0.045	0.047	0.303
Slope length of path, S_0 (m)	1281	200	1069	1081	1347	1380	1527
Second derivative of slope function, y" (m^{-1})	5.2E-04	8.4E-05	4.0E-04	5.0E-04	5.0E-04	6.0E-04	6.0E-04
Vertical height to low point on parabola, H_0 (m)	659	67	619	620	627	655	776
Scale parameter for path profile, H_0y"	0.353	0.047	0.315	0.320	0.325	0.390	0.416
Starting Zone Inclination, θ (°)	37.8	3.70	33	36	38	39	43
Starting Zone Aspect, (SZ_Asp) (deg)	90.0	0	90	90	90	90	90
Starting Zone Elevation, SZ Elev (m)	1774.0	36.30	1725	1760	1780	1780	1825
Runout Zone Elevation, RZ Elev (m)	1201.0	44.35	1140	1171	1220	1223	1250
Surface Roughness, SR (m)	0.30	0	0.30	0.30	0.30	0.30	0.30
Wind Index, WI (unitless)	1.4	0.89	1	1	1	1	3
Width of Start Zone, W (m)	290.6	80.45	173	290	290	300	400
Terrain Profile, TP (unitless)	2.8	0.45	2	3	3	3	3
Winter Precipitation (mm)	360.2	1.10	359	359	361	361	361

Table 4.2 for the Fernie area shows a maximum reference angle ratio "α/β" of 1.02; this is from the Hilda/Pearl path which had an extreme runout (α) point located above the β-point. This path is excluded from the runout ratio and α – β statistical analysis because extreme avalanche damage was not observed past the β-point.

Table 4.3 for the Columbia mountains shows a minimum δ angle of -12.9° which is an exceptionally steep uphill runout (typical runout zone angles are usually around 6-9°). This value was obtained from the "Whitewater 9.5" path in the Selkirks, which has an α-point located on the opposite (uphill) side of a steep creek cut bank.

Since there are only five avalanche paths in the Sparwood area, the data were not statistically analyzed on their own, but are included here for general comparison and completeness. The Sparwood data are revisited as part of Section 4.4, which looks at the relationship between avalanche runout and snowfall.

The normality of the 23 variables in the Fernie and Columbias datasets was evaluated using the Kolmogorov-Smirinov (K-S), with rejection of the null hypothesis of normality at the 5% level ($p < 0.05$).

For the Columbia Mountains dataset, eight variables are considered to be normally distributed namely: β, α, δ, α/β, $\Delta x/X_\beta$, H_β, H_0y'', and the runout zone elevation (*RZ_Elev*). For the Fernie dataset, 15 variables are considered to be normally distributed namely: β, α, δ, α/β, Δx, $\Delta x/X_\beta$, H_β, X_β, H_α, X_α, H_0y'', H_0, S_0, starting zone aspect (*SZ_Asp*), and starting zone elevation (*SZ_Elev*). Excluding the Hilda/Pearl path from the Fernie dataset, results of the Kolmogorov-Smirinov (K-S) are summarized in Table 4.5, and the variables for each dataset that can be classified as normally distributed are bolded.

Table 4.5: *Summary of Kolmogorov-Smirinov test results for Fernie Area and Columbia Mountains avalanche path variables; bolding indicates a normal distribution*

	Fernie		Columbias	
	D value	p-value	D value	p-value
Winter Precipitation (mm)	0.18	0.0086	0.209	8.04E-04
Vertical height to low point on parabola, H_0 (m)	0.11	**0.41**	0.20	0.0022
Second derivative of slope function, y " (m^{-1})	0.27	2.0E-06	0.23	1.5E-04
Scale parameter for path profile, H_0y"	0.18	0.011	0.083	**0.81**
Horizontal reach to β, X_β (m)	0.087	**0.78**	0.22	3.2E-04
Beta angle, β (°)	0.12	**0.29**	0.090	0.79
Runout distance, Δx	0.13	**0.15**	0.20	0.0022
Horizontal reach to α, X_α (m)	0.091	**0.72**	0.18	0.0063
Alpha angle, α (°)	0.12	**0.31**	0.10	**0.52**
Delta angle, δ (°)	0.16	0.040	0.086	**0.78**
Reference angle ratio α/β	0.15	**0.051**	0.13	**0.15**
Runout ratio, $\Delta x/X_\beta$	0.18	0.013	0.18	0.012
Slope length of path, S_0 (m)	0.087	**0.78**	0.12	0.0019
Vertical fall to β, H_β (m)	0.14	**0.11**	0.18	0.011
Vertical fall to α, H_α (m)	0.15	**0.061**	0.20	0.0019
Starting Zone Inclination, θ (°)	0.093	**0.68**	0.20	0.0017
Starting Zone Aspect, (SZ_Asp) (deg)	0.34	4.5E-10	0.18	0.0065
Starting Zone Elevation, SZ Elev (m)	0.14	**0.11**	0.18	0.0092
Runout Zone Elevation, RZ Elev (m)	0.18	0.007	0.16	0.028
Surface Roughness, SR (m)	0.26	9.3E-06	0.20	0.0023
Wind Index, WI (unitless)	0.32	6.4E-09	0.25	1.0E-05
Width of Start Zone, W (m)	0.19	0.0053	0.20	0.00131
Terrain Profile, TP (unitless)	0.42	2.6E-16	0.23	8.5E-05

Excluding the parameters which directly depend on the extreme runout position (α), leaves fifteen remaining independent variables including the following: PRISM winter precipitation *(W_Precip), H_0, y", H_0y", X_β, β, H_β,* starting zone inclination *(SZ_Ang),* starting zone aspect *(SZ_Asp),* starting zone elevation *(SZ_Elev),* runout zone elevation *(RZ_Elev),* surface roughness *(SR),* wind index, *(WI),* starting zone width *(SZ_Width)* and terrain profile *(TP).*

4.3 Alpha-Beta Statistical Runout Models

In this section, multiple regression methods are used to explore the relationship between α (the extreme runout position) and terrain variables for the Fernie area and Columbia Mountain paths.

4.3.1 Description of Multiple Regression Method

Out of the 23 predictor variables described in Table 4.1, eight of these depend on the extreme runout position, α. Since the intent of statistical runout models is to predict the α-point location, variables directly dependent on α were not carried forward for the multiple regression analysis. H_0 and *y"* depend on the selected trajectory for the avalanche path, and although this depends somewhat on the location of the α-point, it is still possible for the field surveyor to select an approximate avalanche path trajectory without knowing the α-point. The surveyor would have to apply some judgement and experience when selecting the trajectory for large, dry avalanches. These large destructive events tend to flow in a straight line and sometimes up and over obstacles, without being significantly deflected by terrain features such as gullies. Since the large, dry avalanche is considered to have the most destructive potential (Mears, 1992), the assumption that the design case avalanche will flow straight downhill is valid.

Spearman rank correlations between predictor variables and α were calculated for the Columbia Mountains and Fernie data, and variables which are significant at the 0.05 level are carried forward for multiple regression analysis. Table 4.6 summarizes the Spearman rank results for both datasets; significant variables with $p < 0.05$ are bolded and variables with p close to 0.05 are shown in italics.

Table 4.6: *Summary of Spearman rank correlations between the response variable α, and possible predictor variables for the Fernie area and Columbia Mountains*

	Columbias (n = 33)		Fernie (n = 31)	
Predictor Variable	R	p-value	R	p-value
Winter Precipitation (mm)	0.26	0.14	0.23	0.21
Vertical height to low point on parabola, H_0 (m)	**0.42**	**0.016**	-0.040	0.83
Second derivative of slope function, y " (m^{-1})	0.024	0.90	**0.57**	**0.0011**
Scale parameter for path profile, H_0y"	**0.65**	**5.9E-05**	**0.73**	**7.8E-06**
Horizontal reach to β, X_β (m)	-0.23	0.20	-0.20	0.29
Beta angle, β (°)	**0.94**	**2.20E-16**	**0.64**	**1.7E-04**
Vertical fall to β, H_β (m)	*0.31*	*0.080*	0.13	0.48
Starting Zone Inclination, θ (°)	0.28	0.12	0.16	0.40
Starting Zone Aspect, (SZ_Asp) (deg)	**0.45**	**0.0094**	-0.031	0.87
Starting Zone Elevation, SZ Elev (m)	-0.15	0.42	-0.022	0.91
Runout Zone Elevation, RZ Elev (m)	-0.22	0.23	-0.18	0.34
Surface Roughness, SR (m)	-0.092	0.61	-0.087	0.64
Wind Index, WI (unitless)	**-0.50**	**0.0042**	0.0021	0.99
Width of Start Zone, W (m)	-0.12	0.49	**-0.51**	**0.004**
Terrain Profile, TP (unitless)	0.071	0.69	0.092	0.62

For the Columbia Mountains, six variables are carried forward for the multiple regression: *H_0, H_0y", β, H_β*, *SZ_Asp*, and *WI*. For the Fernie area, four variables are carried forward for the multiple regression: *y", H_0y", β*, and *SZ_Width*.

4.3.2 Fernie Area Multiple Regression Models

For the Fernie dataset, an initial regression analysis of α on the four predictor variables *y", H_0y", β, SZ_Width*. The backward elimination method was used to eliminate variables which were found to have a minimal effect on the model, based on the F-value at the 1% significance level where $v_1 = k$ (degrees of freedom), and $v_2 = n - (k+1)$. For the initial four predictor regression, the threshold F-value (v_1 =4, v_2 =26), was 4.14 (Mendenhall and Sincich, 1995 p. 1108), such that variables with an F-value less than 4.14 were removed from the regression.

Table 4.7: *F-values for predictor variables for the Fernie area stepwise multiple regression, bolding indicates significance at the 1% level based on the threshold F-value of 4.14*

Variable	F-value
Second derivative of slope function, y " (m^{-1})	**17.76**
Scale parameter for path profile, H_0y"	**13.43**
Beta angle, β (°)	1.55
Width of Start Zone, SZ_Width (m)	3.87

Based on the threshold F-Value, the *SZ_Width* and the β angle were eliminated, resulting in the following regression equation:

$$\propto = 19.46 - 5987.64y" + 22.71H_0y" \qquad \text{Equation 4.2}$$

This model has an R^2 of 0.49, a standard error of 1.5 and uses 31 avalanche paths from the Fernie area for model development. A plot of the residuals is included as Figure 4.2 below and shows that the "Fish Bowl" avalanche path from the Island Lake area is an outlier.

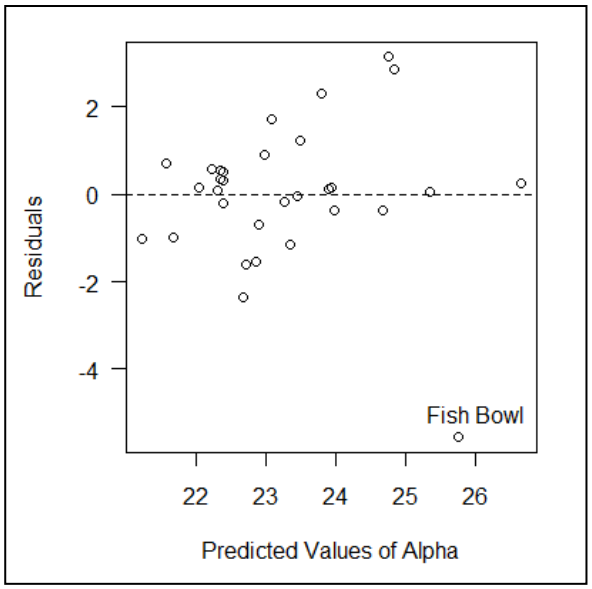

Figure 4.2: *Plot of residuals for Fernie Area multiple regression Equation 4.2 showing the Fish Bowl path as an outlier*

A closer examination of the "Fish Bowl" avalanche path shows two factors which may be contributing to the extraordinarily long runout. The first is that the path is highly channelized in the runout zone where avalanche flow from several portions of a large starting zone and track

coalesce into a single gully approximately 60 m wide. The second contributing factor is that the Fish Bowl path has some large benches in the runout zone, with the slope angle first reaching 8° at an elevation of 1320 m and then steepening back to 10° around 1200 m before reaching the α-point at a slope angle of about 5° at an elevation of 1160 m.

The initial regression analysis and backward elimination was repeated excluding the "Fish Bowl" avalanche path with a threshold F-value (v_1 =4, v_2 =25) of 4.18 (Mendenhall and Sincich, 1995 p. 1108), resulting in the F-values shown in Table 4.8 which show that all four predictor variables are significant.

Table 4.8: *F-values for predictor variables for the Fernie area stepwise multiple regression without the Fish Bowl path, bolding indicates significance at the 1% level based on the threshold F-value of 4.18*

Variable	F-value
Second derivative of slope function, y " (m^{-1})	**31.00**
Scale parameter for path profile, H_0y"	**25.24**
Beta angle, β (°)	**15.82**
Width of Start Zone, W (m)	**10.26**

The resulting regression equation is:

$$\propto = 8.35 - 2529y" + 1.27\mathrm{H}_0\mathrm{y}" + 0.63\beta - 0.00215SZ\_Width \qquad \text{Equation 4.3}$$

This model has an R^2 of 0.73, a standard error of 1.0° and uses 30 avalanche paths from the Fernie area for model development.

Autocorrelation for this model is tested using the Durbin-Watson test which gives a test result d-statistic of 1.6 and a p-value of 0.08, suggesting that autocorrelation is unlikely (Durbin and Watson, 1951). Residuals and the distribution of standard residuals for this model are included as Figure 4.3.

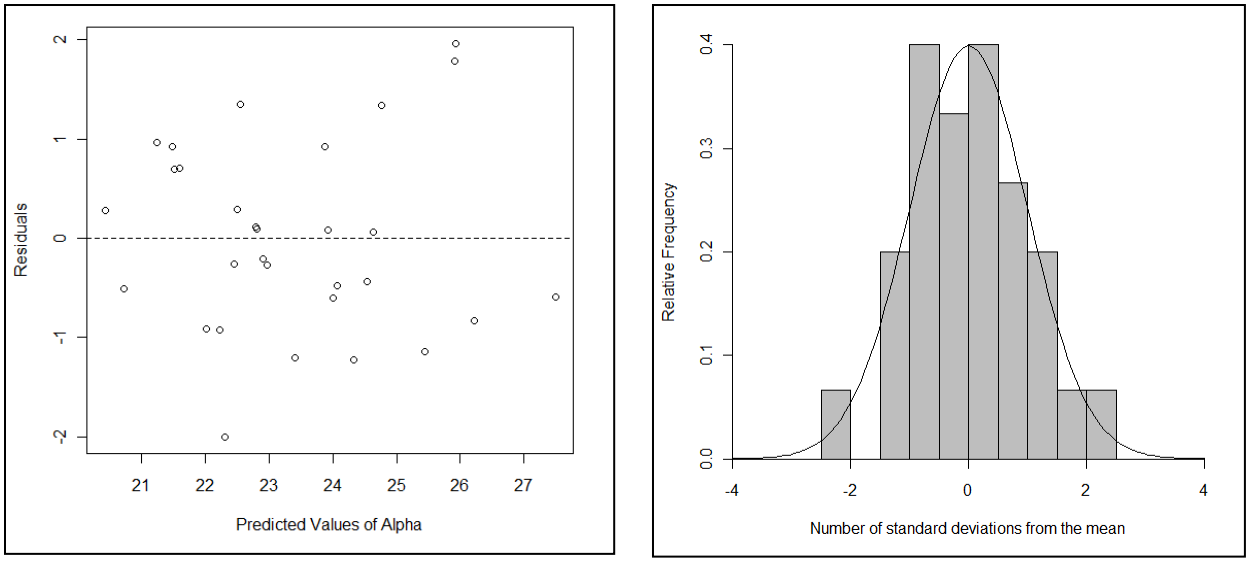

Figure 4.3: *Scatterplot of residuals (left) and distribution of standard residuals (right) for the multi-predictor α – β model (Equation 4.3) for the Fernie area*

The Kolmogorov-Smirinov (K-S) and Lilliefors tests are used to quantitatively test normality. For this test, the null hypothesis is normality, with rejection of the null hypothesis at the 1% level ($p < 0.01$). The p-value of 0.82 indicates that the null hypothesis can be accepted.

Table 4.9 *Kolmogorov-Smirinov and Lilliefors normality test results for Fernie area multi-predictor model (n = 30)*

D-value	p-value
0.0865	0.82

A plot of the vertical fall to β (H_β) against the standard residuals for this model is included as Figure 4.4 below and shows the residuals increasing for increasing values of H_β, or for bigger avalanche paths. This suggests that larger estimation errors may be associated with larger avalanche paths.

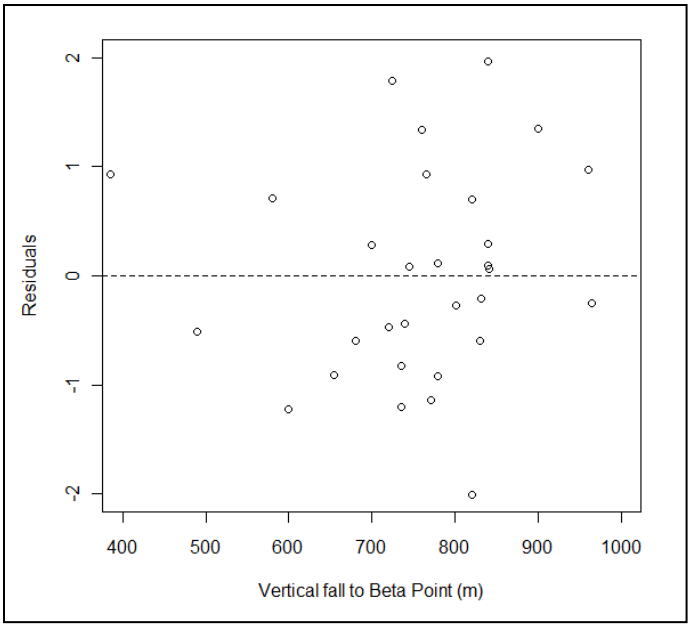

Figure 4.4: Residuals vs. H_β *for Fernie area multi-predictor model (Equation 4.3)*

4.3.3 Fernie Area Simplified Regression Model

Previous studies of extreme avalanche runout by Lied and Bakkehöi (1980), McClung and Lied (1987), and McClung and Mears (1991) found that predictor variables other than β were not significant for avalanche paths with over 300 m vertical fall height. Results in Section 4.2.4 show that for this dataset, β is significantly correlated with α, but that *y"* is the most statistically significant variable followed by H_0*y", β*, and starting zone width (*SZ_Width*). For comparison with the β-only models of Lied and Bakkehöi (1980), McClung and Lied (1987), and McClung and Mears (1991), removing predictor variables other than β from the regression gives the following equation:

$$\alpha = 0.61\beta + 7.60 \qquad \text{Equation 4.4}$$

This equation has an adjusted R^2 = 0.64 and a standard error of 1.2° and uses 30 avalanche paths for model development. The F-statistic is 53.5 with a corresponding p-value of 6E-08 indicating that this model provides a reasonable fit to the data. The p-values for the coefficients C_0 and C_1 are 1.5E-03 and 5.8E-08 respectively, indicating that both the coefficient and the intercept are significant. This model is shown graphically as Figure 4.5 below.

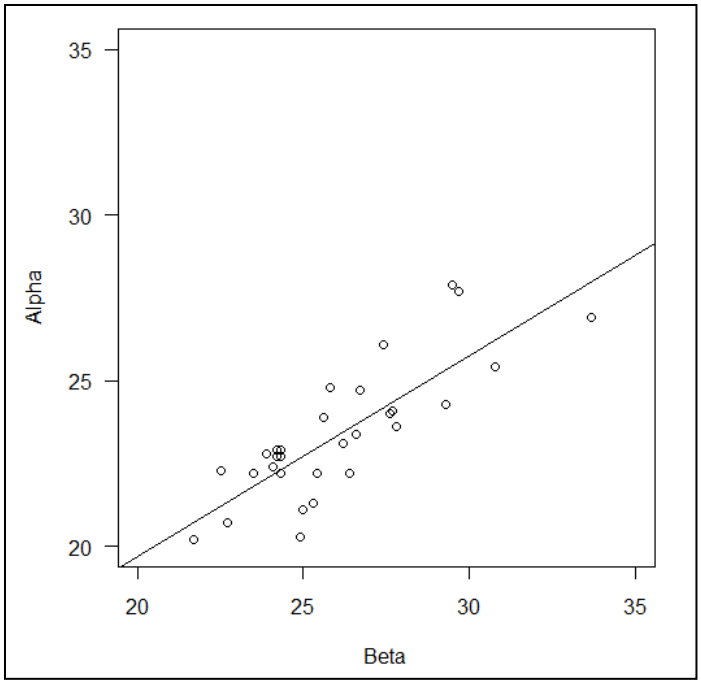

Figure 4.5: *Graphical representation of simplified regression (Equation 4.4) for the Fernie area*

Autocorrelation for the simplified model is tested using the Durbin-Watson test, which gives a test result d-statistic of 1.6 and a p-value of 0.15 suggesting that autocorrelation is unlikely (Durbin and Watson, 1951). Figure 4.6 shows the variation and distribution of the residuals for this model.

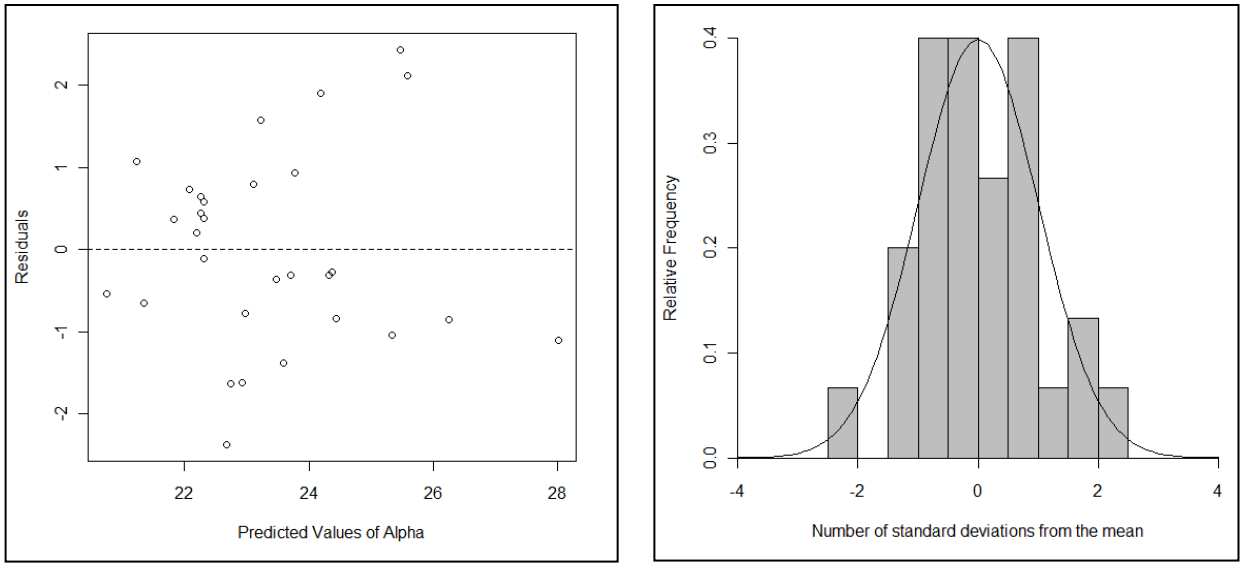

Figure 4.6: *Scatterplot of residuals (left) and distribution of standard residuals (right) for the simplified α – β model (Equation 4.4) for the Fernie area*

The Kolmogorov-Smirinov (K-S) and Lilliefors tests are used to quantitatively test normality. For this test, the null hypothesis is normality, with rejection of the null hypothesis at the 1% level ($p < 0.01$). The p-value of 0.73 indicates that the null hypothesis can be accepted.

Table 4.10: *Kolmogorov-Smirinov and Lilliefors normality test results for Fernie area simplified α – β model (n = 30)*

D-value	p-value
0.093	0.73

A plot of the vertical fall to β (H_β) against the standard residuals for this model is included as Figure 4.7 below and shows the residuals increasing for increasing values of H_β, or for bigger avalanche paths. This suggests that larger estimation errors may be associated with bigger avalanche paths.

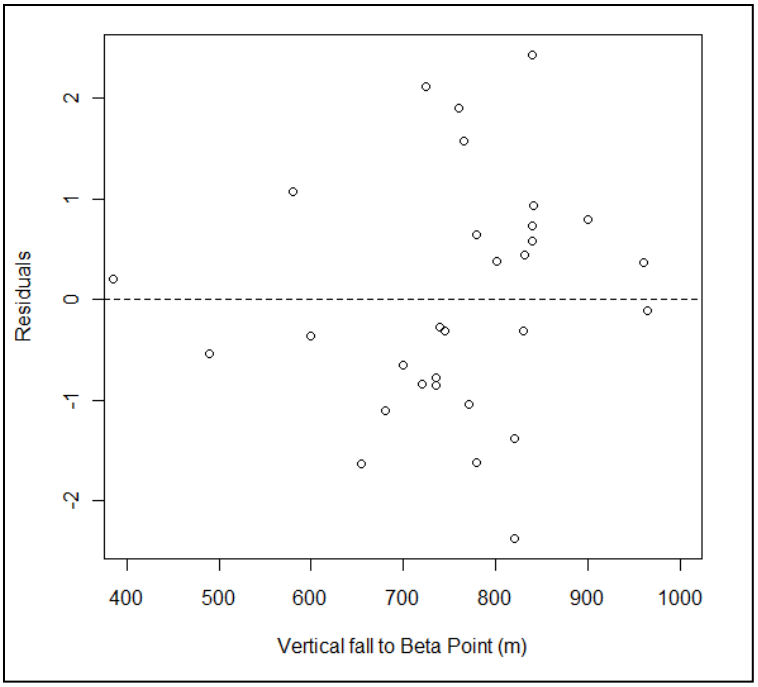

Figure 4.7: Residuals vs. *H_B for Fernie area simplified α – β model (Equation 4.4)*

Table 4.11 summarizes the multiple regression model results developed for the Fernie area using the reduced dataset of 30 avalanche paths, with the "Fish Bowl" avalanche path removed.

Table 4.11: *Summary of regression models developed for the Fernie area, bolding indicates the preferred model*

Equation	n	R^2	SE	p-value
$\alpha = 8.35 - 2529y" + 1.27H_0y" + 0.63\beta - 0.00215SZ\_Width$	30	0.77	1.0	1.31E-07
$\boldsymbol{\alpha = 0.61\beta + 7.60}$	**30**	**0.66**	**1.2**	**5.79E-08**

Although the initial regression equation has the adjusted highest R^2, estimating H_0 and y" requires some knowledge of the extreme avalanche trajectory. In addition, estimating the overall start zone width (*SZ_Width*) requires some amount of interpretation and knowledge of terrain. For this reason, the simplified linear α – β model with the intercept (Equation 4.4) is preferred when there is considerable uncertainty with measurements of *H_0, y"* or *SZ_Width*.

4.3.4 Columbias Mountains Multiple Regression Models

For the Columbias dataset, an initial regression analysis of α on the predictor variables *H_0, H_0y'', β, H_β, SZ_Asp* and *WI* was performed. The backward elimination method was used to eliminate variables which were found to have a minimal effect on the model, based on the F value at the 1% significance level. For the initial six predictor regression (v_1 =6, v_2 =26), the threshold F-value was 3.59 (Mendenhall and Sincich, 1995 p. 1108), and the vertical fall to β (H_β) was eliminated from the regression.

Table 4.12: *F-values for predictor variables for the Columbia Mountains stepwise multiple regression, bolding indicates significance at the 1% level based on a threshold F-value of 3.59*

Variable	F -value
Vertical height to low point on parabola, H_0 (m)	**84.68**
Scale parameter for path profile, H_0y''	**245.98**
Beta angle, β (°)	**121.43**
Vertical fall to β, H_β (m)	0.02
Starting Zone Aspect, SZ_Asp (deg)	**5.53**
Wind Index, WI (unitless)	**15.72**

This results in the following multi-predictor regression equation:

$$\propto = 5.87 + 0.00094H_0 - 0.49H_0y'' + 0.78\beta + 0.002SZ\_Asp - 0.88WI \quad \text{Equation 4.5}$$

This model has an adjusted R^2 of 0.94, a standard error of 1.1° and uses all 33 avalanche paths from the Columbia Mountains for model development, individual coefficient results are summarized in Table 4.13.

Table 4.13: *Results of Columbia Mountains multiple regression analysis for α (adjusted R^2 = 0.94, SE = 0.04°, p = 10^{-16})*

Variable	Coefficient	Std. Error	t-value	p-value
Intercept	5.87	1.86	3.15	3.9E-03
Vertical height to low point on parabola, H_0 (m)	9.44E-04	4.36E-04	2.17	0.039
Scale parameter for path profile, H_0y"	-0.48	3.00	-0.16	0.87
Beta angle, β (°)	0.78	0.08	9.77	2.4E-10
Starting Zone Aspect, SZ_Asp (deg)	2.04E-03	2.59E-03	0.79	0.44
Wind Index, WI (unitless)	-0.88	0.24	-3.67	1.1E-03

Autocorrelation for the multi-predictor model (Equation 4.5) is tested using the Durbin-Watson test which gives a test result d-statistic of 1.9 and a p-value of 0.24 suggesting that autocorrelation is unlikely (Durbin and Watson, 1951). Figure 4.8 shows the distribution of residuals and standard residuals.

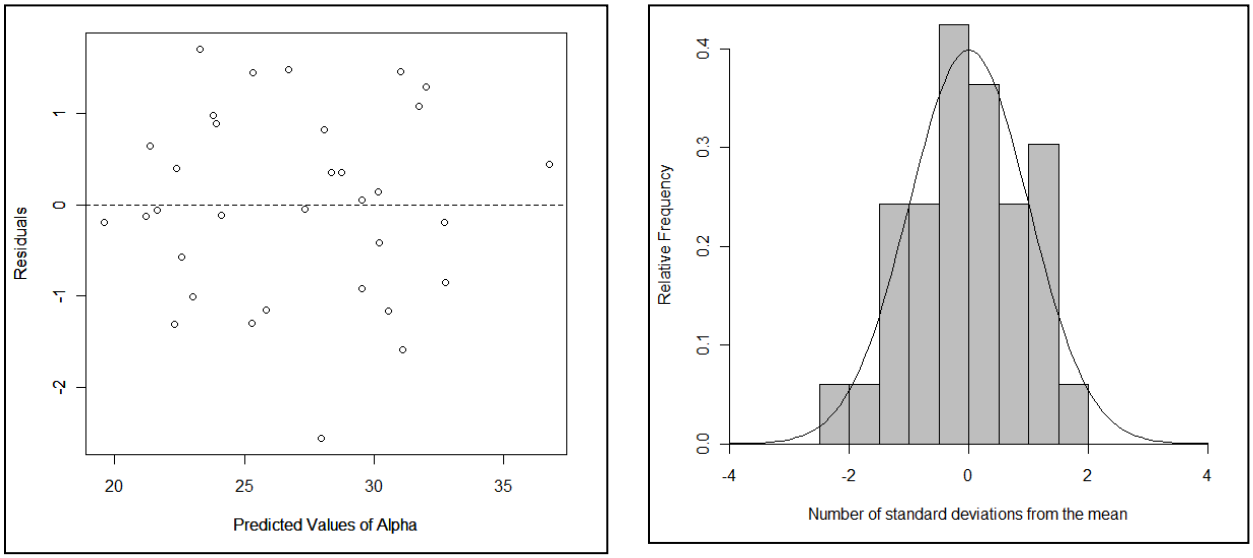

Figure 4.8: *Scatterplot of residuals (left) and distribution of standard residuals (right) for the multi predictor model (Equation 4.5) for the Columbia Mountains*

Visual examination of the residuals shows random variation which suggests that the model is correctly specified (Mendenhall and Sincich, 1995). The Kolmogorov-Smirinov (K-S) and Lilliefors tests are used to quantitatively test normality. For this test, the null hypothesis is normality, with rejection of the null hypothesis at the 1% level ($p < 0.01$). The p-value of 0.73 indicates that the null hypothesis can be accepted.

Table 4.14: *Kolmogorov-Smirinov and Lilliefors normality test results for Columbia Mountains multi predictor model (n = 33)*

D-value	p-value
0.091	0.70

A plot of the vertical fall to β (H_β) against the standard residuals for this model is included as Figure 4.9 below. A visual examination of the distribution shows random distribution of the residuals for increasing values of H_β, with no apparent scale effects.

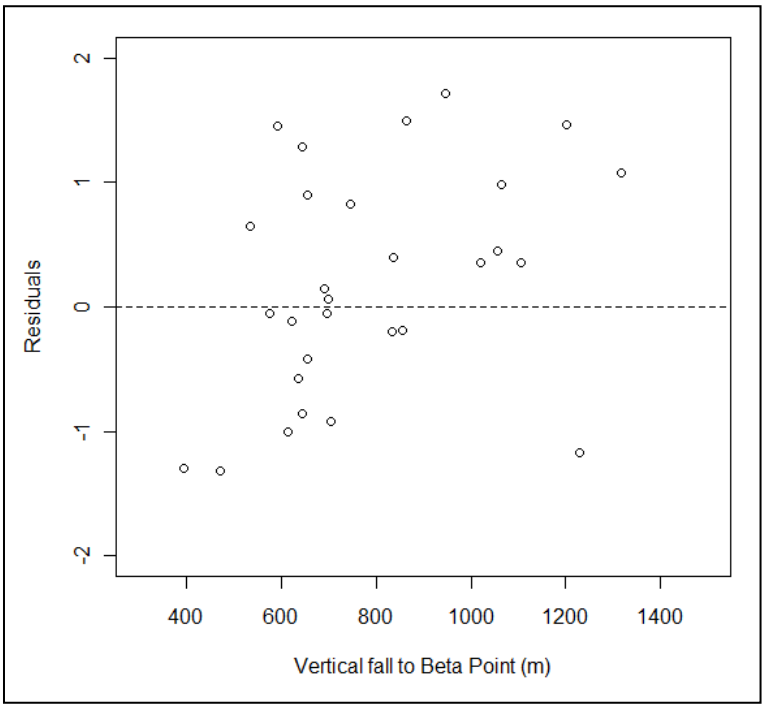

Figure 4.9: Residuals vs. *H_β for Columbia Mountains multi-predictor model (Equation 4.5)*

As shown in Table 4.13, three of the five predictor variables (*H_0*, *H_0y''* and *β*) are terrain parameters derived from the avalanche path slope profile. The other two variables are the starting zone aspect (*SZ_Asp*) and wind index (*WI*). Starting zone aspect (*SZ_Asp*) is also a terrain variable which is based on the average aspect of the avalanche path start zone; the wind index (*WI*) is qualitatively assessed by comparing the avalanche path starting zone to the criteria outlined in Table 3.4 (Schaerer, 1977). Since *SZ_Asp*, *WI* and *β* are not dependent on

the extreme runout position or the avalanche path trajectory, the backwards elimination regression analysis is repeated with these three variables. Eliminating *SZ_Asp* based on an F-value of 3.69 results in the following regression equation which predicts α and a function of β and *WI*:

$$\propto = 4.82 + 0.84\beta - 0.74WI \qquad \text{Equation 4.6}$$

This model has an adjusted R^2 of 0.93, a standard error of 1.2° and uses all 33 avalanche paths from the Columbia Mountains for model development.

4.3.5 Columbia Mountains Simplified Regression Model

To develop a model based only on β as a predictor, as developed for other ranges by Lied and Bakkehöi (1980), McClung and Lied (1987), and McClung and Mears (1991), removing predictor variables other than β from the regression gives the following equation:

$$\alpha = 0.90\beta + 0.69 \qquad \text{Equation 4.7}$$

This equation has an $R^2 = 0.90$ and a standard error of 0.045 and uses all 33 avalanche paths for model development. Summary t-value and p-value statistics for this model are included as Table 4.15 and show that the intercept C_0 is insignificant.

Table 4.15: *Summary of t-value and p-value statistics for the simplified Columbia Mountains regression model (Equation 4.7)*

	value	t-value	p-value
C_0	0.69	0.043	0.67
C_1	0.90	7.31	2.0E-16

If we force the linear model through the origin, we obtain Equation 4.8 which has an R^2 of 0.90 and a standard error of 0.042°.

$$\alpha = 0.92\beta \qquad \text{Equation 4.8}$$

Figure 4.10 shows a graphical plot of α and β values for the Columbia Mountains along with the two models presented here, visual analysis shows that the models are almost identical.

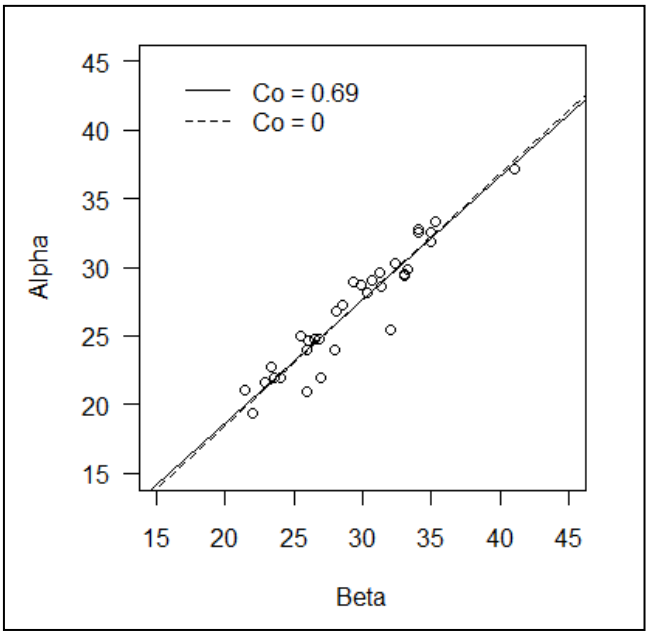

Figure 4.10: *Scatter plot of α and β and graphical representation of Equations 4.7 and 4.8 for the Columbia Mountains models*

A plot of the residuals versus the predicted values of α and of the distribution of the standard residuals is included as Figure 4.11.

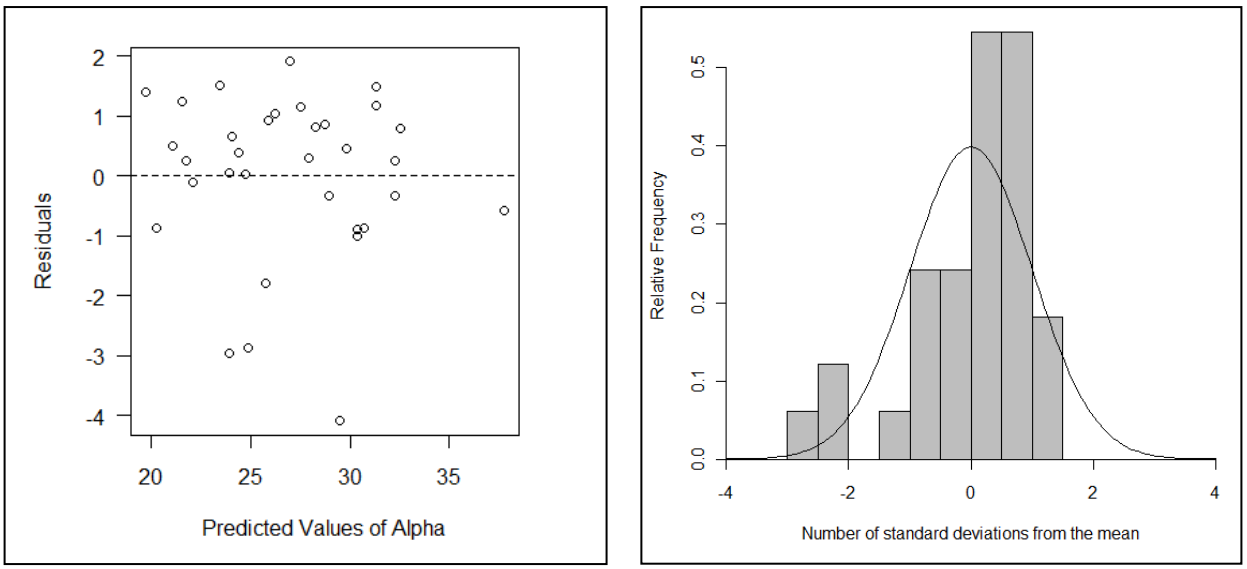

Figure 4.11: *Scatter of residuals (left) and distribution of standard residuals (right) for simplified α – β model forced through the origin (Equation 4.8) for the Columbia Mountains*

Visual inspection of Figure 4.11 shows random distribution of the residuals. Visual examination of the histogram does not show obvious non-normality. The Kolmogorov-Smirinov (K-S) and Lilliefors tests are used to quantitatively test normality. For this test, the null hypothesis is normality, with rejection of the null hypothesis at the 1% level ($p < 0.01$). The p-value of 0.08 indicates that the null hypothesis can be accepted.

Table 4.16: *Kolmogorov-Smirinov and Lilliefors normality test results for Columbia Mountains simplified α – β model (n = 33)*

D-value	p-value
0.1463	0.08

A plot of the vertical fall to β (H_β) against the standard residuals for the simplified α - β model (Equation 4.8) is included as Figure 4.12 below. A visual examination of the distribution shows no trend in the residuals as H_β increases for $H_\beta > 500$ m. The single low residual for $H_\beta \approx 400$ m is interesting but insufficient to indicate scale effects.

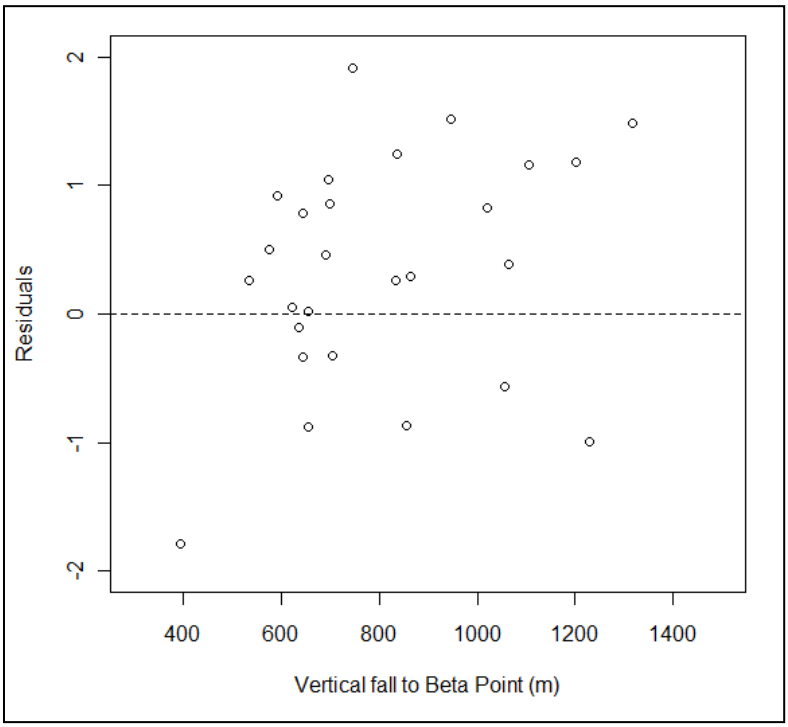

Figure 4.12: Residuals vs. *H_β for Columbia Mountains simplified α – β model (Equation 4.8)*

Table 4.17 summarizes the multiple regression model results developed for the Columbia Mountains and shows that the R^2 value is maximized for the multiple regression model *with H_0,*

H_0y", SZ_Asp, and *WI* as variables. The preferred multi-predictor and simplified regression models are bolded (Equations 4.5 and 4.8).

Table 4.17: *Summary of regression models developed for the Columbia Mountains*

Equation	n	R^2	SE (°)	p-value
$\boldsymbol{\alpha = 5.87 + 0.00094H_0 - 0.49H_0y" + 0.78\beta + 0.002SZ\_Asp - 0.88WI}$ **(Equation 4.5)**	**33**	**0.94**	**1.1**	**5.6E-16**
$\alpha = 4.82 + 0.84\beta - 0.74\mathrm{WI}$ (Equation 4.6)	33	0.93	1.2	2.2E-16
$\alpha = 0.90\beta + 0.69$ (Equation 4.7)	33	0.90	1.4	2.2E-16
$\boldsymbol{\alpha = 0.92\beta}$ **(Equation 4.8)**	**33**	**0.90**	**1.3**	**2.2E-16**

Obtaining reasonable values for H_0 and $H_0y"$ depend on having some knowledge of avalanche trajectory and extreme runout position. The interpretation of the start zone aspect and the wind index are both somewhat subjective, but are expected to be fairly consistent between surveyors, so for some avalanche paths, this model may be more useful. Table 4.14 also shows that the fit is similar for the simplified model whether the constant is included or not.

4.3.6 Columbia Mountains Simplified Regression Models by Sub-Range

The simplified regression model for the Columbia Mountains is further explored on a sub-range basis by separately analyzing the avalanche paths from the Selkirk, Cariboo and Monashee Mountains. Similar to the combined range model, results of the simplified regression show that the intercept (C_0) is insignificant for the sub-range models, based on p-value statistics of 0.62, 0.58 and 0.42 for the Selkirks, Cariboos and Monashees. Resulting regression equations with C_0 = 0 and summary statistics are summarized in Table 4.18, and a plot of the three models is included as Figure 4.13.

Table 4.18: *Summary of simplified regression models developed for the Columbia Mountain sub-ranges: Selkirk, Cariboo and Monashee Mountains*

Sub-Range	Equation	n	R^2	SE (°)	p-value
Selkirks	$\alpha = 0.91\beta$	13	0.86	1.5	2.2E-16
Cariboos	$\alpha = 0.94\beta$	6	0.85	0.91	1.6E-08
Monashees	$\alpha = 0.92\beta$	14	0.82	1.4	2.2E-16

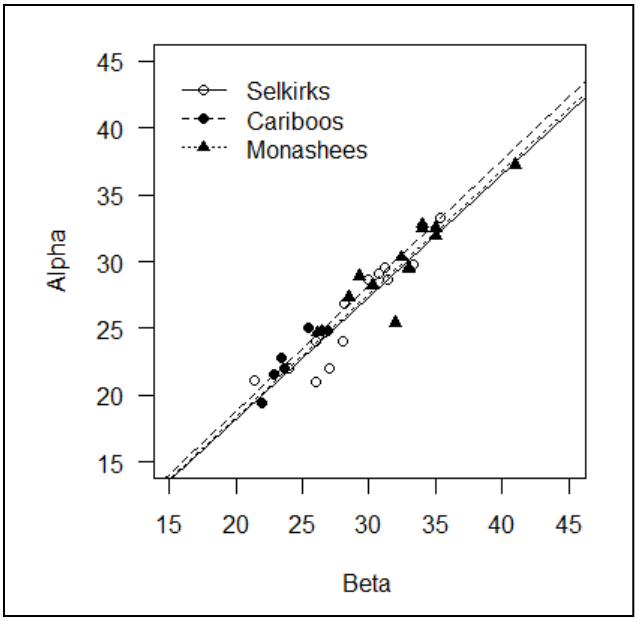

Figure 4.13: *Graphical representation of the simplified regression models for the Selkirk, Cariboo and Monashee sub-ranges of the Columbia Mountains*

The α – β fit for the combined ranges (R^2 = 0.90), is higher than the fits for the sub-range models, and other than the Cariboos, the standard error is also smaller for the combined range model. A visual analysis of the linear model fits shows that the avalanches in the Selkirks tend to run further than the avalanches in the Monashees, with the avalanches in the Cariboos having the steepest α - β line indicating that avalanches from this range have relatively shorter run outs. Although this analysis suggests some trends within the sub-ranges, the combined range model is preferred because of the better model fit and the larger number of paths.

4.3.7 Summary of Alpha-Beta Model Parameters

In this section, multi-predictor and simplified α – β model parameters shown below (Equation 4.9, 4.10, 4.11 and 4.12) are developed and presented for the Fernie Area and for the Columbia Mountains.

Fernie Area multi-predictor (R^2 = 0.73, SE = 1.0°, n = 30):

$$\propto = 8.35 - 2529y" + 1.27\mathrm{H}_0y" + 0.63\beta - 0.00215SZ\_Width$$

Equation 4.9

Fernie Area simplified (R^2 = 0.66, SE = 1.19°, n = 30):

$$\alpha = 0.61\beta + 7.60 \quad \text{Equation 4.10}$$

Columbia Mountains multi-predictor (R^2 = 0.90, SE = 1.3°, n = 33):

$$\propto = 5.87 + 0.00094H_0 - 0.49H_0y'' + 0.78\beta + 0.002SZ\_Asp - 0.88WI \quad \text{Equation 4.11}$$

Columbia Mountains simplified (R^2 = 0.90, SE = 1.3°, n = 33):

$$\alpha = 0.92\beta \quad \text{Equation 4.12}$$

Analysis of the distribution of the fit and the residuals of the models indicates that these α – β model parameters are relevant for estimating extreme avalanche runout for typical tall avalanche paths in these regions. This includes paths with greater than 350 m vertical fall height, paths with little to no uphill or cross valley runout, and paths which are not highly confined or channelized in the runout zones. Some of the limitations of these models are discussed further in Section 4.6.

4.4 Runout Ratio Statistical Models

The objective of this section is to develop runout ratio model parameters for the Fernie area and for the Columbia Mountains that can be used to predict extreme avalanche runout in these areas. Previous studies by McClung and Lied (1987), McClung and Mears (1989) and McClung et al. (1991) showed that a set of avalanche path runout ratios ($\Delta x/X_\beta$) from a specific mountain range can be analyzed using Extreme Value Type 1 (Gumbel) statistics. Section 4.3.1 describes this statistical method, and results of the analysis for the two mountain ranges are presented in Sections 4.3.2 (Fernie area) and 4.3.3 (Columbia Mountains).

4.4.1 Description of Runout Ratio Method

The work of McClung and Lied (1987) and McClung and Mears (1991) showed that for a set of avalanche paths in a given mountain range, the runout ratio ($\Delta x/X_\beta$), obeyed a Gumbel distribution of the form:

$$P = e^{-e^{\frac{\left(\frac{\Delta x}{X_\beta}\right)_P - u}{b}}}$$

Equation 4.13

Replacing $\left(\frac{\Delta x}{X_\beta}\right)_P$ with x_P and rearranging gives Equation 4.14:

$$x_p = u + b(-\ln(-\ln(P))$$

Equation 4.14

In the above equation, u and b are location and scale parameters, respectively, and P is a chosen non-exceedence probability with a value between 0 and 1 which represents the proportion of paths in the dataset with runout ratios not exceeding x_P. The term $(-\ln(-\ln(P))$ is called the "reduced variate" which can be defined by ranking a set of runout ratios for a given mountain range according to:

$$\left(\frac{\Delta x}{X_\beta}\right)_1 < \left(\frac{\Delta x}{X_\beta}\right)_i < \left(\frac{\Delta x}{X_\beta}\right)_n$$

Equation 4.15

The non-exceedence probability P can be determined from the ranked runout ratio using several methods described by McClung at al. (1989). For this analysis we have ranked the data according to Weibull (Gumbel, 1958) where:

$$P_i = \frac{rank}{n+1}$$

Equation 4.16

For both the Columbia Mountains and the Fernie area, the runout ratio method is applied to derive the location and scale parameters u and b unique to each mountain range. Unlike the

multiple regression method which rejects paths with an α-point located higher in elevation than the β-point which would result in a negative runout ratio, this method can incorporate paths with a negative runout ratio.

4.4.2 Fernie Area Runout Ratio Model

The runout ratio model for the 31 tall avalanche paths in the Fernie area is shown as Figure 4.14 with the runout ratio, x_p, plotted as a function of the reduced variate, -ln(-ln(P)).

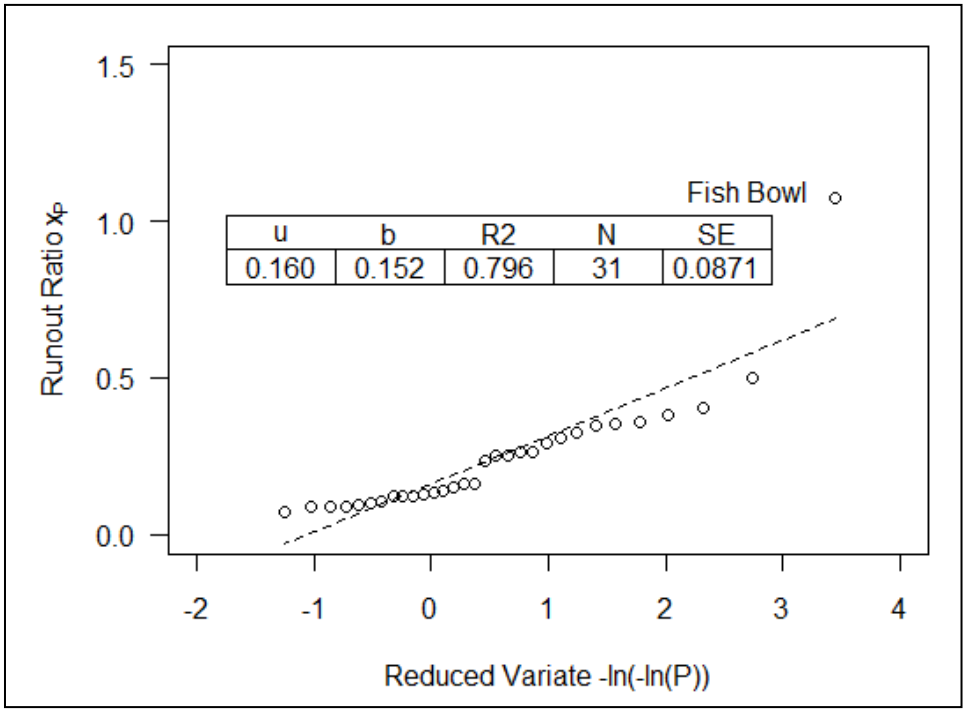

Figure 4.14: *Runout ratio model for 31 tall avalanche paths in the Fernie area*

The coefficients of the regression line fit to the model are u = 0.160 and b = 0.152 with an adjusted R^2 of 0.796 and SE = 0.0871. Since both of the variables, x_p and the reduced variate are functions of the field-observed runout ratio, only high adjusted R^2 values ($R^2 > 0.95$) are considered an acceptable fit to a Gumbel distribution. The R^2 for this dataset does not show an acceptable fit.

Similar to the multiple regression model, analysis of the residuals shows the "Fish Bowl" path as an outlier, for the reasons discussed in Section 4.2.2, this path is removed and the analysis is repeated to give the model shown in Figure 4.15 which has an acceptable R^2 of 0.957 and a SE =

0.02 and uses 30 of the 31 avalanche paths for model development. Given the dramatic change in the model fit, the "Fish Bowl" path is not included in further analysis.

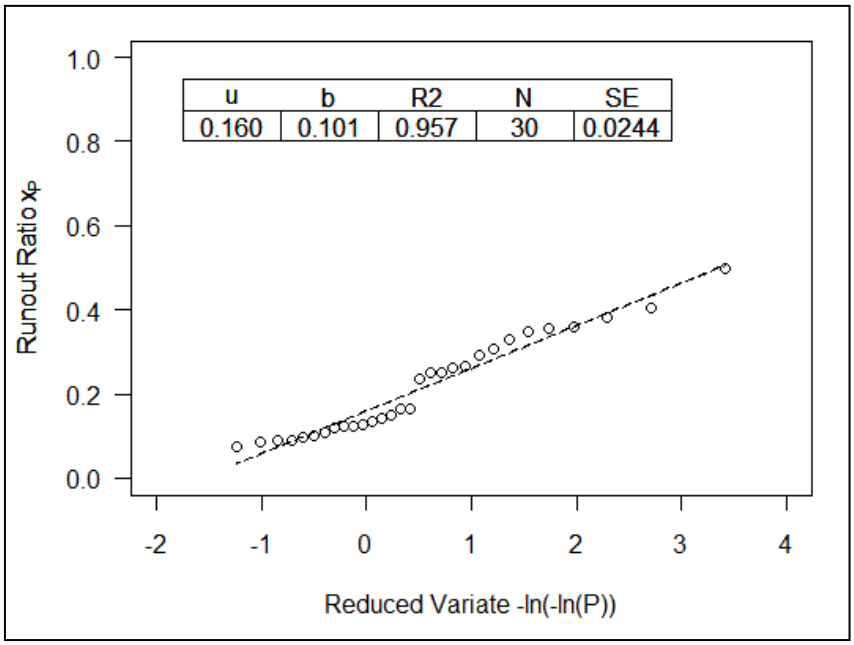

Figure 4.15: *Runout ratio model for 30 tall avalanche paths in the Fernie area (Fish Bowl path removed)*

A visual examination of the plot shows a jump in the data at about $x_p = 0.2$. If we analyze and plot these data separately, we get the runout ratio models shown in Figure 4.16 and 4.17 respectively.

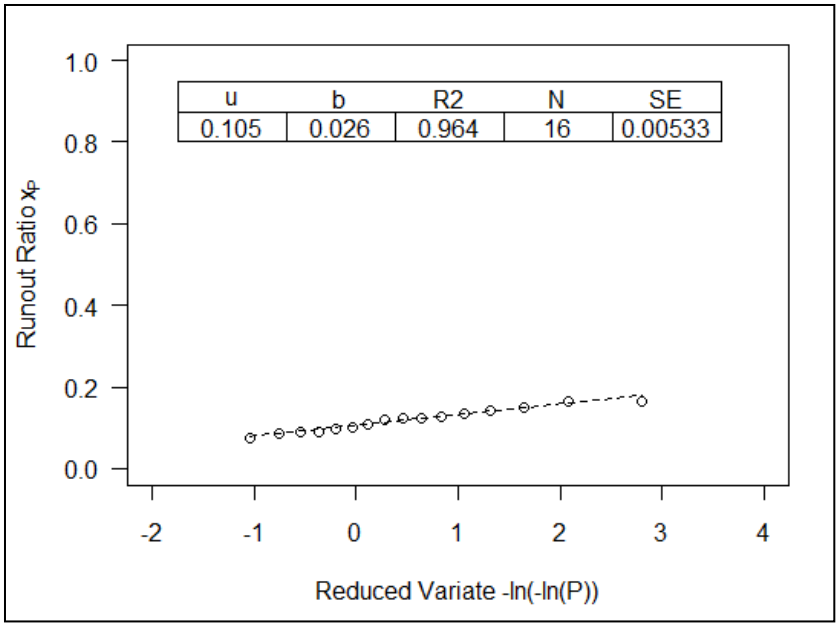

Figure 4.16: *Runout ratio model for 16 tall avalanche paths in the Fernie area with $x_p < 0.2$*

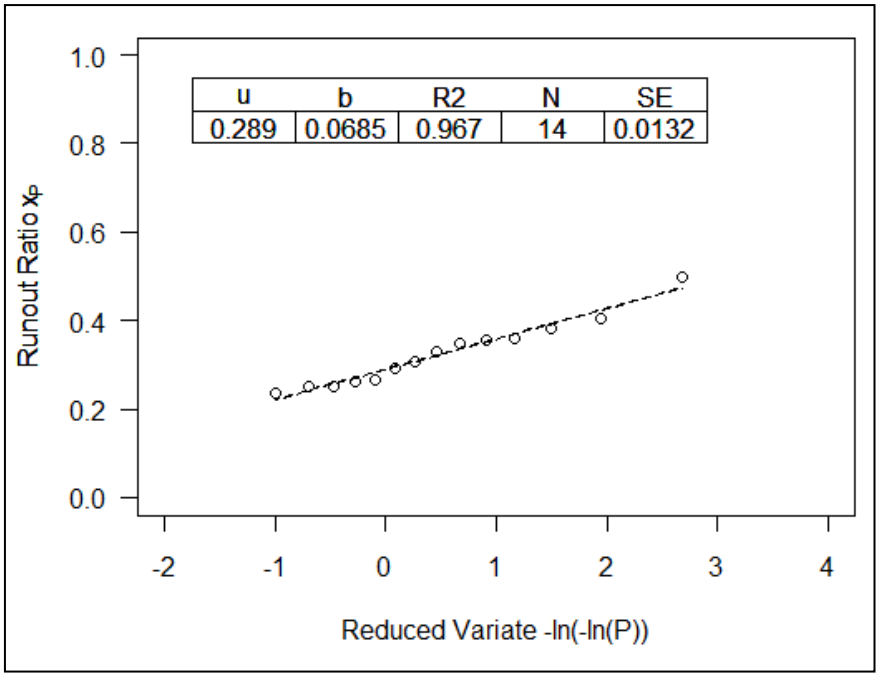

Figure 4.17: *Runout ratio model for 14 tall avalanche paths in the Fernie area with $x_p > 0.2$*

Although separating the dataset for values of x_p above and below 0.2 improves the fit for the avalanche paths with shorter runout ratios ($R^2 = 0.96$) and with longer runout ratios ($R^2 = 0.97$), the sample size of the divided datasets (n=16 and n=14) are small, and the larger data sets are preferred for conducting statistical analyses with reasonable levels of confidence. This

approach may still be useful for identifying trends in the data and for directing future runout studies in the Fernie area. Possible reasons for the poor fit to the longer running avalanche paths are explored and discussed in Section 4.5.

After McClung and Mears (1991), the full dataset of 30 avalanche paths is censored for the shorter running paths at the value of $P = e^{-1}$. The runout ratio model for the censored dataset is included as Figure 4.18.

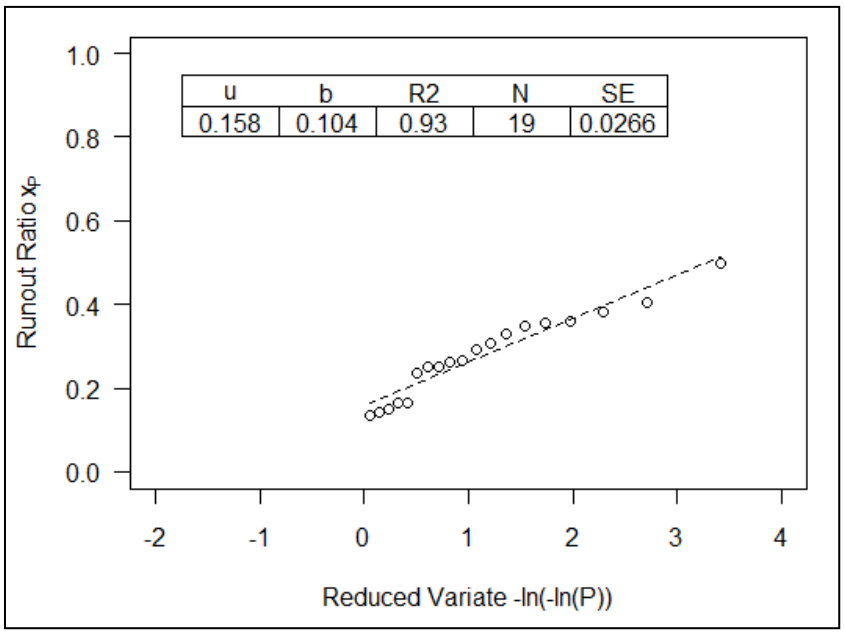

Figure 4.18: *Fernie area runout ratio model for 19 tall avalanche paths, censored for values of P < e^{-1}*

For this censored dataset, the coefficients of the regression line fit to the 20 avalanche paths are u = 0.158, b = 0.104 with a R^2 of 0.93 and SE = 0.027. Censoring the dataset to remove values below $P = e^{-1}$ effectively removes the shorter running avalanches from the dataset and provides a better fit to the higher values of the runout ratio, building additional conservatism into the estimated runout. For land use planning, these longer running avalanches are generally of more interest than the shorter running paths. In this case, censoring the dataset does not provide a better fit to the data.

Table 4.19 summarizes the model parameters and fits derived for the Fernie area:

Table 4.19: *Summary of runout ratio model parameters and fits for the Fernie area models, bolding indicates the preferred model*

Model	n	u	b	R^2	SE
Full dataset	31	0.160	0.152	0.796	0.087
Fish Bowl removed	**30**	**0.160**	**0.101**	**0.957**	**0.024**
Censored for x_p >0.2	16	0.105	0.026	0.964	0.005
Censored for x_p <0.2	14	0.289	0.0685	0.967	0.013
Censored for P<e^{-1}	19	0.158	0.104	0.930	0.026

Table 4.19 shows that the best fit of the model is achieved when the dataset is censored for runout ratio values (x_p) above 0.2. Although this indicates that splitting the dataset into shorter and longer running avalanches, the divided datasets are small. The model with the "Fish Bowl" avalanche path removed has both the sufficient number of paths, and an acceptable fit (R^2 > 0.95) to be a potentially useful predictive model. Applying the Durbin-Watson test to explore the presence of residual correlation gives a test result d-statistic of 0.39 and a p-value of 1.3E-09 which suggests that autocorrelation is likely. A positive correlation implies that small runout ratio estimate errors (residuals) are associated with shorter running avalanche paths and longer runout ratio errors are associated with long running avalanche paths, this has been previously identified by Mears and McClung (1991) and Nixon and McClung (1993) as "scale" effects. To explore this further, a plot of the residuals versus the vertical fall height to β (H_β) is included as Figure 4.19, although an increase in the value of the residuals for increasing values of H_β is expected, this is not evident.

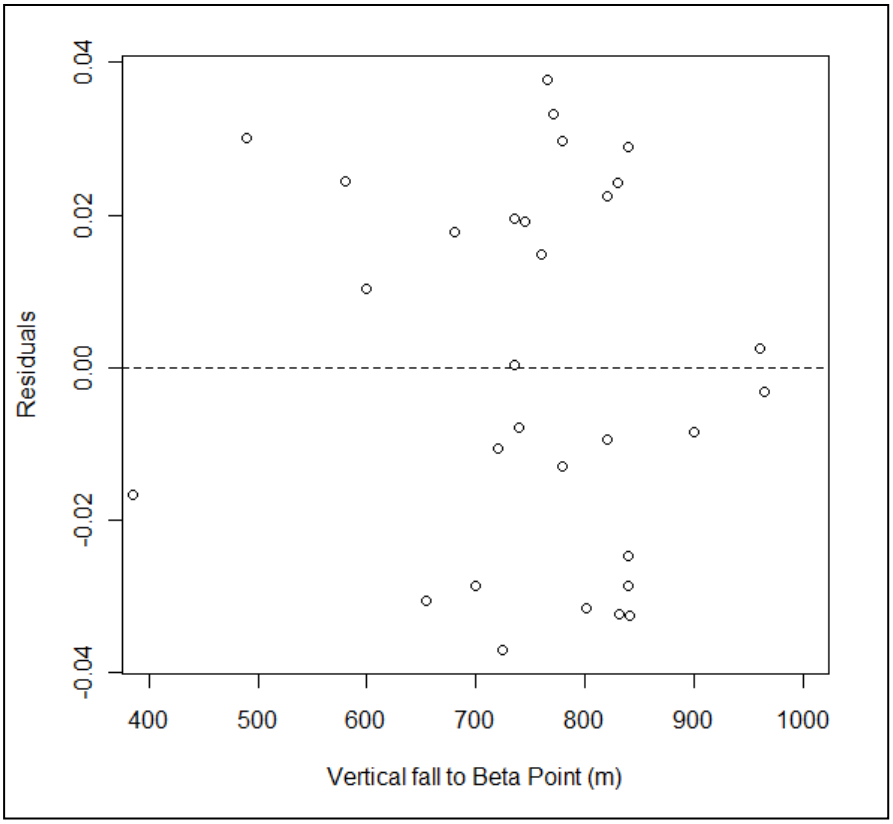

Figure 4.19: *Residuals vs. H_β for the Fernie area preferred runout ratio model*

A plot of the residuals and of the distribution of the standard residuals for this model are included as Figure 4.20 below, and a visual inspection shows non-monotonic trends for increasing values of x_p. This plot also shows all residuals lying between the +0.04 and -0.04 with no apparent outliers. Visual examination of the histogram does not show obvious non-normality.

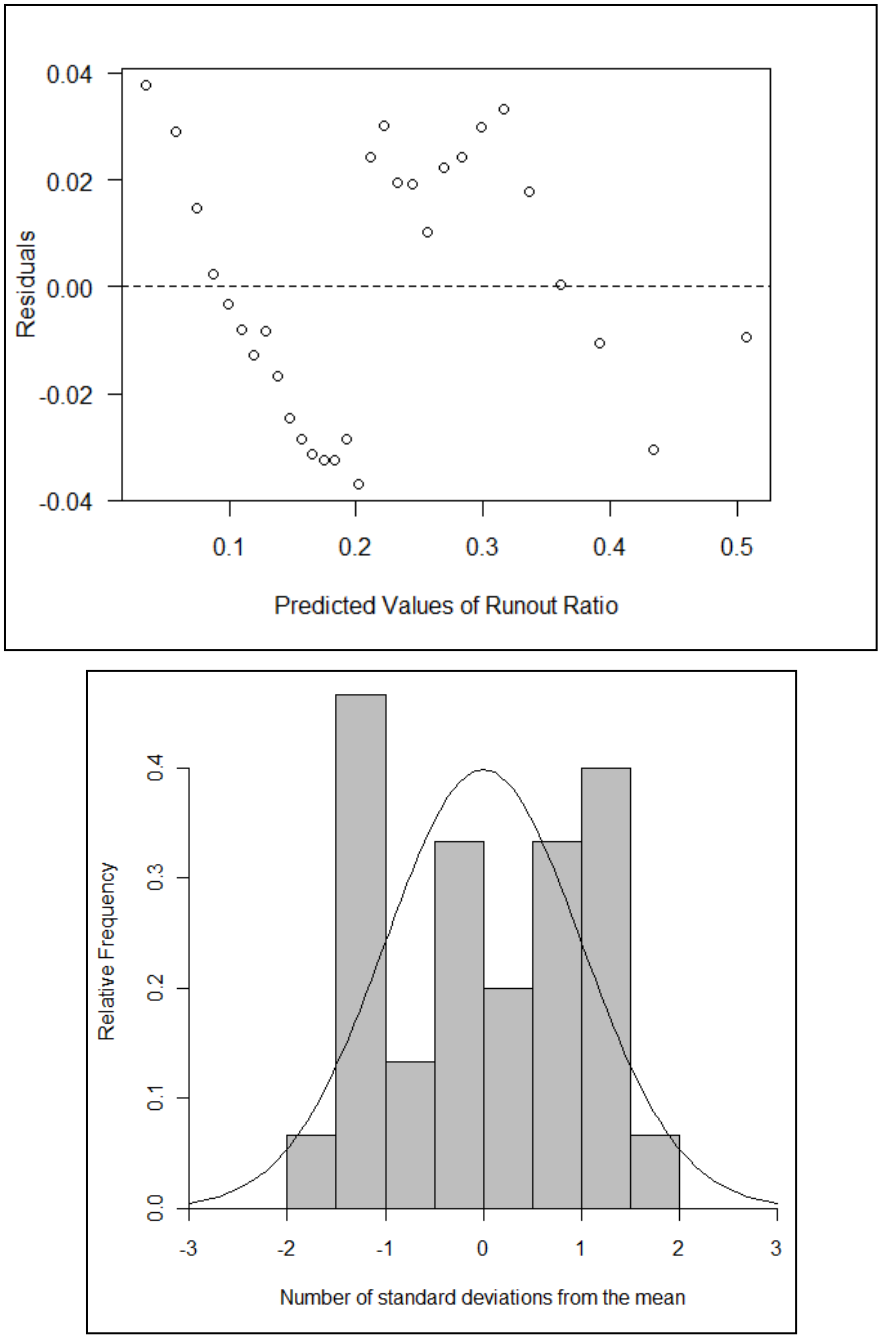

Figure 4.20: *Scatter of residuals (top) and distribution of standard residuals (bottom) for preferred runout ratio model (Figure 4.15) for the Fernie Area*

The Kolmogorov-Smirinov (K-S) and Lilliefors tests are used to quantitatively test normality with rejection of the null hypothesis of normality at the 1% level ($p < 0.01$). Results are shown in Table 4.20.

Table 4.20: *Kolmogorov-Smirinov and Lilliefors normality test results for Fernie area preferred runout ratio model (n = 30)*

D-value	p-value
0.1372	0.159

So the hypothesis of normality is not rejected and the model parameters are considered acceptable.

4.4.3 Columbia Mountains Runout Ratio Model

The runout ratio model for the 33 tall avalanche paths in the Columbia mountains is shown as Figure 4.21, with runout ratio (x_p) plotted as a function of the reduced variate, -ln(-ln(P)). The coefficients of the regression line fit to the model are u = 0.110 and b = 0.137 with an R^2 = 0.848 and SE = 0.0662. A visual examination of this plot shows a reasonably good fit to the central part of the data, with obvious outliers at the upper end. Since both the variables, x_p and the reduced variate are functions of the field observed runout ratio, only high adjusted R^2 values ($R^2 > 0.95$) are considered an acceptable fit to a Gumbel distribution.

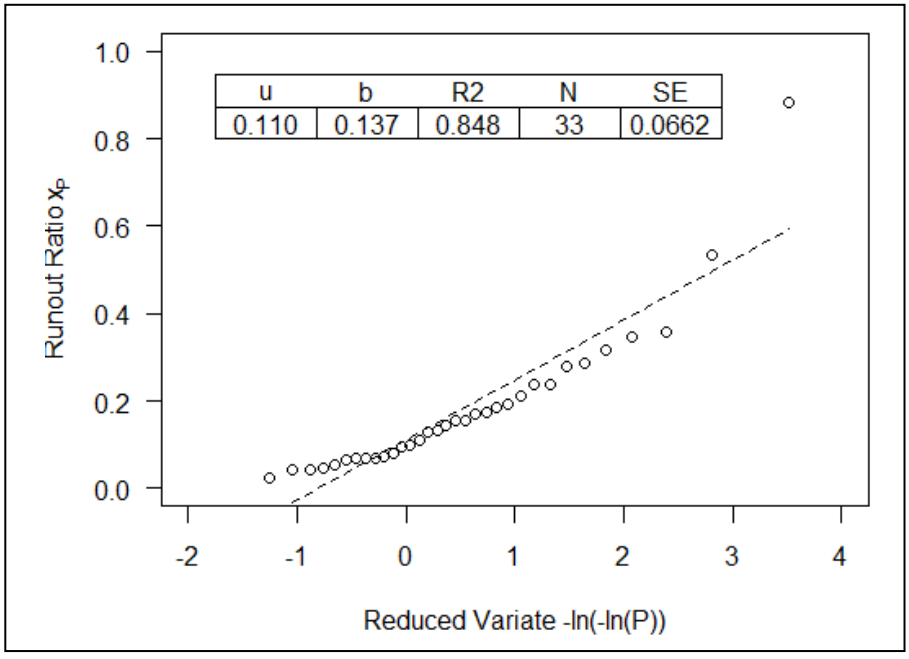

Figure 4.21: *Columbia Mountains runout ratio model for 33 tall avalanche paths*

The two upper end outliers are avalanche paths from the Oliver Creek area of the Selkirk Mountains named “Oliver Creek 11.1-11.4” ($\Delta x / X_\beta$ = 0.884) and “Oliver West 20” ($\Delta x / X_\beta$ =

0.532). These path data were provided by others, and examination of the photos and field summaries for Oliver Creek 11.1-11.4 shows that the runout zone for this path is in a 20 year old cut block which would have made identification of the extreme runout position particularly difficult since the 30-100 year vegetation record would have been removed.

Examination of the photos and field summaries for "Oliver West 20" shows that the lower track and runout zone for this path have some bench-like features which could be contributing to either a poorly defined β-point, or extraordinary long runout. This path may not be representative of a "typical" path as described in Section 3.5. For these reasons, these two paths are excluded from the remainder of the runout ratio analysis, and a plot of the runout ratio model for Columbia Mountains without these two paths is shown as Figure 4.22.

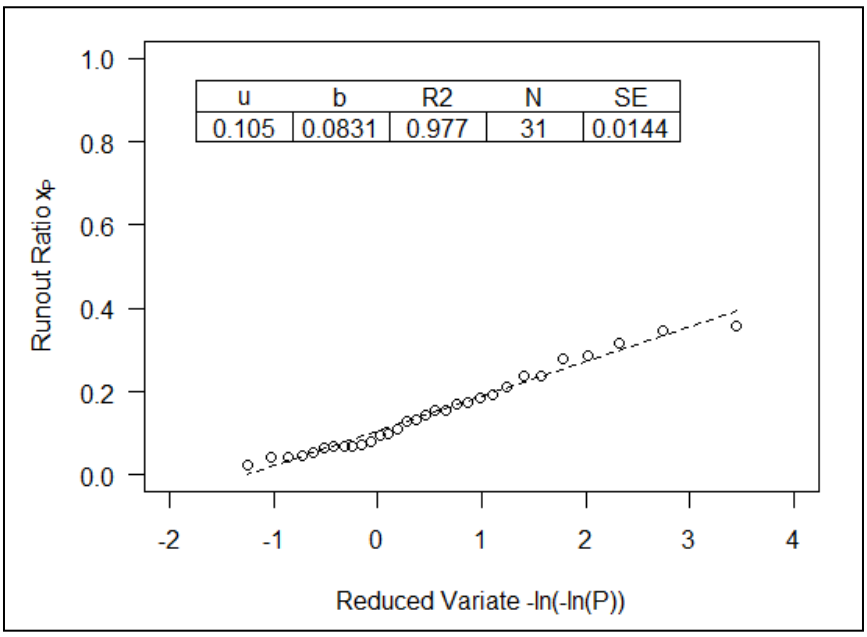

Figure 4.22: *Columbia Mountains runout ratio model for 31 tall avalanche paths with two Oliver Creek outlying paths removed*

For this model with the outliers removed, the coefficients of the regression line fit to the 31 avalanche paths are u = 0.105, b = 0.083 with a R^2 of 0.977 and SE = 0.0144. After the work of McClung and Mears (1991), Figure 4.23 shows the runout ratio model for a reduced dataset censored for values of $P < e^{-1}$.

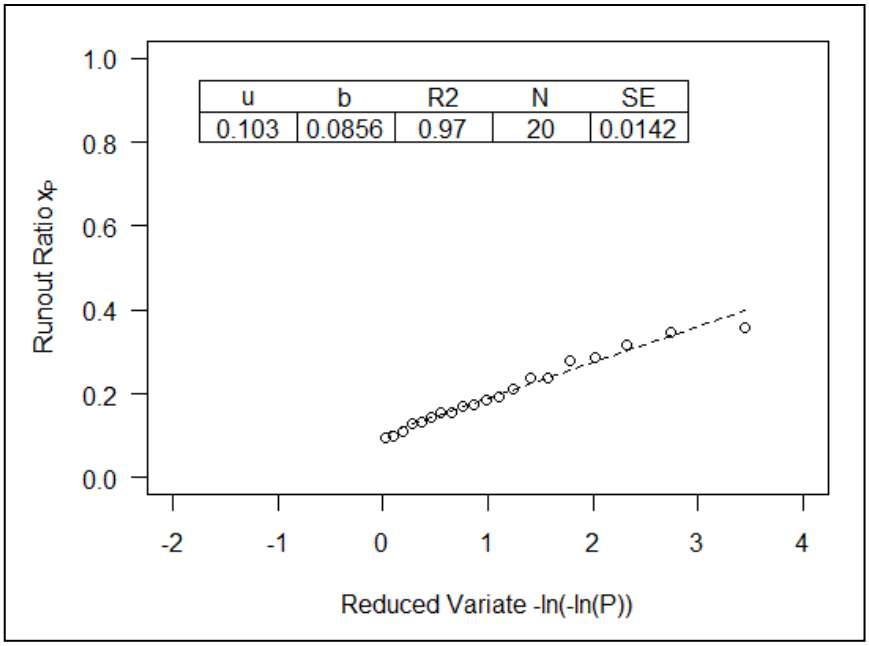

Figure 4.23: *Columbia Mountains runout ratio model for 20 tall avalanche paths, censored for values of $P < e^{-1}$*

For this censored dataset, the coefficients of the regression line fit to the 20 avalanche path are u = 0.103, b = 0.086 with a R^2 of 0.97 and SE = 0.0142. Censoring the dataset to include only P values above e^{-1} ($P > e^{-1}$) effectively removes the shorter running avalanches from the dataset and provides a better fit to the higher values of the runout ratio, building additional conservatism into the estimated runout. Although providing an acceptable fit to the data ($R^2 > 0.95$), the censored sample size of n = 20 is less than n = 30 which is typically considered a representative sample size for developing these models, this censored dataset may still provide a useful comparison for estimating extreme runout positions since the influence of long running paths is increased.

Table 4.21 summarizes the model parameters derived for the three Columbia Mountains runout ratio models.

Table 4.21: *Summary of runout ratio model parameters and fits for the Columbia Mountains models, bolding indicates preferred models*

Model	n	u	b	R^2	SE
Full dataset	33	0.110	0.137	0.848	0.062
Outliers removed	**31**	**0.105**	**0.083**	**0.977**	**0.014**
Censored for $P < e^{-1}$	**20**	**0.103**	**0.086**	**0.970**	**0.014**

The best runout ratio model fit is achieved when the outlying paths “Oliver Creek 11.1-11.4” and “Oliver West 20” are removed from the dataset; this is the preferred runout ratio model for the Columbia Mountains. Although an acceptable fit ($R^2 > 0.95$) is also achieved for the censored dataset, the number of avalanche paths is small ($n < 30$), and larger datasets are preferred. A plot of the residuals and distribution of standard residuals for the preferred model are included as Figure 4.24 below, and a visual inspection shows some increasing and decreasing linear trends for increasing values of x_p. This plot also shows all residuals lying between the +0.03 and -0.04.

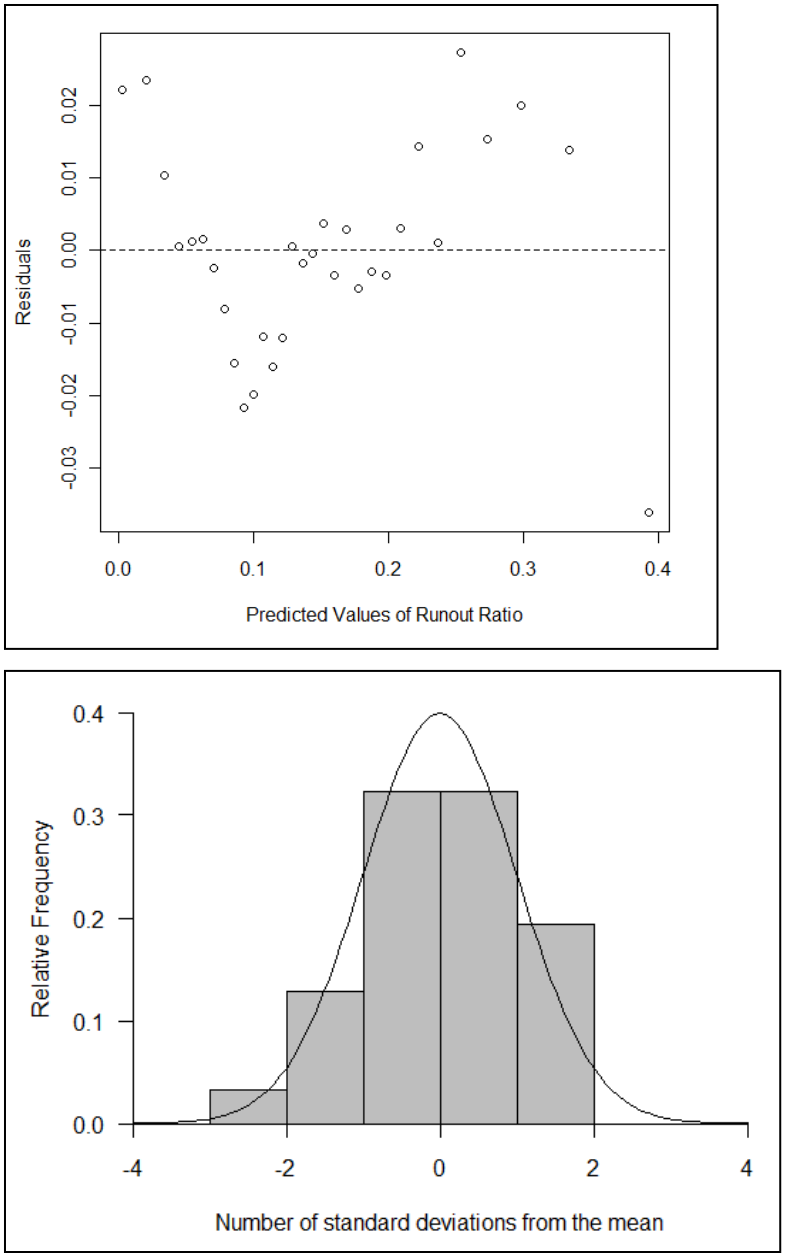

Figure 4.24: *Scatterplot of residuals (top) and distribution of standard residuals (bottom) for the preferred runout ratio model for the Columbia Mountains*

A visual examination of the histogram does not show obvious non-normality. The Kolmogorov-Smirinov (K-S) and Lilliefors tests are used to quantitatively test normality without rejection of the null hypothesis of normality at the 1% level ($p < 0.01$), summarized in Table 4.22.

Table 4.22: *Kolmogorov-Smirinov and Lilliefors normality test results for Columbia Mountains preferred runout ratio model (n=31)*

D-value	p-value
0.1383	0.137

The effect of avalanche path height is further explored by comparing the residuals against the vertical fall to β (H_β) shown in Figure 4.25. Visual inspection shows a slight increase in residuals for increasing values of H_β, suggesting that larger estimation errors may be associated with bigger avalanche paths.

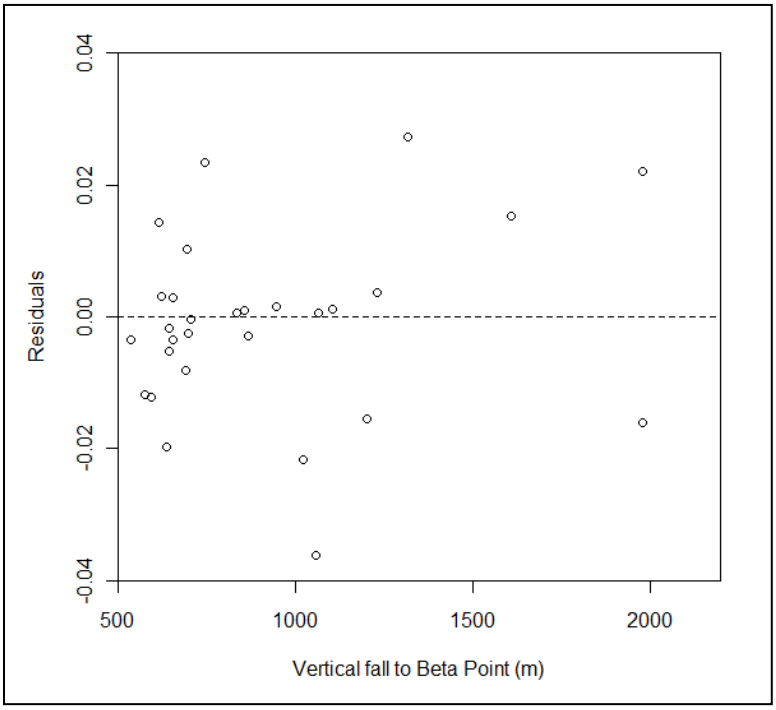

Figure 4.25: *Residuals vs. H_β for Columbia Mountains preferred runout ratio model*

4.4.4 Summary of Runout Ratio Model Parameters

In this section, runout ratio model parameters shown below (Equation 4.17 and 4.18) are presented for the Fernie Area and for the Columbia Mountains.

Fernie Area (R^2 = 0.96, SE = 0.024, n = 30):

$$x_p = 0.160 + 0.101(-\ln(-\ln(P)) \quad \text{Equation 4.17}$$

Columbia Mountains (R^2 = 0.98, SE = 0.014, n = 31):

$$x_p = 0.105 + 0.083(-\ln(-\ln(P)) \quad \text{Equation 4.18}$$

Analysis of the distribution of the fit and the residuals of the models indicates that these runout ratio model parameters are relevant for estimating extreme avalanche runout for typical tall avalanche paths in these regions. This includes paths with greater than 350 m vertical fall height, paths with little to no uphill or cross valley runout and paths which are not highly confined or channelized in the runout zones.

4.5 Climatic Influence on Runout

As described in Section 2.3.4, past studies of extreme avalanche runout have mostly excluded climate parameters from the analysis. This is based partly on the assumption that climatic conditions favouring the longest running avalanches will occur in every mountain range over a 100 year period (McClung et al., 1989), and partly on the lack of reliable, high-elevation climate records for individual avalanche paths. In this section, the potential correlations between extreme runout parameters and snowfall records are explored using several sources of climate data.

To explore the relationship between snowfall and runout, the data for the Columbia Mountains, the Fernie area and the Sparwood area were combined into a single dataset of 70 avalanche paths. In this section, the relationship between runout and climate is examined using PRISM winter precipitation data along with extreme *snow water equivalent (SWE)* data from nearby provincial snow observation sites and snowpack height data from federal weather stations. Derivation of winter snowfall from the PRISM data is summarized in Section 3.2.3, the other snowfall data sources are described here.

4.5.1 British Columbia Snow Course Data (Provincial Snow Observation Sites)

The British Columbia Provincial snow course and snow pillow sites are maintained and used for monitoring the snowpack within stream drainage basins. These consist of sites located at a variety of elevations throughout the province where the water equivalent of the snowpack is measured manually (snow courses) or electronically (snow pillows). The SWE data in mm are

made available online. The length of the record and the recording frequency varies from station to station. For each avalanche path surveyed, the nearest snow course or snow pillow site was identified. SWE values were examined for the full period of record for each station, and the largest recorded value of SWE was extracted from the data record. This value represents the extreme snow water equivalent for the site for the period of record. The length of the record varied from as long as 83 years (1928-2011) for some sites in the Selkirk Mountains to as short as 10 years (2001-2011), with a mean of 52.4 years. The distance between the snow course station and avalanche path start zone coordinates ranged from 2.9 to 130.5 km. The snow course records were collected from a variety of elevations ranging from 673 to 2062 m-asl, and were generally located at a lower elevations than the avalanche path starting zones.

4.5.2 Environment Canada: Canadian Daily Climate Data (Federal Weather Stations)

The federal weather station sites consist of Environment Canada weather stations generally located near populated centers and airports. These data were accessed through the Canadian Daily Climate Data (CDCD) database which contains daily records from 1898 to 2007. Snow height at these stations is generally recorded manually in cm by probing the ground within the study plot and averaging the measurements. The closest weather station with the longest monitoring record was chosen for each avalanche path, and the extreme snow height value in cm for the recorded period was extracted. The length of record for the CDCD weather stations used in this analysis ranged from 24 to 91 years, and the distance between the weather station and the avalanche path starting zone ranged from 2.7 to 67.6 km. These sites are generally located at valley bottom elevations which are much lower than the avalanche path start zones.

To compare between the different values and to facilitate the elevation corrections in Section 4.4.3, the CDCD data were converted from cm of snow to mm of water equivalent using an assumed density of 250 kg/m^3 for snow on the ground. The error introduced by this assumption is discussed further in Section 4.5.2.

4.5.3 Elevation Correction for Snow Water Equivalent

Two methods were used to convert the snow course SWE and CDCD snow height readings to a representative SWE at the elevation of the avalanche path starting zones. The first method, after Claus et al. (1984), involved using the parameters for the "Interior Average", "North Kootenay", "Rogers Pass" and "Rocky Mountain Dry" to calculate a constant for each reference snow course site (Equation 4.19) and then to calculate the associated extreme SWE at the avalanche path start zone elevation. The parameters "B" and "C" for each region are summarized in Table 4.21.

$$Extreme\ Water\ Equivalent\ (mm) = Constant + B(elevation) + C(elevation)^2$$

Equation 4.19

Table 4.23: *Regional parameters to calculate elevation specific SWE for Equation 4.18 (Claus et al., 1984) for western Canadian mountain ranges*

Region	B	C
Rogers Pass	-0.723	0.000801
North Kootenay	-0.572	0.000222
Interior Average	-0.694	0.000149
Rocky Mountain Dry	-1.863	0.004815

The second method involved calculating snow height at the starting zone after Margreth and Gruber (1998), by assuming an increase in snow height of 0.05 m for every 100 m in elevation. Although this method is based upon two reference sites in Switzerland, it is commonly used in other parts of the world in the absence of a more accurate relationship. To convert from cm of snow to mm of water equivalent, a density of 250 kg/m^3 was assumed.

For comparison, Figure 4.26 shows the SWE for each avalanche path using the three data sources and two elevation correction methods (five values for each site):

1) PRISM Winter Precipitation

2) Snow Course: elevation correction after Claus et al. (1984)

3) Snow Course: elevation corrected after Margreth and Gruber (1998)

4) CDCD: elevation correction after Claus et al. (1984)

5) CDCD: elevation correction after Margreth and Gruber (1998)

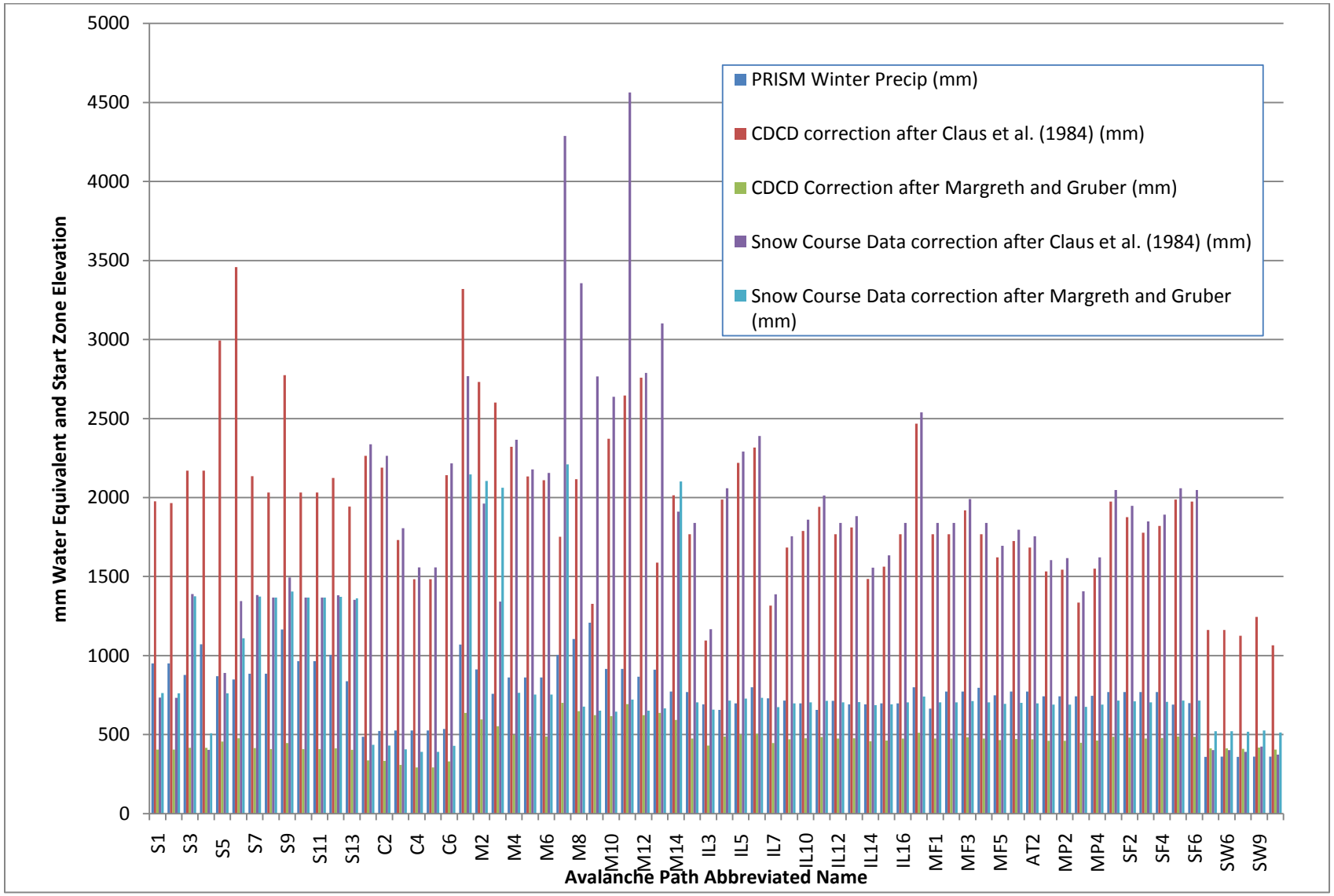

Figure 4.26 ; *Elevation corrected average winter snowfall and maximum recorded SWE for 70 avalanche paths in the Columbia Mountains, Fernie and Sparwood areas*

4.5.4 Correlation between Snow Water Equivalent and Avalanche Runout

As an initial step in analyzing the SWE and runout data, Pearson correlation coefficients were examined for the combined range dataset (n = 70). The Pearson R is a dimensionless value between -1 and 1 which provides a quantitative measurement of the strength of the relationship (Mendenhall and Sincich, 1995). A large (closer to 1) positive or negative number indicates that a linear trend may exist between the variables. The Pearson R and associated p-values between runout parameters (α angle and runout ratio) and the various SWE values are summarized in Table 4.24 below. Shaded values indicate acceptance of the null hypothesis at the 5% level ($p < 0.05$).

Table 4.24: *Pearson Correlation Coefficients between SWE and field observed α angle and runout ratio for combined mountain ranges (n=70). Bolding indicates significance at the 5% level*

	Field Observed α Angle		Field Observed Runout Ratio	
	Pearson R	p-value	Pearson R	p-value
PRISM	0.21	0.073	**0.24**	**0.042**
Snow Course: elevation corrected after Claus et al. (1984)	0.097	0.42	**0.26**	**0.029**
Snow Course: elevation corrected after Margreth and Gruber (1998)	**0.32**	**0.0074**	-0.13	0.28
CDCD: elevation corrected after Claus et al. (1984)	0.082	0.50	-0.017	0.89
CDCD: elevation corrected after Margreth and Gruber (1998)	**0.33**	**0.0049**	**0.28**	**0.019**

In an attempt to improve the correlation between SWE and avalanche path runout, the avalanche paths with a reference snow course station or CDCD weather station located greater than 10 km away from the starting zone were removed from the dataset. 10 km was chosen as an arbitrary distance which could improve the snowfall estimates without resulting in an unreasonably small sample size. Removing the sites with snowfall records further than 10 km away resulted in a subset of 35 avalanche paths from combined mountain ranges for the snow course data, and a subset of 42 avalanche paths from the combined mountain ranges for the CDCD data.

The Pearson correlation coefficients were re-calculated for the reduced datasets to give the R and p values summarized in Table 4.25.

Table 4.25: *Pearson correlation coefficients between SWE and field observed α angle and runout ratio for combined mountain ranges with reference sites within 10 km. Bolding indicates significance at the 5% level*

		Field Observed α Angle		Field Observed Runout Ratio	
		Pearson R	p-value	Pearson R	p-value
Reference Snow Course within 10 km (n = 35)	PRISM	**0.52**	**1.3E-03**	-0.16	0.36
	Elevation corrected after Claus et al. (1984)	-0.29	0.087	0.26	0.13
	Elevation corrected after Margreth and Gruber (1998)	**0.73**	**6.0E-08**	-0.17	0.34
Reference CDCD station within 10 km (n = 42)	PRISM	**-0.28**	**6.5E-03**	0.23	0.14
	Elevation corrected after Claus et al. (1984)	**-0.55**	**1.4E-04**	**0.30**	**0.048**
	Elevation corrected after Margreth and Gruber (1998)	**0.31**	**0.046**	0.010	0.95

For the significant correlations highlighted in Table 4.25 ($p < 0.05$), the Pearson R values suggest both positive and negative correlations between snowfall data and runout parameters (α angle and runout ratio). Physically, we would expect the relationship between SWE and α to be negative, since higher snowfall areas are more likely associated with longer running avalanches and smaller α angles. Similarly, we would expect a positive correlation between the runout ratio and SWE since a bigger runout ratio implies a longer running avalanche which should be physically associated with a high SWE. This is discussed further in Section 4.5.3.

To further examine the relationship between the runout parameters and snow water equivalents, linear regression and outlier analyses were examined for the possible significant relationships which are highlighted in Table 4.25.

From Table 4.25, the relationship between winter precipitation from the PRISM dataset and the observed α angle was analyzed by performing a linear regression as shown in Figure 4.27.

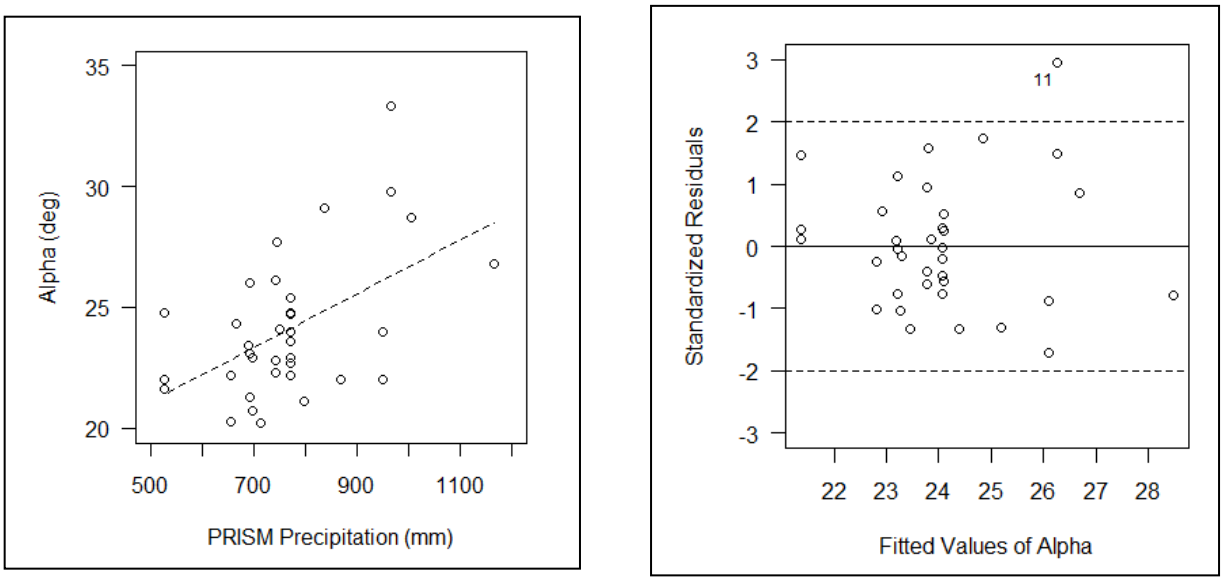

Figure 4.27: *Linear regression (left) and outlier analysis (right) of PRISM winter precipitation and α (n=35)*

Linear regression of the PRISM precipitation data and fitted α angle shows that path 11 is an outlier with a standard error greater than 2. This path is from the Kokanee Glacier Road near Nelson, BC, which only had a 10 year snow course record. Although there is no physical explanation for this outlier such as extraordinary long or short runout, or atypical terrain parameters, this path were removed from the dataset and the correlation was re-calculated for comparison. With the outliers removed, the recalculated Pearson R was 0.51 with a p-value of 1.9E-03 (n=31) indicating a slightly lower correlation.

Similarly, from Table 4.25, the relationship between the snow course extreme SWE value corrected for elevation after Margreth and Gruber (1998) and the observed α angle was analyzed by performing a linear regression and analysis of residuals as shown in Figure 4.28.

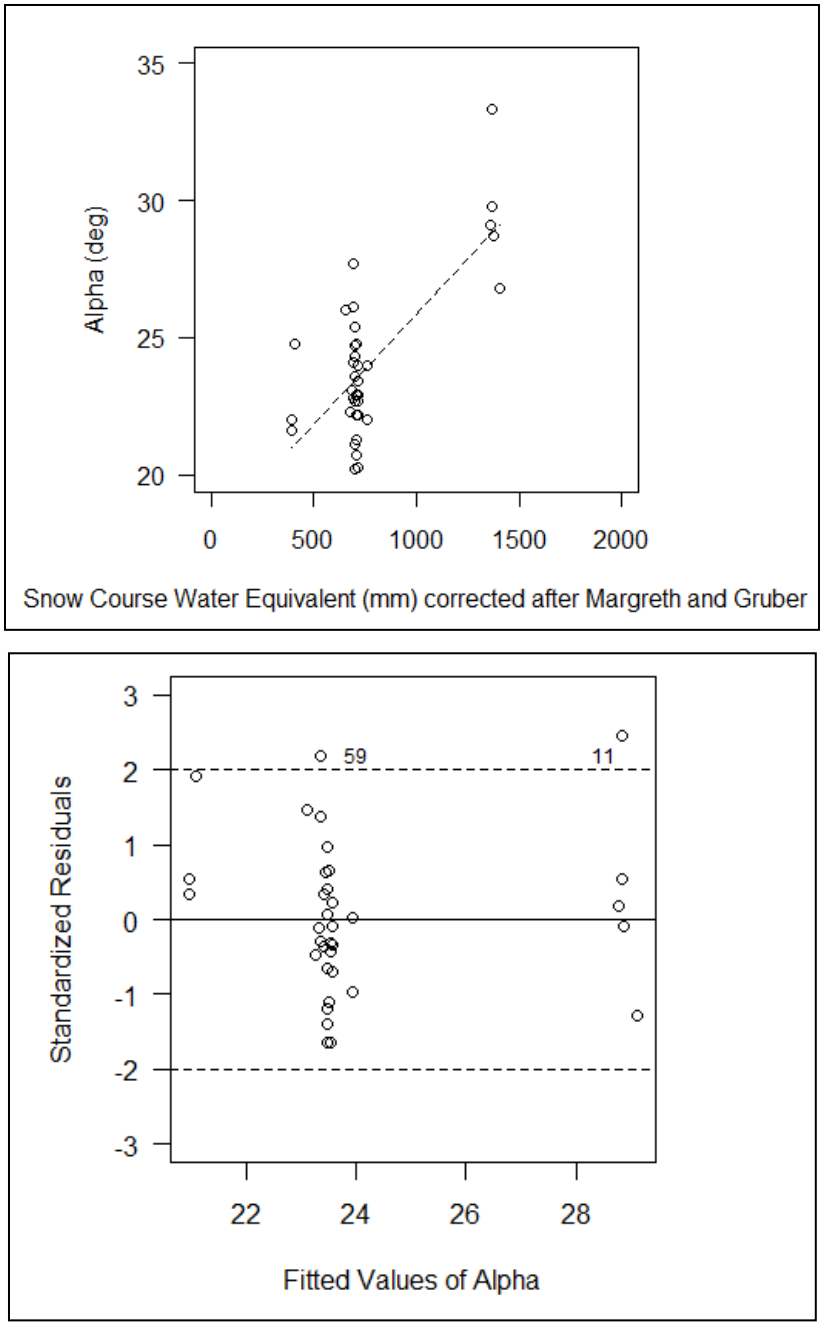

Figure 4.28: *Linear regression (top) and outlier analysis (bottom) of snow course data elevation corrected after Margreth and Gruber (1998) and α (n = 35)*

This analysis shows that paths 59 and 11 of the dataset are potential outliers. These paths are from Alpine Trails in Fernie BC (59) and from the Kokanee Glacier Road near Nelson, BC (11). Similar to the previous analysis, the Kokanee Glacier path is considered an outlier due to the shorter record used for the snow course extreme snowfall value (only 10 years of data available). Although there is no physical explanation for the other path such as extraordinary

long or short runout, or atypical terrain parameters, these paths were treated as statistical outliers and were removed from the dataset. With the outliers removed, the recalculated Pearson R was 0.72 with a p-value of 9.4E-07 (n = 33) indicating a slightly lower correlation.

Suggested correlations from the data subset with CDCD weather stations within 10 km were also examined by performing a linear regression and analysis of residuals as shown in Figures 4.29, 4.30 and 4.31.

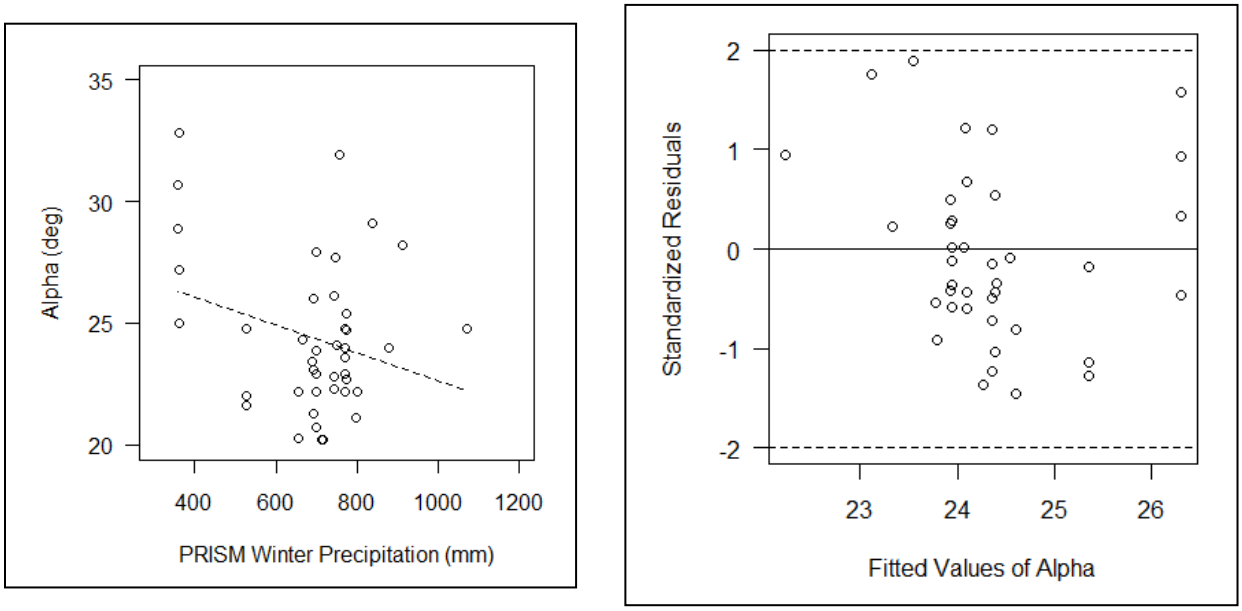

Figure 4.29: *Linear Regression (left) and outlier analysis (right) of PRISM Winter Precipitation and α for reduced dataset with Environment Canada stations within 10 km (n = 42)*

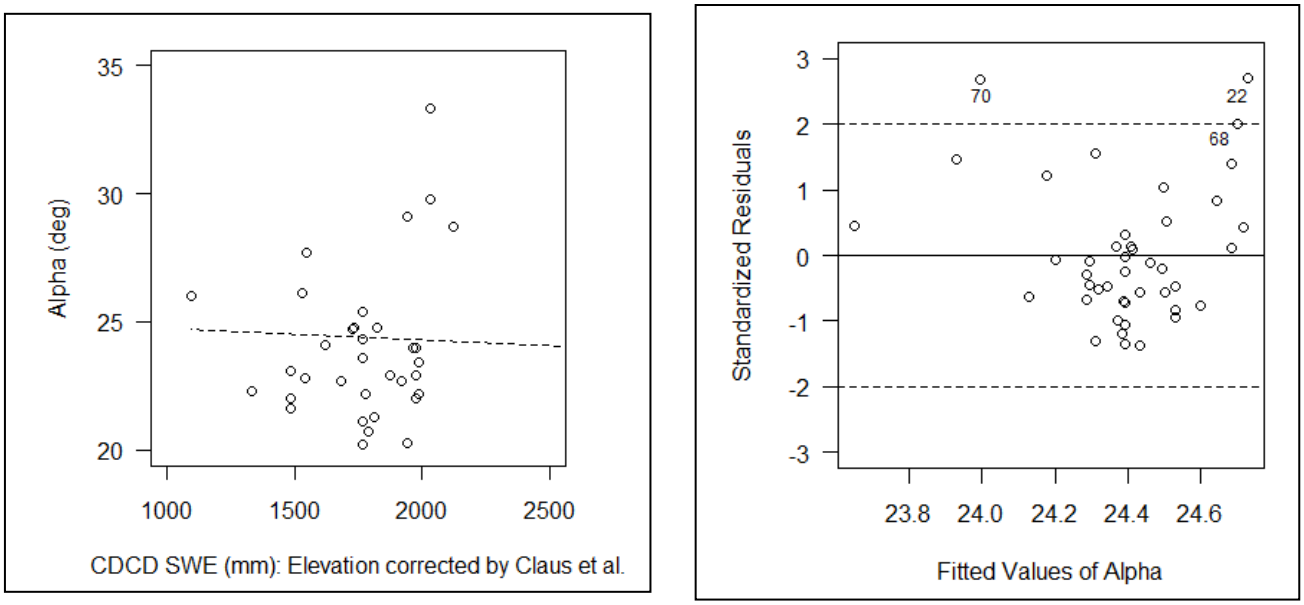

Figure 4.30: *Linear regression (left) and outlier analysis (right) of CDCD sites corrected for elevation by Claus et al. (1984) and α for the reduced dataset with Environment Canada stations within 10 km (n = 42)*

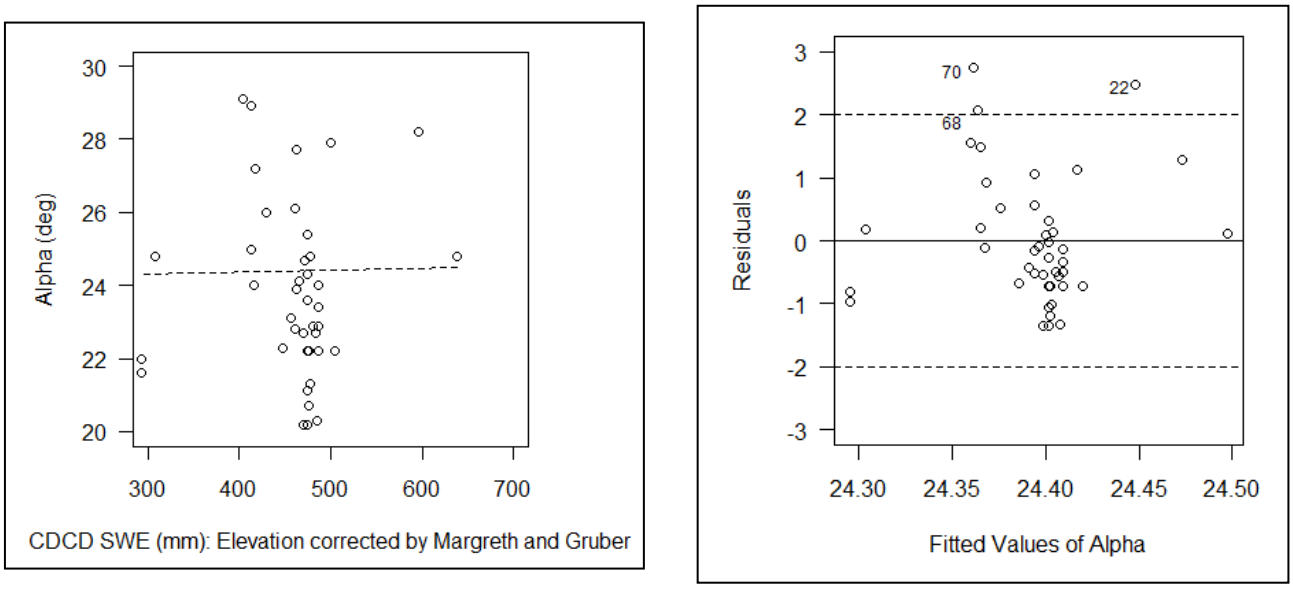

Figure 4.31: *Linear regression (left) and outlier analysis (right) of CDCD sites corrected for elevation Margreth and Gruber (1998) and Observed Alpha Angle for reduced dataset with Environment Canada stations within 10 km (n=42)*

Figure 4.29 does not show any outliers based on a standard error of 2.0. The Pearson R and p-value of -0.28 and 6.5E-03 are unchanged.

Figure 4.30 shows that avalanche paths 22, 68 and 70 are outliers for this correlation based on a standard error of 2. These paths are from Mt. MacPherson near Revelstoke, BC (22) and from two residential development sites in Sparwood (68 and 70). These outlying paths were removed from the dataset and the correlation was re-calculated for comparison. With the outliers removed, the recalculated Pearson R was -0.068 with a p-value of 0.67 (n = 39), indicating that the correlation is not significant.

Figure 4.31 shows these same three paths 22, 68 and 70 are outliers. These outlying paths were removed from the dataset and the correlation was re-calculated for comparison. With the outliers removed, the recalculated Pearson R was 0.01 with a p-value of 0.94 (n = 39), indicating that the correlation is not significant.

From Table 4.25, the only potential correlation with the field observed runout ratio and snowfall was for the data subset with Environment Canada stations within 10 km which were corrected for elevation after Claus et al. (1984). Figure 4.32 shows this linear regression and plot of the standard residuals.

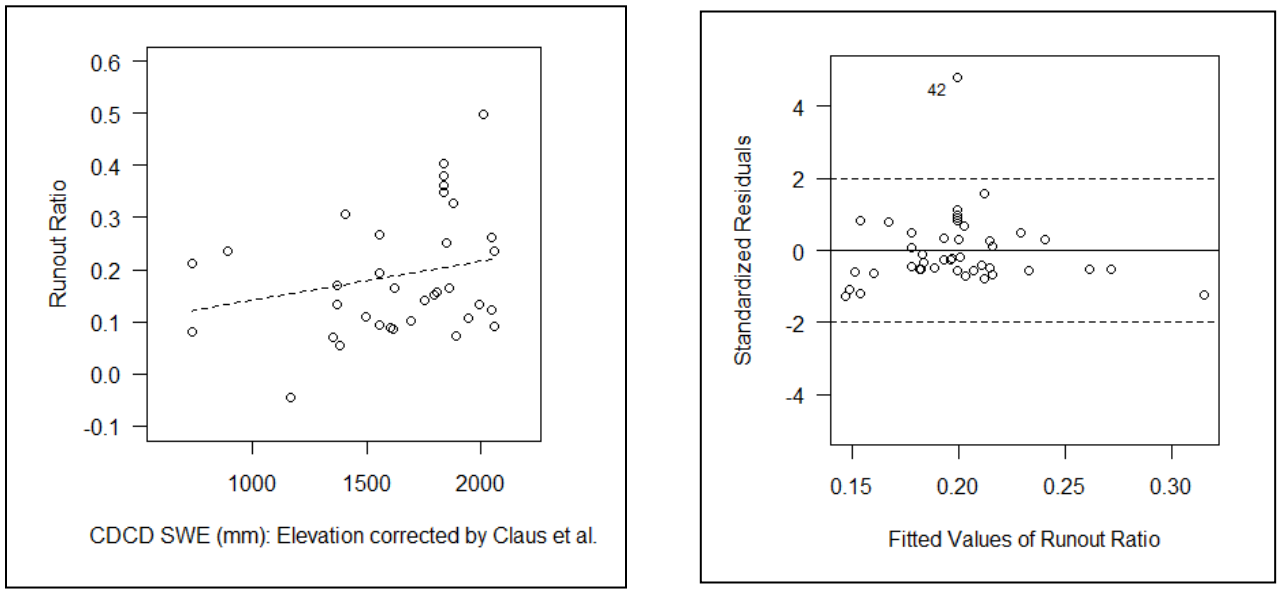

Figure 4.32: *Linear regression (left) and outlier analysis (right) of CDCD sites corrected for elevation by Claus et al. (1984) and observed runout ratio for reduced dataset with Environment Canada Stations within 10 km (n = 42)*

This analysis shows that path 42 (Big Steep Mother) from the Island Lake area in Fernie, BC is an outlier. Although there is no physical basis for the rejection of 'Big Steep Mother', this outlier was removed and the Pearson R was recalculated at 0.16 with a p-value of 0.33, indicating that the correlation is not significant.

4.5.5 Stepwise Multiple Regression between Snow Height and Terrain Variables

For the significant ($p < 0.05$) correlations identified in Section 4.4.4, a backwards elimination stepwise regression was performed to see if the snowfall data could be used to improve estimates of extreme avalanche runout. This analysis was done using the same procedure described in Section 4.2.1. Since the PRISM data were obtained directly for each starting zone location (not interpolated from a nearby weather station), this dataset consisted of the combined mountain range avalanche paths with the outliers identified in Section 4.4.4 removed. As an initial step, Pearson correlation coefficients were calculated between the dependent variable, α, and the independent terrain variables summarized in Table 4.26.

Table 4.26: *Summary of Pearson rank correlations between the response variable α, and predictor variables for the combined mountain range dataset with identified outliers removed (n =65)*

	Combined Ranges, Outliers Removed (n = 65)	
Predictor Variable	Pearson R	p-value
Winter Precipitation, W_Precip (mm)	**0.30**	**0.018**
Vertical height to low point on parabola, H_0 (m)	**0.45**	**1.6E-04**
Second derivative of slope function, y " (m^{-1})	0.19	0.13
Scale parameter for path profile, H_0y"	**0.68**	**3.5E-10**
Horizontal reach to β, X_β (m)	-0.19	0.14
Beta angle, β (°)	**0.85**	**2.2E-16**
Vertical fall to β, H_β (m)	0.20	0.10
Starting Zone Inclination, θ (°)	0.20	0.10
Starting Zone Aspect, SZ_Asp (deg)	**0.40**	**8.7E-04**
Starting Zone Elevation, SZ Elev (m)	0.050	0.69
Runout Zone Elevation, RZ Elev (m)	-0.21	0.087
Surface Roughness, SR (m)	-0.15	0.23
Wind Index, WI (unitless)	**-0.33**	**0.0080**
Width of Start Zone, W (m)	-0.13	0.29
Terrain Profile, TP (unitless)	0.13	0.31

For this combined mountain range dataset, an initial regression analysis of α on the predictor *variables H_0, H_0y'', β,* PRISM Precipitation (*W_Precip*), *SZ_Asp* and *WI* was performed. The backward elimination method was used to eliminate variables which were found to have a minimal effect on the model, based on the F value at the 1% significance level. For the initial 6 predictor regression (v_1 =6, v_2 =58), the threshold F-value was 3.12 (Mendenhall and Sincich, 1995, p. 1108). F-value results are summarized in Table 4.27.

Table 4.27: *F-values for six predictor stepwise regression for multi-range snowfall model (n=65); bolding indicates significance at the 1% level based on the threshold F-value of 3.12*

Variable	F-value
PRISM Winter Precipitation, W_Precip	0.0042
Vertical height to low point on parabola, H_0 (m)	**73.6**
Scale parameter for path profile, H_0y''	**160.0**
Beta angle, β (°)	**45.5**
Starting Zone Aspect, (SZ_Asp) (deg)	**4.60**
Wind Index, WI (unitless)	**17.8**

The resulting regression equation is included as Equation 4.20, and does not include the PRISM Winter Precipitation.

$$\propto = 10.03 + 0.00229H_0 + 7.56H_0y'' + 0.494\beta + 0.00631SZ\_Asp - 0.959WI$$

Equation 4.20

This model has an R^2 of 0.82, a standard error of 1.7 and uses 65 avalanche paths from the Columbia Mountains, Fernie Area and Sparwood area for model development.

A similar analysis was completed for the data subset with snow course stations within 10 km. Correlation coefficients between the dependent variable (α) and independent terrain variables are summarized in Table 4.28 and show that eight variables are carried forward for the backwards elimination stepwise multiple regression.

Table 4.28: *Summary of Pearson rank correlations between the response variable α, and predictor variables for the combined mountain range dataset with snow course stations within 10 km*

Predictor Variable	Combined Ranges, Outliers Removed (n = 29) Pearson R	p-value
Snow Course Water Equivalent elevation corrected by Margreth and Gruber (1998) (mm)	**0.72**	**5.8E-07**
Vertical height to low point on parabola, H_0 (m)	**0.38**	**0.021**
Second derivative of slope function, y " (m^{-1})	0.29	0.088
Scale parameter for path profile, H_0y"	**0.61**	**7.5E-05**
Horizontal reach to β, X_β (m)	-0.32	0.059
Beta angle, β (°)	**0.76**	**9.1E-08**
Vertical fall to β, H_β (m)	0.15	0.39
Starting Zone Inclination, θ (°)	-0.16	0.35
Starting Zone Aspect, SZ_Asp (deg)	**0.66**	**1.0E-05**
Starting Zone Elevation, SZ Elev (m)	0.092	0.59
Runout Zone Elevation, RZ Elev (m)	-0.029	0.87
Surface Roughness, SR (m)	-0.14	0.42
Wind Index, WI (unitless)	**-0.34**	**0.046**
Width of Start Zone, W (m)	**-0.47**	**0.0041**
Terrain Profile, TP (unitless)	**0.38**	**0.020**

For this combined mountain range dataset, an initial regression analysis was performed of α on the predictor variables listed here: Snow Course Water Equivalent (SC_{mm}), H_0, H_0y'',β, *SZ_Asp*, *WI, SZ_Width*, and *TP*. The backward elimination method was used to eliminate variables which were found to have a minimal effect on the model, based on the F value at the 1% significance level. For the initial eight predictor regression (v_1 =8, v_2 =22), the threshold F-value was 3.45(Mendenhall and Sincich, 1995 p. 1108).

Table 4.29: *F-values for six predictor stepwise regression for multi-range snowfall model with weather stations within 10 km (n = 29); shading indicates significance at the 1% level based on the threshold F-value of 3.45*

Variable	F-value
Snow Course Water Equivalent, corrected after Gruber and Margreth (1998), SC_{mm}	**6.83**
Vertical height to low point on parabola, H_0 (m)	**18.72**
Scale parameter for path profile, H_0y''	**54.86**
Beta angle, β (°)	**11.12**
Starting Zone Aspect, SZ_Asp (deg)	0.40
Wind Index, WI (unitless)	**5.44**
Terrain Profile, TP (unitless)	1.30

The resulting regression equation is as follows:

$$\propto = 12.64 + 0.0038SC_{mm} + 0.0016H_0 + 8.78H_0y'' + 0.290\beta - 0.893WI$$

Equation 4.21

This model has an R^2 of 0.72, a standard error of 1.5° and uses 29 avalanche paths from the Columbia Mountains, Fernie Area and Sparwood area. The significance and limitations of these models are compared to the previously developed regression models and discussed in Section 4.5.3.

4.6 Discussion of Results

4.6.1 Discussion of Alpha-Beta Model Results

In Section 4.2, α – β statistical runout models were developed for the Columbia Mountains and for the Fernie area. Table 4.28 summarizes previously developed model parameters along with the model parameters developed in this study for comparison.

Table 4.30: *Comparison of previously developed α – β model parameters and preferred α – β model parameters from this study*

Area	C_0	C_1	R^2	SE (°)	n	Reference
Rocky and Purcell Mountains	0.93	-	0.75	1.75	126	McClung and Mears, 1991
Sierra Nevada	0.67	2.50	0.60	-	90	McClung and Mears, 1991
Coastal Alaska	0.74	3.67	0.58	-	52	McClung and Mears, 1991
Colorado Rockies	0.63	4.68	0.50	-	130	McClung and Mears, 1991
Western Norway	0.93	-	0.93	2.1	192	McClung and Mears, 1991
Coast Mountains	0.90	-	0.74	1.70	31	Nixon and McClung, 1993
Iceland	0.85	-	0.72	2.2	44	Johannesson, 1998
Columbia Mountains (40 Year Observation Period)	0.93	-	0.89	1.10	35	Delparte et al., 2008
Columbia Mountains	0.90	0.69	0.90	1.4	33	this study
Columbia Mountains ($C_1 = 0$)	0.92	-	0.90	1.3	33	this study
Fernie Area	0.61	7.60	0.66	1.19	30	this study

Although the Columbia Mountains dataset is small, the model has an R^2 of 0.90 which indicates a better fit than most of the other regions except for Norway ($R^2 = 0.93$). Standard errors for the model parameters developed in this study are smaller than most of the other regions. The Fernie area model has an R^2 of 0.66 which is about the same as the fits for the Sierra Nevada, Coastal Alaska and the Colorado Rockies. Increasing the number of avalanche paths used to derive the model parameters for the Columbia Mountains and the Fernie area could improve the fits.

Figure 4.25 shows a graphical representation of previously developed α – β models along with the models developed as part of this study. This plot shows that over typical angle values for β (20-35°); avalanche paths from the Colorado Rockies and Sierra Nevada relatively further than in other regions.

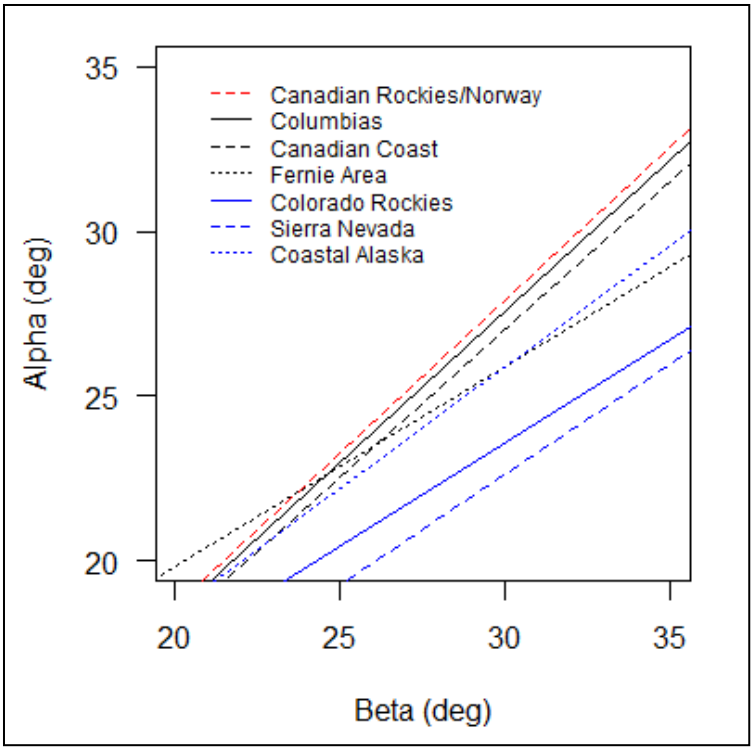

Figure 4.33: *Graphical comparison of α – β runout model parameters for North American and Norwegian Mountain ranges*

Figure 4.33 also shows that the models for the Canadian Rockies/ Purcells, Coast and Columbias are very similar, and that the estimated α angles in the Rockies are slightly bigger, indicating shorter runout distances, and the estimated α angles on the Coast are slightly smaller indicating longer runout distances than the Columbia Mountains.

The Fernie area and coastal Alaska models show that for higher β angles, the α angles are relatively smaller, and for lower β angles the alpha angles are relatively larger, or that scale effects are more pronounced in these areas. A possible physical explanation for this could be that both coastal Alaska and the Fernie area experience temperature fluctuations below and above 0° from starting zone to runout zone elevations, and it is not unusual for mountain top rain events to occur during any winter. However, this same climate occurs in the Canadian Coastal mountains, which have an α – β relationship much more like the Canadian Rockies and Columbias.

Delparte et al. (2008) developed an α – β model for the Columbia mountains (Selkirk Mountain sub-range) using avalanche path profiles obtained from high and low resolution digital elevation models (DEMs) along with avalanche runout observations recorded during a 40 year period in Glacier National Park. Comparing the models developed by Delparte et al. (2008) to the preferred model for the Columbias from this study shows that α angles calculated using the α – β method relationship presented in this study (α = 0.92β) are slightly smaller than the α angles calculated using the results of Delparte et al. (2008) (α = 0.93β). This is consistent with the fact that Delparte et al. (2008) used avalanche runout observed during a 40 year observation period, while the runout positions typically identified from observations of vegetative damage in western Canada are on the order of 50 – 300 years (McClung and Mears, 1991).

Although a co-efficient difference of 0.01 may seem of questionable importance, over the path length of a typical tall avalanche path this can translate to 10 – 20 m of runout distance, which is important for land use planning.

4.6.2 Discussion of Runout Ratio Model Results

In Section 4.3, runout ratio statistical models were developed for the Columbia Mountains and for the Fernie area. For both the Fernie area and Columbia mountain datasets, the runout ratio models showed acceptable fit to an extreme value distribution ($R^2 > 0.95$), and appropriate distribution of the residuals.

Table 4.31 summarizes previously developed model parameters along with the model parameters developed in this study for comparison. These parameters are also shown graphically in Figure 4.26.

Table 4.31: *Comparison of previously developed runout ratio model parameters and preferred runout ratio model parameters from this study*

Area	β (°)	u	b	Se	R^2	n	Reference
Rocky and Purcell Mountains	10	0.079	0.070	0.012	0.98	79	McClung and Mears, 1991
Sierra Nevada	10	0.374	0.206	0.041	0.98	90	McClung and Mears, 1991
Colorado Rockies	10	0.288	0.202	0.040	0.98	130	McClung and Mears, 1991
Western Norway	10	0.143	0.077	0.011	0.98	80	McClung and Mears, 1991
Coastal Alaska	10	0.185	0.108	0.023	0.97	52	McClung and Mears, 1991
Southwest Montana	18	0.0343	0.173	-	0.931	24	McKittrick and Brown, 1993
Canadian Coast Mountains (uncensored)	10	0.107	0.088	0.020	0.97	31	Nixon and McClung, 1993
Canadian Coast Mountains (censored)	10	0.096	0.092	0.021	0.96	20	Nixon and McClung, 1993
Canadian Short Slopes	24	0.494	0.441	0.08	0.98	46	Jones and Jamieson, 2004
Columbia Mountains	10	0.105	0.083	0.014	0.977	31	this study
Fernie Area	10	0.160	0.101	0.024	0.957	30	this study

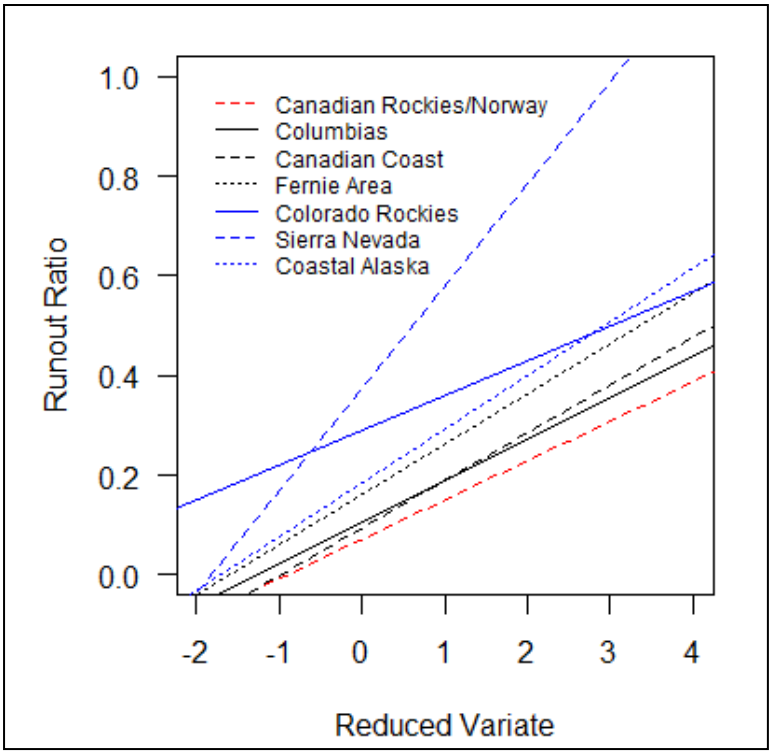

Figure 4.34: *Graphical comparison of runout ratio model parameters for North American and Norwegian Mountain ranges*

For land use planning, avalanche runout is typically estimated for non-exceedence probabilities from P= 0.5 to 0.85, or reduced variates (-ln-ln(P)) ranging from 0.36 to 1.8. Comparing the regional model parameters over this range shows that avalanche runouts in the Sierra Nevada are the longest followed by the Colorado Rockies, Coastal Alaska, Fernie, and then the Canadian Coast, Columbias and Rockies Mountains. This is consistent with the findings of McClung and Mears (1991), who observed that the highest runout ratio values came from regions with the gentlest terrain, specifically, the Colorado Rockies and the Sierra Nevadas. Comparing the models developed in this study (Figure 4.34) shows that the Fernie model is quite similar to that developed for coastal Alaska, and does not show marked effect of extremely gentle terrain like the Colorado Rockies or Sierra Nevada.

McClung et al. (1989) state that an advantage of the runout ratio model is that the extreme runout position can be calculated independently of the runout zone slope angle. However, $\alpha - \beta$ models may better reflect reality since real avalanches tend to run further on steeper runout zones. Nevertheless, McClung et al. (1989) statement implies that the runout ratio method can

tolerate some amount of uphill runout and that reasonable predictions for runout distances can be obtained without prior knowledge of the runout zone slope angle.

4.6.3 Discussion of Effect of Snow Water Equivalent

In Section 4.4.1, the correlation between SWE and runout parameters was explored by comparing three different methods of snowfall measurement to extreme runout parameters. Significant correlations from this analysis are summarized in Table 4.32.

Table 4.32: *Summary of significant snow water equivalent (SWE) and runout correlations*

	Pearson R	p-value	n
PRISM precipitation and α angle	0.58	4.5E-04	28
PRISM precipitation and α angle	0.54	0.0011	39
Snow course SWE and α angle	0.75	5.0E-07	29

For the significant correlations summarized above, the Pearson R values indicate positive correlations with α. Intuitively, we would expect this correlation to be negative, since extreme avalanche runout generally increases with snowfall in Canada (from the Rocky to Columbias to Coastal Mountains). Work completed by Fitzharris and Schaerer (1981) in the Rogers Pass area of the Columbia Mountains shows that winters with large avalanches may not have a heavy snowpack. A possible physical explanation for this could be that shallower snowpacks are usually associated with having a weaker base structure and more persistent weak layers throughout the season, which may promote longer running avalanches. For example, multiple regression runout models developed for mountain ranges in the United States (Table 4.30) show longer relative runout for the Sierra Nevada and Colorado Rockies (McClung, et al. 1989), both of which would have lower expected snowfall than Coastal Alaska.

This analysis is based on extreme snowpack water equivalent which is a measure of the amount of snow on the ground. For coastal snowpacks which generally have fewer persistent weak layers, climax avalanches may be related more to large storm events than to deep snowpacks. This has been shown in the dynamic runout model work of Margreth and Gruber (1998) and Schweizer (2009).

In Section 4.4, multiple regression methods were used to incorporate SWE for avalanche path starting zones into a model for avalanche runout. After removing outliers and performing a backwards elimination stepwise multiple regression, Equation 4.19 which incorporates extreme snow pack water equivalent was developed. This equation uses the extreme SWE value from the nearest snow course (within 10 km of the avalanche path starting zone) corrected after Margreth and Gruber (1998) for the starting zone elevation. The period of record for the snow courses used in this analysis ranged from 10 to 83 years. The elevation correction used is a linear correction which assumes that snow height increases by 5 cm for every 100 m increase in elevation.

For comparison, this model (Equation 4.19) is summarized in Table 4.33 along with the cross range and individual range full regression models.

Table 4.33: *Comparison of cross range and regional multiple regression models*

Description	Equation	R^2	SE	n
Cross range model (Equation 4.20)	$\propto = 10.03 + 0.00229H_0 + 7.56H_0y" + 0.494\beta + 0.00631SZ\_Asp - 0.959WI$	0.82	1.7	65
Cross range regression incorporating snow course data (Equation 4.21)	$\propto = 12.64 + 0.0038SC_{mm} + 0.0016H_0 + 8.78H_0y" + 0.290\beta - 0.893WI$	0.72	1.5	29
Columbia Mountains (Equation 4.5)	$\alpha = 5.87 + 0.00094H_0 - 0.49H_0y" + 0.78\beta + 0.002SZ\_Asp - 0.88WI$	0.93	1.3	33
Fernie Area (Equation 4.3)	$\propto = 8.35 - 2529y + 1.27\mathrm{H_0y"} + 0.63\beta - 0.002SZ\_Width$	0.73	1.0	30

The intent of incorporating snowfall into the regression equation would be to provide practitioners with an improved model for estimating extreme runout by incorporating the extreme SWE value from the nearest snow course station (within 10 km to the starting zone). Table 4.33 shows that the fit for Equation 4.20 is no better than the fits for the individual range models which do not incorporate the SWE data. This agrees with the work of others which has shown the best statistical avalanche runout models derived to date are based solely on terrain

parameters and are independent of climate (McClung et al. 1989; Lied and Bakkehöi, 1980; Bovis and Mears, 1976;)

One problem with this analysis is that there are several interpretations and assumptions involved in extrapolating snow course data to avalanche path starting zones. Even by excluding snow course sites further than 10 km from each starting zone, the distance between the starting zones and snow courses still ranged from 2.9 to 9.9 km, and the length of record ranged from 10 to 83 years of data.

The bigger limitation of this analysis, likely has to do with the fact that extreme avalanches are related more to extreme storm events than to extreme snowpack water equivalent or to average weather conditions.

4.6.4 Limitations of Statistical Models

The statistical models presented in this paper were developed using "typical" avalanche paths from the Columbia Mountains and the Fernie area with vertical fall heights over 350 m. This analysis excluded paths with significant uphill runout (such as those found in narrow valleys) or paths with a high degree of channelization in the track and/or runout zone. This analysis included paths which were not substantially channelized and which had little uphill runout.

Paths with uphill runout will usually have a smaller Δx than paths with no uphill runout and paths which are channelized in the track or runout zone will typically run further than paths without confinement (Johnston et al., 2011). Caution must be exercised when applying these runout models to atypical paths.

McClung and Mears (1991) indicated that these methods can be applied to complete or censored datasets of at least 30 paths which have records of producing major (100-year) avalanches. For the Columbia Mountains and Fernie area models developed in this study, the number of paths meet, but do not exceed this criteria. Repeating this analysis with a larger dataset could increase the accuracy of these estimates and also improve user confidence with using statistical runout models in these areas.

4.7 Summary

In this chapter, multiple regression methods and extreme value statistics were used to develop α – β and runout ratio statistical model parameters for the Columbia Mountains and for the Fernie Area.

After removing an outlier from the Fernie data, a simplified α – β model (R^2 = 0.64, SE = 1.19°, n = 30) was developed which can be used to estimate the extreme runout for a given path based on the definition of the β-point defined as the position where the slope incline first decreases to 10°. Inclusion of other terrain variables, *y", H_0y"* and starting zone width (*SZ_Width*) improved the fit of this model (R^2 = 0.77, SE = 1.0°, n = 30); however, since some knowledge of extreme runout position is required to accurately estimate H_0 and *H_0y",* the simplified model may prove more useful.

For the Columbia Mountains, a simplified α – β model (R^2 = 0.90, SE = 1.3°, n = 33) was proposed which can be used to estimate the α angle for a given path also based on the 10° definition of the β-point. Inclusion of other terrain variables: *H_0, H_0y",* starting zone aspect (*SZ_Asp*) and wind index (*WI*) give a slightly improved the fit of this model (R^2=0.93, SE=1.1°, n=33). Avalanche path data from sub-ranges in the Columbia Mountains (Selkirk, Cariboo and Monashee Mountains) was also analyzed separately to look for potential trends on a sub-range basis. This analysis showed that avalanche paths in the Monashee Mountains may run farther than paths in the Selkirks, but that the overall fit was not improved for sub-ranges.

Extreme value statistical analysis was also used to develop runout ratio model parameters for both mountain ranges. Similar to the multiple regression analysis, the "Fish Bowl" avalanche path was removed from the Fernie data set which dramatically improved the fit of the runout ratio model for this region (R^2 = 0.957, SE = 0.024, n = 30). The Fernie dataset shows a distinct jump in the data at a runout ratio of about 0.2, and analyzing the data above and below the jump separately slightly improved the fit of the model, although the sample sizes of the split dataset are too small to be considered representative.

For the Columbia Mountains, two avalanche paths were removed from the dataset for the runout ratio analysis based on physical terrain properties. Removal of these two paths resulted in an acceptable fit for the runout ratio analysis (R^2 = 0.977, SE = 0.014, n = 31), and censoring the dataset (removing paths with low runout ratio) did not improve the fit.

To explore the relationship between climate and extreme runout, SWE data were interpreted for each avalanche path starting zone using an available raster dataset (PRISM monthly average precipitation) and by analyzing available provincial snow course and federal weather station data. Two different elevation corrections were applied to the snow course and weather station data to come up with extreme SWE values for each avalanche path starting zone. Pearson correlation coefficients and multiple regression methods were used in an attempt to incorporate SWE into extreme runout estimations, and all but one model was rejected. The accepted model uses data from the combined mountain ranges with reliable snow course records and uses *SWE, H_0, H_0y'', β*, and wind index (*WI*) to estimate the α angle (R^2 = 0.72, SE = 1.52, n = 29). Neither the fit, nor the size of the dataset is improved for this model. One challenge identified with this analysis includes the difficulty with obtaining accurate extreme SWE data for avalanche starting zone locations. The most important obstacle to this analysis is that extreme avalanche runout is related more to extreme storm events (Schweizer et al., 2009) rather than snowpack water equivalent or average winter precipitation.

5.0 CONCLUSIONS

5.1 Thesis Conclusions

α – β and runout ratio statistical models are common methods which are used to estimate extreme avalanche runout for land zoning purposes. These model results are combined with dynamic model estimates, historical observations, aerial photo analysis and field observations of vegetative damage to determine hazard lines for zoning. Expert judgment of the avalanche hazard mapper is critical to determining the level of confidence which can be placed on model estimates, field observations and historical data.

This study expanded on the work of others by deriving α – β and runout ratio parameters for tall avalanche paths (H > 350 m) in the Columbia Mountains and for the area around Fernie, BC. Terrain parameters and extreme runout observations from 33 avalanche paths in the Columbia Mountains were used to derive model parameters which can be used for tall paths in this range. For the area near Fernie, BC, terrain parameters and extreme runout observations from 31 tall avalanche paths are used to derive model parameters for this area. The statistical models developed in this study can be used to predict extreme avalanche runout for "typical" avalanche paths including those without significant channelization or uphill runout.

In accordance with the objectives outlined in Section 1.11, the conclusions of this thesis are summarized in the following sections.

5.1.1 Fernie Area Statistical Models

A total of 31 avalanche paths from the Fernie area were analyzed using multiple regression and extreme value statistics to give the following results:

- After removing an outlier (the "Fish Bowl" avalanche path), the remaining 30 paths were used to develop a model (Equation 4.3) using multiple regression methods. The terrain parameters *H_0y", β* and *SZ_Width* were used to estimate the *α* angle for extreme runout (adjusted R^2 = 0.73, SE = 1.03).
- A simplified regression model (Equation 4.4) which used β as the only predictor for α is also presented (R^2 = 0.64, SE = 1.19).

- Runout ratios for the remaining 30 paths from the Fernie area are well fit to a Gumbel distribution (adjusted R^2 = 0.96, SE = 0.024). This model (Figure 4.15) can be used to estimate extreme runout for other avalanche paths in the region.
- The best runout ratio fit was obtained by limiting the dataset to the 14 avalanche paths (Figure 4.17) with runout ratios above x_p = 0.2 (R^2 = 0.97, SE = 0.013). Although this gives a favourable fit to the longer running avalanche paths in this range, the model developed with the larger dataset is preferred.

5.1.2 Columbia Mountains Statistical Models

A total of 33 avalanche paths from the Columbia Mountains were analyzed using multiple regression and extreme value statistics to give the following results:

- The 33 paths were used to develop a model using multiple regression methods (Equation 4.5). The terrain parameters H_0, H_0y'', β, *SZ_Asp*, and *Wind_I* can be used to estimate the α angle for extreme runout (adjusted R^2 = 0.94, SE = 0.041).
- A simplified regression model (Equation 4.8) is also presented which uses β as the only predictor and forces the constant C_0 = 0. This simplified model predicts the extreme runout angle α (R^2 = 0.90, SE = 0.045), and can also be used to estimate extreme avalanche runout is this region.
- Avalanche paths from the Monashee, Selkirk and Cariboo sub-ranges of the Columbias were analyzed individually using multiple regression methods. Results suggest that avalanche paths in the Monashees run further than paths in the Selkirks and Cariboos; however, the sample sizes are small and are only useful for comparing general trends.
- After removal of two outlying paths, runout ratio analysis for the Columbia mountains shows an acceptable fit to a Gumbel distribution (R^2 = 0.98, SE = 0.014, n=30). Censoring the dataset for longer running avalanches does not have a large effect on the fit (R^2 = 0.97, SE = 0.014, n = 20), and the model developed using the full dataset is preferred.

5.1.3 Influence of Climate on Runout

The relationship between climate and runout was analyzed using a dataset of 70 avalanche paths from the Fernie Area (n=31), Columbia Mountains (n=33) and Sparwood Area (n=6). For

this analysis, extreme and average snowfall and SWE values were obtained from a number of sources including a modeled raster dataset and available snow course and weather stations. Pearson rank correlations and multiple regression methods were used to explore the relationship between SWE and avalanche runout with the following results:

- Pearson correlation coefficients between extreme snowfall values and α angles ranged between -0.548 and 0.725. Physically, the correlation coefficients are expected to be negative assuming that higher snowfall relates to longer running avalanches and therefore smaller α angles.
- Including the SWE_{ex} obtained from snow course stations within 10 km of avalanche path starting zones results in a multiple regression relationship between α and H_0, H_0y'', β, and *Wind_I* (adjusted R^2 = 0.72, SE = 1.52, n = 29). This model has a higher SE than the individual range models (Equation 4.3 and 4.5) which exclude SWE data.
- Although this analysis suggests that extreme SWE may be a useful parameter for extreme runout predictions, the lack of reliable and representative snowfall records for avalanche path start zones limits the practical application of this method.

5.2 Recommendations for Further Research

The Fernie area is known for having a much higher snowfall and milder temperatures than other parts of the Rocky Mountains. Local knowledge suggests that this heavy snowfall area includes, but is not limited to local Rocky Mountain sub-range known as the Lizard Range. Quantifying the boundaries of this climatic region would be useful for choosing which runout model parameters to apply in this area.

Model parameters were derived for the Fernie area using a dataset of 30 avalanche paths with vertical drops over 350 m. Assuming that short avalanche paths (H < 350 m) in this area also run proportionally farther than other areas of the Rocky Mountains, extending this analysis to short avalanche slopes could improve accuracy for short slope runout estimations in this region.

Similar to the work done by McKittrick and Brown (1993) in Montana and by Jones and Jamieson (2004) for Canadian short slopes, the α - β regression analysis for the Fernie area may be improved by re-defining the β-point at a position farther upslope.

The runout models developed for the Columbia Mountains used 13 avalanche paths from the Selkirks, 14 paths from the Monashees and 6 paths from the Cariboo sub-ranges. Analysis of data from the individual sub-ranges suggests trends in runout distances between the sub-ranges, but the sample sizes in this study are small. A larger dataset incorporating 30 paths from each sub-range could be used to develop sub-range model parameters and increase accuracy for runout estimates on a sub-range basis.

The snowfall and runout analysis was complicated by several sources of uncertainty, mainly to do with extrapolating snowfall data from measurement stations to avalanche path starting zones. Reliable, high-elevation snowfall data and snowpack water equivalent data could greatly improve this analysis. Specifically, new snow data including the 3-day storm snowfall could be used to compare extreme snow storm data to long running avalanches.

REFERENCES

Bakkehöi, S. 1987. Snow Avalanche Prediction using a Probabilistic Method. Avalanche Formation, Movement and Effects. Proceedings of the Davos Symposium, Semptember 1986.

Bovis, M., Mears, A., 1976. Statistical Prediction of Snow Avalanche Runout from Terrain Variables in Colorado. Arct. Alp. Res. 8, 115-132.

British Columbia Government, 2002. Biogeoclimatic Zones of British Columbia. Victoria, British Columbia: Ministry of Forests and Range.

British Columbia Government, 2010. British Columbia Water Resources Atlas. Accessed via the world wide web: http://www.env.gov.bc.ca/wsd/data_searches/wrbc/index.html

Campbell,C., Bakermans, L., Jamieson, B., Stethem, C., 2007. Current and Future Snow Avalanche Threats and Mitigation Measures in Canada. Revelstoke: Canadian Avalanche Association.

Campbell, C.B. 2008. Avalanche threats and mitigation measures in Canada. Proceedings of the 2008 International Snow Science Workshop in Whistler, BC, Canada, (pp. 836-844). Whistler, British Columbia.

Canadian Avalanche Association (CAA), 2002. Guidelines for Snow Avalanche Risk Determination and Mapping in Canada. McClung, D.M., Stethem, C.J., Schaerer, P.A, Jamieson, J.B. (eds.). Canadian Avalanche Association, Revelstoke, BC, Canada.

Canadian Avalanche Association (CAA), 2002. Land Managers Guide to Snow Avalanche Hazards in Canada. Jamieson, J.B., Stethem, C.J., Schaerer, P.A., McClung, D.M. (eds.). Canadian Avalanche Association, Revelstoke, BC, Canada.

Canadian Avalanche Association (CAA). 2007. Observation Guidelines and Recording Standards for Weather and Avalanches. Revelstoke, British Columbia: Canadian Avalanche Association.

Daly, C.N., 1993. A Statistical - Topographical Model for Mapping Climatological Precipitation over Mountainous Terrain. J. Appl. Meteorol., 33, 140 - 158.

Delparte, D. 2008. Avalanche terrain modeling in Galcier National Park, Canada, PhD Thesis. Unviersity of Calgary, Department of Geography, Calgary, Alberta.

Delparte, D., Jamieson, B., Waters, N., 2008. Statistical runout modelling of snow avalanches using GIS in Glacier National Park, Canada. Cold Reg. Sci. Technol. 54, 183-192.

Durbin, J.W., Watson, G. 1951. Testing for Serial Correlation in Least Squares Regression II. Biometrika, 38, 159-177.

Environment Canada. 2000. Canadian Daily Climate Data CDCD V1.02. Climate Information Branch Atmospheric Environment Service.

Gumbel, E. 1958. Statistics of Extremes. New York: Columbia University Press.

Gubler, H. 1987. Measurements and modelling of snow avalanche speeds. Avalanche formation, movement and effects. Proceedings of the Davos Symposium (405-420). September, 1986.

Jamieson, B. 2009. Snow Avalanche Hazard Mitigation. Universty of Calgary ENCI 751 Course Notes. Calgary, Alberta.

Jamieson, B., Haegeli, P., Gauthier, D. 2010. Avalanche Accidents in Canada Volume 5, 1996 - 2007. Revelstoke, British Columbia: Canadian Avalanche Association.

Johannesson, T. 1998. A tographic model for Icelandic avalanches. Reykjavik, Iceland: Icelandic Meteorological Office Report Vi-G980003-UR03.

Johnson, R. 2005. Miller and Freund's Probability and Statistics for Engineers 7th Ed. Upper Saddle River: Pearson Prentice Hall.

Johnston, K., Jamieson, B. 2010. Estimating Extreme Avalanche Runout for the Lizard Range, Fernie, British Columbia. Proceedings of the 2010 International Snow Science Workshop, (252-257). Tahoe, CA.

Johnston, K., Jamieson, B., Jones, A. 2011. Estimating extreme snow avalanche runout for the Columbia Mountains, British Columbia, Canada. Proceedings of the 5th Canadian Conference on Geotechnique and Natural Hazards. Kelowna, BC.

Jones, A., Jamieson, B., 2004. Statistical avalanche runout estimation for short slopes in Canada. Ann. Glaciol. 38, 363-372.

Lied, K., Bakkehöi, S., 1980. Empirical calculations of snow avalanche runout distance based on topographic parameters. J. Glaciol. 26, 165-177.

Maindonald, J. B. 2010. Data Analysis and Graphics Using R - an Example-Based Approach 3rd Edition. Cambridge: Cambridge University Press.

Margreth, S., Gruber, U. 1998. Use of Avalanche Models for Hazard Mapping. Proceedings of the Symposium: Snow as a Physical, Ecological and Economic Factor. Davos, Switzerland.

McClung, D.L. 1987. Statistical and Geometric Definition of Snow Avalanche Runout. Cold Reg. Sci. Technol. 13 (2), 107-119.

McClung, D., Mears, A.I., Schaerer, P., 1989. Extreme avalanche runout: data from four mountain ranges. Ann. Glaciol. 13, 180 – 184.

McClung, D. 1999. The Encounter Probability for Mountain Slope Hazards. Can. Geotech. J., (36) 1195 -1196.

McClung, D., Mears, A., 1991. Extreme value prediction of snow avalanche runout. Cold Reg. Sci. Technol. 19, 163-175.

McClung, D., 2001. Extreme Avalanche Runout: A Comparison of Empirical Methods. Can. Geotech. J., 1254-1265.

McClung, D., Schaerer, P., 2006. The Avalanche Handbook (3rd Ed.). The Mountaineers Books, Seattle, Washington.

McKittrick, L., Brown, R. 1993. A statistical model for maximum avalanche run-out distances in southwest Montana. Ann. Glaciol. 18, 295-299.

Mears, A. 1984. Climate Effects on Snow Avalanche Travel Distances. Proceeding of the International Snow Science Workshop, 80-83. Aspen, Colorado.

Mears, A. 1988. Comparisons of Colorado, E.Sierra, Coastal Alaska and Western Norway Avalanche Runout Data. Proceedings of the International Snow Science Workshop, 232-238. Whistler, British Columbia.

Mears, A. 1989. Regional comparison of avalanche-profile and runout data. Arct. Alp. Res. 21, 283-287.

Mears, A. 1992. Snow-Avalanche Hazard Analysis for Land-Use Planning and Engineering. Colorado Geological Survey, Denver, Colorado.

Mendenhall, W.S., Sincich, T. 1995. Statistics for Engineering and the Sciences 4th Edition. Prentice Hall.

Nixon, D., McClung, D., 1993. Snow avalanche runout from two Canadian mountain ranges. Ann. Glaciol. 18, 1-6.

Perla, R. Cheng, T., McClung, D. 1980. A two-parameter model of snow-avalanche motion. J. Glaciol. 26. 197-207.

Perla, R., Lied, K., Kristensen, K. 1984. Paricle simulation of snow avalanche motion. Cold Reg. Sci. Technol. 9, 191-202.

Perla, R., & Martinelli, M. 1976. Avalanche Handbook. US Department of Agriculture, Forest Service Agriculture Handbook No. 489.

Schaerer, P. 1977. Analysis of snow avalanche terrain. Can. Geotech. J. 14, 281-287.

Schaerer, P. 1971. Relation between the mass of avalanches and characteristics of terrain at Rogers Pass, British Columbia, Canada. Proceedings of the Moscow Snow and Ice Symposium held August 1971. 378-380.

Schweizer, J. Mitterer, C., Stoffel, L. 2008 Determining the critical new snow depth for a destructive avalanche by considering the return period. Proceedings of the International Snow Science Workshop, 292-298. Whistler, BC.

Schweizer, J., Mitterer, C., Stoffel, L. 2009. On forecasting large and infrequent snow avalanches. Cold Reg. Sci. Technol, 59, 234-241.

Smith, M., McClung, D. 1997. Avalanche frequency and terrain characteristics at Rogers Pass, British Columbia, Canada. J. of Glaciol. 43, 165-171.

Tremper, B. (2008). Staying Alive in Avalanche Terrain (2nd ed.). Seattle, Washington: The Mountaineers Books.

APPENDIX A: Example Field Notes

WP002 - lots of dead trees + down timber, not facing downhill + down from the root bulbs.

WP003 - 5+ broken off trees, different heights + ages: see photos
- mostly facing downhill but variable
~ 45-60cm diameter.

WP004 - hemlock, well over 1.5 m diameter, see photo of leaves.
- lots of timber down here also.

WP005 - ignore

WP006 - RZ below deposit
- still some older trees, for the most part forest is getting younger

WP007 - high point on alluvial fan/RZ where flow seems to split into 2 fingers

No. 612
J.L. DARLING CORP. TACOMA, WA 98424-1017
www.RiteInTheRain.com
DURA

WP008- standing on debris

WP009- looking into deep channel full of wet debris
~ 8m deep
- ground cover is nil (v small 0.20m aldr) + small rocks.

- avalanche clearly ricochets off sides of channel (see trimline photos)

- 2 seperate SZ's, probably don't release together, but more photos to come.

WP010- photos towards RZ note v. trimline: looks like alluvial fan: difficult to tell difference betwn any trim line + fan trim line

- under also recent wet deposit following gullied terrain stairs RHS of fan.

- bottom of incised channel: much more damage on stairs RHS, vegetation on RHS of channel mainly aspen up to 0.20m diameter, high frequency in channel, also looks high frequency.

WP011 ground cover mainly aldr ~ 0.40m high
some 3 year old conifers.
- very nice view of trimlines in RZ
- just above us (maybe 10m) there is exposed bedrock in channel.

No. 612
J.L. DARLING CORP. TACOMA, WA 98424-1017
www.RiteintheRain.com

No. 612
J.L. DARLING CORP. TACOMA, WA 98424-1017
www.RiteintheRain.com

WP	ALT	SLOPE (y)	ψ	Comments
011	1010	xx	xx	start survey
xx		28y	22	below gully
012	1000	~~x~~	~~x~~	W= 30+164y
		37	22.5	W= 147+33
013/014(FL)	985			W= 125+64
		39	21.5	widens on bot/su
015	970			W= 115+108
		42	22	
016	955			bear in path.
		33	21.5	W= 126+132
017	940			W= 196+114
		54	215	(RHS)
018	920			W= 159+?
		55	20.5	
019	900			W= ?
		29	20	
020	895			
		35	18.5	W?
021	885	break in slope where debris stopped.		
		41	17	
022	870			
		38	13	
x23				

WP030 - increment bore of stand of trees in middle of RZ.
Age ~ 50 yrs.
*see photos.

P033 - see photo of damage on aspen, also lots of recent timber facing downhill + newly broken stumps trees on ground ~ 50 yrs.

P036 - increment bore of aspen here ~ 30 yrs
moving more into a mixed age forest

*heading straight down to river from here

No. 612
J. L. DARLING CORP. TACOMA, WA 98424-1017
www.RiteintheRain.com

WP	ALT	SLOPE	↺	Comments
024	865			near LHIs.
		52	10	on debris f.
025/026	FL 850			
		20	11	bigger alder ~ 1.5m.
027	845			
		28	7.5	
028	840			some older trees / tree island.
		24	9.5	
029	840			
		28	6.0	btwn flow
031	840			
		34	7.5	more debris on ground lined up
032	835			
↳ following	longest fuga	34	6.0	@ aspen trm line
033	830			primarily aspen here.
↳ vegetation change		23	5.5	
↳ 034	825			conifers ~ 20 yrs.
		20	6.0	no damage.
035	825		~~6.5~~	@ aspen.
		22	6.5	still diff debris on ground.
036	820			
		16	6.0	trees lined up @ SRHs.
037	825			
		23	4.0	

039- move to SLHS for fall line for large slides, lots of lined up timber on ground here.

040- flagging on conifers.

041- increment bore of conifer: moving move into a mixed age forest
age ~ ~~years~~ 100yrs
- shll some snapped + damaged trees + timber on ground.
- diam ~ 20"

042- almost e river: shll some debris on ground.

046- SLHS trim line e river

047- vegetative damage from erosion, not avalanche.

WP	ALT	Slope	W	Comm:
038	825			shll damage on
		20	4.0	trees, 30y+
039/040	FL 830			trees in leaders.
		20	2.5	
041	830			see notes.
		19	3.5	
042	830			
		23	4.0	
043	825			
		7	6.5	top of river bank
044	825			flagging on tree.
		68	0	middle of
045	825			river bed
		81	0	
048	830	81	to	across river
		~~EL~~	for side	flagging
		22	-2.0	
049	835			* small trees, floodplain here.
		26	-1.0	
050	835			
		28	-0.5	
051	830			* channel here
		29	-1.0	

No. 612
J.L. DARLING CORP. TACOMA, WA 98424-1017
www.RiteInTheRain.com
DURASTEEL

047 - below avalanche path @ river: floodplain here, smaller trees + uniform ages ~ 20yrs.

050 - another branch of river, small, unhealthy trees on floodplain (bar)

look back @ SZ: 4 observations
- lookers left seems to be biggest + capeable of producing biggest slides.
- distinct sections of SZ probably not likely to release together, but possible.

055 - not natural forest hole (possibly cleared) @ snow point)
- increment bore of conifer = 40+ yrs old.

APPENDIX B: Example Avalanche Path Plot

Profile of Mica Mountain 2

Sources: Above 1500 m: Contour Map 1:20,000 TRIM, June 2010
Below 1500 m: Field Survey by Mike Smith and Katherine Johnston, July 20, 2010

Segment/ GPS	Elevation	Horizontal distance	Slope distance	Incline	Width
	2220				
1		80	82.4621	14.036	250
	2200				
2		170	197.231	30.466	250
	2100				
3		140	172.047	35.538	250
	2000				
4		120	126.491	18.435	250
	1960				
5		80	100	36.87	250
	1900				
6		180	205.913	29.055	250
	1800				
7		240	260	22.62	250
	1700				
8		180	189.737	18.435	270
	1640				
9		120	126.491	18.435	270
	1600				
10		120	126.491	18.435	270
	1560				
11		120	134.164	26.565	270
	1500				
12		22.200213	24.7	26	270
	1490				
13		26.970792	29.3	23	
	1485				
14		20.920191	22.9	24	
	1470				
15		27.799247	30.2	23	
	1465				
16		30.714796	32.9	21	
	1450				
17		31.62551	32.9	16	
	1445				
18		34.808668	36.6	18	
	1435				
19		33.517626	34.7	15	
	1425				
20		33.669262	34.7	14	
	1415				
21		31.289759	32.9	18	
	1405				
22		18.456225	19.2	16	
	1400				
23		28.429665	29.3	14	
	1390				
24		15.3	15.7025	13	
	1390				
25		24.9	25.6623	14	
	1385				
26		18.963616	19.2	9	
	1380				
27		21	21.3931	11	
	1380				
28		12.564828	12.8	11	
	1380				
29		20.88496	21	6	
	1375				
30		13.169285	13.7	16	
	1370				
31		17.900101	18.3	12	
	1360				
32					
	Slope distance to alpha		2210.78		

X	Y	Ground/Terrain Features and Comments
0	2220	
80	2200	
250	2100	
390	2000	
510	1960	
590	1900	
770	1800	
1010	1700	
1190	1640	
1310	1600	
1430	1560	
1550	1500	
1572	1490	
1599	1485	
1620	1470	
1648	1465	
1679	1450	
1710	1445	
1745	1435	
1779	1425	
1812	1415	
1844	1405	
1862	1400	
1890	1390	
1906	1390	
1931	1385	Beta
1950	1380	
1971	1380	
1983	1380	
2004	1375	
2017	1370	
2035	1360	Alpha

X	Y					E	N	Elev (m)	horizontal distance
			yds	m					
0	2220		27	24.7					22.01
80	2200		32	29.3		725	333938.9	5862668.9	1485.351
250	2100		25	22.9					27.43
390	2000		33	30.2		726	333961.3	5862684.8	1472.854
510	1960		36	32.9					19.89
590	1900		36	32.9		727	333977.3	5862697	1463
770	1800		40	36.6					27.60
1010	1700		38	34.7		728	333997.5	5862715	1451.47
1190	1640		38	34.7					34.02
1310	1600		36	32.9		729	334026.8	5862733	1440.89
1430	1560		21	19.2					32.56
1550	1500		32	29.3		730	334051.2	5862754	1431.52
1572.2	1490		20	18.3					36.32
1599.17	1485		20	18.3		731	334083.2	5862771	1424.07
1620.09	1470		21	19.2					29.55
1647.89	1465		15	13.7		732	334105.9	5862790	1408.93
1678.61	1450		14	12.8					36.71
1710.23	1445		23	21.0		733	334137.1	5862810	1404.36
1745.04	1435		15	13.7					28.38
1778.56	1425		20	18.3		734	334162.4	5862823	1391.38
1812.23	1415								20.47
1843.52	1405					735	334177.4	5862836	1387.3
1861.97	1400								29.43
1890.4	1390					736	334203.5	5862850	1384.65
1908.23	1390								15.32
1925.99	1385					737	334217.4	5862857	1392.1
1944.95	1380								24.86
1958.4	1380					738	334237.9	5862871	1378.41
1970.97	1380								13.95
1991.85	1375					739	334247	5862881	1382.01
2005.02	1370								20.96
2022.92	1360					740	334258.6	5862899	1379.85
									13.85
						741	334265.4	5862911	1369.51
									20.53
						742	334278.3	5862927	1373.36
									19.54
						743	334297.7	5862928	1361.34

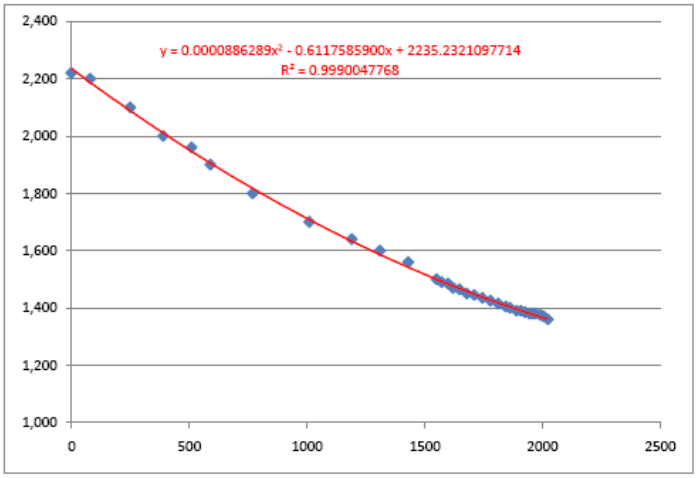

Delta X	87
H Beta	835
X Beta	1931
Beta	23.38884882
H Alpha	850
X Alpha	2035
Alpha	22.66897785

APPENDIX C: Summary of Avalanche Path Data

Path_ID	Range	Easting	Northing	W_Precip	X_0	H_0	y''	X_β	β	Δx	X_α	H_α
S1	Selkirks	486231	5478389	951	1525	628	5.41E-04	1364	24.0	109	1473	1465
S2	Selkirks	485939	5477834	951	1449	633	6.03E-04	1177	26.0	249	1426	1454
S3	Selkirks	477024	5494874	877	1006	419	8.28E-04	760	28.0	242	1002	1733
S4	Selkirks	496277	5438240	1071	1501	515	4.57E-04	968	26.0	336	1304	1655
S5	Selkirks	487028	5538424	869	1354	617	6.73E-04	1133	27.0	267	1400	1901
S6	Selkirks	510360	5555208	848	8476	2260	6.29E-05	5055	21.4	120	5175	640
S7	Selkirks	480907	5516072	886	1512	752	6.58E-04	1156	31.4	165	1321	1425
S8	Selkirks	480920	5515894	886	2028	881	4.28E-04	1152	31.2	78	1230	1423
S9	Selkirks	489417	5510345	1165	2886	972	2.33E-04	1109	28.1	121	1230	1780
S10	Selkirks	489949	5506008	965	1553	743	6.16E-04	999	33.3	171	1170	1430
S11	Selkirks	489718	5505731	965	2096	995	4.53E-04	912	35.3	122	1034	1420
S12	Selkirks	491592	5500725	1004	4171	1559	1.79E-04	1919	29.9	106	2025	1030
S13	Selkirks	491411	5500213	838	3386	1344	2.34E-04	1721	30.7	123	1844	1035
C1	Cariboos	330197	5864911	486	3274	987	1.84E-04	2114	22.0	501	2615	1330
C2	Cariboos	332727	5862150	522	3451	1056	1.77E-04	1931	23.4	87	2018	1370
C3	Cariboos	339437	5851234	526	1635	684	5.11E-04	1292	26.9	202	1494	1330
C4	Cariboos	339434	5851335	526	1739	608	4.02E-04	1362	22.9	130	1492	1310
C5	Cariboos	339437	5851646	526	1931	622	3.33E-04	1224	23.6	237	1461	1310
C6	Cariboos	334174	5857212	536	3896	1195	1.57E-04	1979	25.5	127	2106	1220
M1	Monashees	409940	5643390	1069	6282	1856	9.41E-05	2135	26.5	275	2410	985
M2	Monashees	411496	5643130	913	2306	950	3.58E-04	1481	30.3	273	1754	820
M3	Monashees	412409	5643081	758	1550	767	6.38E-04	920	35.0	158	1078	750
M4	Monashees	374835	5660863	861	2748	1035	2.74E-04	1325	29.3	58	1383	1435
M5	Monashees	374359	5660875	861	1638	773	5.76E-04	1086	32.4	76	1162	1440
M6	Monashees	374199	5660912	861	2478	923	3.00E-04	1279	28.5	56	1335	1420
M7	Monashees	425675	5639893	1005	5822	2144	1.27E-04	4041	26.1	395	4436	555
M8	Monashees	361153	5748536	1105	4532	1903	1.85E-04	1906	34.0	534	2440	789
M9	Monashees	362974	5744602	1208	5215	2097	1.54E-04	1125	35.0	995	2120	814
M10	Monashees	360215	5740604	916	3528	1511	2.43E-04	2113	33.0	327	2440	896
M11	Monashees	360170	5739226	916	5316	2023	1.43E-04	2500	33.0	720	3220	901
M12	Monashees	362440	5737683	867	6019	2837	1.57E-04	1187	41.0	423	1610	951

Path_ID	α	δ	H_s	SZ_Ang	SZ_Asp	SZ_Elev	RZ_Elev	SR	WI	SZ_Width	TP
S1	22.0	-12.9	635	34	135	2075	1440	5	3	300	2
S2	24.0	-1.6	623	38	135	2070	1447	5	3	250	2
S3	24.0	7.5	395	45	45	2160	1765	1	3	340	2
S4	21.0	5.9	470	36	135	2160	1690	3	5	760	1.5
S5	22.0	-7.7	615	40	90	2480	1865	1	5	500	2
S6	21.1	9.5	1980	40	90	2640	660	5	4	470	1
S7	28.6	5.2	705	35	270	2145	1440	5	2	110	2
S8	29.6	1.5	698	32	270	2100	1425	5	2	110	2
S9	26.8	12.6	593	30	180	2400	1807	5	4	150	3
S10	29.8	5.0	655	35	315	2100	1445	2	3	170	3
S11	33.3	16.0	645	30	315	2100	1455	2	3	160	2
S12	28.7	2.7	1105	35	270	2140	1035	2	3	320	3
S13	29.1	2.3	1020	35	270	2060	1040	2	3	370	2
C1	19.4	7.4	855	27	90	2250	1395	3	5	610	2
C2	22.8	9.8	835	30	45	2220	1385	2	3	260	1
C3	24.8	9.8	655	45	90	2020	1365	5	4	300	2
C4	21.6	6.6	575	30	90	1900	1325	5	3	150	2
C5	22.0	13.1	535	30	90	1900	1365	5	4	280	1.5
C6	25.0	15.4	945	35	45	2200	1255	5	4	720	1
M1	24.8	10.3	1065	30	45	2100	1035	5	5	550	1
M2	28.2	15.4	865	33	45	1760	895	3	4	340	2
M3	31.9	9.0	645	35	45	1420	775	8	1	100	3
M4	28.9	19.0	745	35	180	2200	1455	5	2	100	1
M5	30.3	-7.5	690	40	180	2120	1430	5	2	100	2
M6	27.3	-5.1	695	30	180	2110	1415	2	2	100	2
M7	24.7	9.3	1980	35	225	2600	620	1	3	1500	2
M8	32.8	25.7	1318	45	225	2364	1046	2	3	1000	1
M9	32.5	27.3	833	40	225	2161	1328	2	3	540	1
M10	29.4	-2.3	1230	40	225	2113	883	3	3	860	1.5
M11	29.5	16.6	1609	50	225	2724	1115	3	3	300	1
M12	37.2	21.0	1056	45	45	2169	1113	2	4	1000	1

Path_ID	Range	Easting	Northing	W_Precip	X_0	H_0	y''	X_β	β	Δx	X_α	H_α
M13	Monashees	362916	5734120	911	4906	1771	1.47E-04	1182	32.0	629	1811	1051
M14	Monashees	399009	5646250	773	2507	1431	4.55E-04	1780	34.0	125	1905	528
IL2	Fernie	635400	5480561	770	2686	849	2.36E-04	1367	27.8	521	1888	1174
IL3	Fernie	633955	5483318	692	1612	554	4.26E-04	1110	25.5	-50	1060	1122
IL4	Fernie	632995	5482582	656	2959	988	2.26E-04	2210	23.5	200	2410	1117
IL5	Fernie	630725	5483239	698	2406	913	3.15E-04	1485	29.5	190	1675	1314
IL6	Fernie	630298	5483529	800	2427	850	2.89E-04	1650	26.4	480	2130	1370
IL7	Fernie	630378	5486546	730	1370	435	4.64E-04	860	24.1	105	965	1372
IL9	Fernie	630808	5486712	715	2240	609	2.43E-04	1230	21.7	310	1540	1394
IL10	Fernie	633478	5487110	698	2748	801	2.12E-04	1675	22.7	275	1950	1275
IL11	Fernie	633524	5482262	656	3341	1010	1.81E-04	1770	24.9	880	2650	1100
IL12	Fernie	634850	5481126	714	2895	854	2.04E-04	1100	31.7	1184	2284	1160
IL13	Fernie	634279	5481624	692	3132	915	1.87E-04	1650	25.3	542	2192	1165
IL14	Fernie	634983	5482175	692	2536	785	2.44E-04	1220	26.2	324	1544	1200
IL15	Fernie	631551	5483226	698	3278	1035	1.93E-04	1881	25.6	227	2108	1165
IL16	Fernie	631799	5482576	698	3750	1111	1.58E-04	2136	24.3	204	2340	1175
IL17	Fernie	629087	5485392	800	1294	693	8.28E-04	1020	33.7	361	1381	1600
MF1	Fernie	643100	5487755	665	1945	816	4.31E-04	1375	29.3	480	1855	1180
MF2	Fernie	637093	5487322	772	1707	786	5.39E-04	1233	30.8	445	1678	1205
MF3	Fernie	636806	5487248	772	2332	861	3.17E-04	1776	24.3	238	2014	1230
MF4	Fernie	635088	5487606	797	2262	715	2.79E-04	1403	25.0	567	1970	1240
MF5	Fernie	634832	5486843	749	1660	726	5.27E-04	1407	27.7	144	1551	1235
AT1	Fernie	637735	5487717	772	2285	892	3.42E-04	1673	26.7	252	1925	1096
AT2	Fernie	637819	5487852	772	2486	889	2.88E-04	1847	24.2	262	2109	1077
MP1	Fernie	640049	5490089	743	2261	863	3.37E-04	1465	27.4	130	1595	1120
MP2	Fernie	640164	5490393	743	2432	868	2.94E-04	1900	23.9	165	2065	1034
MP3	Fernie	640361	5490620	743	2878	760	1.83E-04	1400	22.5	430	1830	1030
MP4	Fernie	638041	5487947	746	1934	815	4.36E-04	1268	29.7	209	1477	1124
SF1	Fernie	635869	5480673	770	3281	974	1.81E-04	1426	27.6	375	1801	1220
SF2	Fernie	636153	5480335	770	3346	902	1.61E-04	1735	24.2	185	1920	1240
SF3	Fernie	636267	5480105	770	2532	781	2.44E-04	1550	25.4	390	1940	1215
SF4	Fernie	636521	5479822	770	2214	758	3.09E-04	1585	25.8	115	1700	1240
SF5	Fernie	636765	5479628	690	2232	832	3.34E-04	1654	26.6	390	2044	1215
SF6	Fernie	636653	5478880	699	2954	933	2.14E-04	1863	24.3	230	2093	1210
SW3	Sparwood	649692	5514387	359	1568	627	5.10E-04	996	29.2	-60	936	1264
SW6	Sparwood	649934	5513471	361	1562	620	5.08E-04	973	28.6	295	1268	1190
SW7	Sparwood	649764	5514389	359	1401	618	6.30E-04	886	31.4	40	926	1210
SW9	Sparwood	649832	5511677	361	1928	776	4.18E-04	1285	36.8	60	1345	1134.0
SW10	Sparwood	650035	5511894	361	1435	655	6.35E-04	910	31.3	-71	839	1185

Path_ID	α	δ	H_s	SZ_Ang	SZ_Asp	SZ_Elev	RZ_Elev	SR	WI	SZ_Width	TP
M13	25.4	4.2	1182	30	45	2279	1097	2	5	900	1
M14	32.5	2.7	1201	35	180	1735	534	5	3	350	3
IL2	23.6	11.5	720	28	45	2000	1280	1	4	740	2
IL3	26.0	13.5	530	28	45	1640	1110	2	2	260	2
IL4	22.2	6.6	960	23	45	2100	1140	1	4	810	2
IL5	27.9	13.6	840	25	45	2200	1360	1	4	310	2
IL6	22.2	5.9	820	33	45	2240	1420	1	4	1430	2
IL7	22.4	7.1	385	28	135	1770	1385	10	1	510	2
IL9	20.2	13.8	490	30	135	1960	1470	5	2	480	2
IL10	20.7	7.3	700	35	180	2010	1310	3	3	920	1
IL11	20.3	10.3	820	38	45	2080	1260	3	4	700	2
IL12	20.2	7.7	680	45	45	2000	1320	3	4	960	2
IL13	21.3	7.9	780	37	45	2020	1240	5	4	850	2
IL14	23.1	10.5	600	30	45	1860	1260	10	2	150	2
IL15	23.9	8.8	900	33	45	1900	1200	4	4	800	1
IL16	22.2	-2.8	965	30	45	2000	1165	4	4	450	1
IL17	26.9	3.2	680	40	45	2300	1620	2	4	400	3
MF1	24.3	7.7	771	40	135	2000	1245	4	3	400	2
MF2	25.4	7.7	735	45	135	2000	1265	4	3	400	2
MF3	22.7	9.5	802	45	180	2070	1270	10	3	150	2
MF4	21.1	10.5	655	34	180	2000	1345	5	3	760	2
MF5	24.1	9.8	740	37	180	1930	1260	2	3	250	2
AT1	24.7	9.7	841	41	135	1980	1139	5	4	100	2
AT2	22.7	11.2	831	36	135	1960	1129	5	3	140	2
MP1	26.1	8.7	760	36	135	1885	1140	5	3	240	1
MP2	22.8	9.0	840	34	135	1891	1060	3	3	240	1
MP3	22.3	21.6	580	34	135	1780	1200	5	3	300	1
MP4	27.7	14.0	724	35	90	1894	1176	10	2	300	2
SF1	24.0	8.3	745	49	45	2095	1275	1	4	740	1
SF2	22.9	9.2	780	46	45	2050	1270	1	4	250	1
SF3	22.2	8.0	735	45	45	2005	1270	1	4	340	2
SF4	24.8	9.9	765	43	45	2025	1260	1	4	150	2
SF5	23.4	8.0	830	41	45	2100	1270	1	4	350	2
SF6	22.9	11.1	840	38	90	2095	1255	1	4	300	2
SW3	28.9	34.3	557	39	90	1780	1223	10	1	290	3
SW6	25.0	11.5	530	33	90	1780	1250	10	1	400	3
SW7	30.7	14.0	540	38	90	1760	1220	10	1	290	3
SW9	27.2	5.7	960	36	90	1825	1140	10	3	300	3
SW10	32.8	11.2	554	43	90	1725	1171	10	1	173	2